

NORWEGIAN UNIVERSITY OF SCIENCE AND TECHNOLOGY  
&  
NORDIC SEMICONDUCTOR



BACHELOR THESIS  
ELECTRICAL ENGINEERING

TELE3001

PROJECT NUMBER E1821

---

## Energy Harvesting Stop Button

ENERGIHØSTENDE STOPP KNAPP

---

*Authors:*

Jonathan L. LUNDAAS  
Tor André MELHEIM  
Besart OLLURI  
Simon RØMO  
Simen S. RØSTAD

*E-mail:*

jonathll@stud.ntnu.no  
toramel@stud.ntnu.no  
besarto@stud.ntnu.no  
simonro@stud.ntnu.no  
simensr@stud.ntnu.no

*Supervisors:*

Audun KORNELIUSSEN  
Torolv SKJØLSVIK  
Rolf K. SNILSBERG

*E-mail:*

audun.korneliussen@nordicsemi.no  
torolv.skjolsvik@nordicsemi.no  
rolf.k.snilsberg@ntnu.no

May 28, 2018

Faculty of Information Technology and Electrical Engineering  
Department of Electronic Systems



NTNU

## *Preface*

Bachelor thesis

### **Energy Harvesting Stop Button**

by Lundaas, Melheim, Olluri, Rømo and Røstad

The bachelor thesis "Energy Harvesting Stop Button" is written by five students studying electrical engineering at NTNU between January and May of 2018. We are satisfied with the effort done in the project period, which hopefully is reflected in the project report. This has been a highly educational process that has given us the opportunity to evolve as both students and co-workers. We have all experienced a steep learning curve throughout the project in our respective assigned tasks, something that has been pushed through by dedication and our general interest for electronics. We also hope that this bachelor thesis, and the documentation provided ([EHSB GitHub](#)) may aid someone in the future. In the end, we are proud to have completed a project of this scale successfully.



## Declaration of Authorship

We, Lundaas, Melheim, Olluri, Rømo and Røstad, hereby declare that this thesis called “Energy Harvesting Stop Button” is our own original work except where otherwise indicated. Any work by any other author is properly acknowledged at given points of use.

---

Jonathan L. Lundaas

---

Tor André Melheim

---

Besart Olluri

---

Simon Rømo

---

Simen S. Røstad



NTNU

## *Abstract*

Bachelor thesis

### **Energy Harvesting Stop Button**

by Lundaas, Melheim, Olluri, Rømo and Røstad

### **English**

This thesis presents the design and construction of a Bluetooth Low Energy system. The system consists of three units; a uniquely identifiable energy harvesting button transmitter, a central observer that sets an LED stop sign on an identified signal, and a relayer to carry signals for longer range applications.

The combination of Bluetooth Low Energy and an energy harvesting circuit leads to a wireless and self-sufficient button. The application for the system will be presented as a stop button which can be used in public transportation, although the same system can be applied to numerous similar situations.

Energy harvesting means exploiting ambient energy naturally surrounding a given system. Even though the energy harvested is mainly in the order of milliamps, today's microcontrollers are energy efficient enough that these minuscule energy sources suffice. The energy harvesting circuit created for this project was ultimately able to harvest a total energy of  $\approx 0.27\text{mWs}$  per button push.

The Bluetooth Low Energy protocol stack allows the system on a chip nRF52, with the energy harvesting circuit described in this paper, to advertise one Bluetooth Low Energy event for 24ms at an energy consumption of  $23.2\mu\text{Ws}$ , and to start up for 8ms with an energy consumption of  $61.7\mu\text{Ws}$ .

This resulted in a solution able to advertise five Bluetooth Low Energy events over the span of  $\approx 100\text{ms}$  by one push of the stop button. This concludes with a proof of concept solution that can be utilized in its intended environment.

---

Norsk

---

Denne bacheloroppgaven tar for seg designet og konstruksjonen av et blåtann lavenergi system. Systemet består av tre enheter; en unikt gjenkjennbar energihøstende sender i form av en knapp, en sentral observatør som opererer en LED indikator på gjenkjent signal, og en videresender til bruk ved lengre avstander.

Kombinasjonen av blåtann lavenergi og energihøsting fører til en trådløs og selvforsynt knapp. Systemet vil bli presentert som en stoppknapp til bruk i offentlig transport, men det skal nevnes at det samme systemet kan anvendes i flerfoldige lignende situasjoner.

Energihøsting betyr at et system utnytter energi fra omgivelsene sine. Selv om energien som blir høstet sjeldent er mer enn milliampere, er dagens mikrokontrollere energieffektive nok til å kjøre på disse strømmene. Energihøstekretsen som er konstruert for dette prosjektet, var til slutt kapabel til å høste en total energi på  $\approx 0.27\text{mW}$  per knappetrykk.

Blåtann lavenergi protokollen lar systemet på en brikke nRF52, med energihøstekretsen beskrevet i denne oppgaven, sende et blåtann lavenergi signal på 24ms med et energiforbruk på  $23.2\mu\text{Ws}$ , samt oppstart på 8ms som bruker  $61.7\mu\text{Ws}$ .

Resultatet ble en stoppknapp som klarer å sende fem blåtann lavenergi event over  $\approx 100\text{ms}$  på et knappetrykk. Dette konkluderer med en fungerende prototyp som fungerer som den skal i sitt bruksområde.

NTNU

## *Acknowledgement*

Bachelor thesis

**Energy Harvesting Stop Button**

by Lundaas, Melheim, Olluri, Rømo and Røstad

We are grateful for the chance to complete a bachelor's degree in Electrical engineering here at the Norwegian University of Science and Technology, and want to thank the university and faculty for providing the equipment and facilities necessary for completing this assignment. We want to express our gratitude to Nordic Semiconductor for invaluable guidance and for funding this project. Thanks to our supervisors, Rolf Kristian Snilsberg, Torolv Skjølsvik and Audun Korneliussen, for their patience and advice in our bi-weekly meetings, for their quick replies to our frequent questions, and for their availability throughout this project.

There is also great gratitude towards the student association Elektra, as they have provided various tools, equipment, components, and for letting us use their workshop. A special thanks to Arne Midjo, Hans Elias Josephsen, Even Johan Christiansen, Stein-Olav Lund, Dag Roar Hjelme, Dominik Osinski, Christian Wilgaard, Bjørn Spockeli, Martin Koen Hongset, Shkurta Olluri, and Kosovare Olluri. Thanks to AtB for providing useful information about their buses.



# List of Abbreviations

<b>AC</b>	Alternating Current	<b>I/O</b>	Input/Output
<b>ADC</b>	Analog to Digital Converter	<b>IC</b>	Integrated Circuit
<b>AHB</b>	Advanced High-performance Bus	<b>IDE</b>	Integrated Development Environment
<b>APB</b>	Advanced Peripheral Bus	<b>IEEE</b>	Institute of Electrical and Electronics Engineers
<b>API</b>	Application Programming Interface	<b>ISP</b>	In-System Programming
<b>ATT</b>	Attribute Protocol	<b>LDO</b>	Low Dropout (regulator)
<b>BLE</b>	Bluetooth Low Energy	<b>LED</b>	Light Emitting Diode
<b>BR/EDR</b>	Basic Rate/Enhanced Data Rate	<b>LFCLK</b>	Low-Frequency Clock
<b>BT</b>	Bluetooth	<b>LFRC</b>	Low-Frequency Resistor-Capacitor
<b>CPU</b>	Central Processing Unit	<b>LFSYNT</b>	Low-Frequency Synthesised
<b>CRC</b>	Cyclic Redundancy Check	<b>LFXO</b>	Low-Frequency External Oscillator
<b>DC</b>	Direct Current	<b>MCU</b>	Microcontroller Unit
<b>DCR</b>	Direct Current Resistance	<b>MOSFET</b>	Metal-oxide-semiconductor field-effect transistor
<b>DK</b>	Development Kit	<b>NFC</b>	Near Field Communication
<b>DSP</b>	Digital Signal Processing	<b>NMOS</b>	N-type metal-oxide-semiconductor
<b>EHSB</b>	Energy Harvesting Stop Button	<b>NTNU</b>	Norwegian university of science and technology (Norges teknisk-naturvitenskapelige universitet)
<b>ESD</b>	Electrostatic Discharge	<b>OPP</b>	Online Power Profiler
<b>FW</b>	Firmware	<b>PCB</b>	Printed Circuit Board
<b>GAP</b>	Generic Access Profile	<b>PPK</b>	Power Profiler Kit
<b>GATT</b>	Generic Attribute Profile	<b>RAM</b>	Random Access Memory
<b>GPIO</b>	General-Purpose Input/Output		
<b>HFCLK</b>	High-Frequency Clock		

---

**X**

<b>RF</b>	Radio Frequency	<b>SMPS</b>	Switch Mode Power Supply
<b>ROM</b>	Read-Only Memory	<b>SOC</b>	System on a Chip
<b>RSSI</b>	Received Signal Strength Indicator	<b>SW</b>	Software
<b>SDK</b>	Software Development Kit	<b>TX</b>	Transmission
<b>SIG</b>	Special Interest Group	<b>UUID</b>	Universally Unique Identifier
<b>SMD</b>	Surface Mount Device		

# Contents

<b>Preface</b>	<b>I</b>
<b>Declaration of Authorship</b>	<b>III</b>
<b>Abstract</b>	<b>V</b>
<b>Acknowledgement</b>	<b>VII</b>
<b>List of Abbreviations</b>	<b>IX</b>
<b>1 Introduction</b>	<b>1</b>
1.1 Background . . . . .	1
1.2 Project Scope . . . . .	1
1.3 Outline . . . . .	2
1.4 Disposition . . . . .	2
<b>2 Theory</b>	<b>3</b>
2.1 Microcontrollers and System on a Chip . . . . .	3
2.2 Bluetooth . . . . .	4
2.2.1 Bluetooth Low Energy (BLE) . . . . .	5
Bluetooth Low Energy Advertising Packet . . . . .	5
2.2.2 Generic Access Profile (GAP) . . . . .	6
2.2.3 Generic Attribute Profile (GATT) . . . . .	6
Services and Characteristics . . . . .	7
2.3 SoftDevice . . . . .	7
2.3.1 SoftDevice S132 . . . . .	8
2.4 Energy Harvesting . . . . .	9
2.4.1 The General System of Energy Harvesting . . . . .	9
2.4.2 Electro-mechanical Generator (Inductive Transducer) . . . . .	11
2.4.3 Piezoelectric Transducers . . . . .	11
2.5 Rectifier Topologies . . . . .	12
2.5.1 Half-wave Bridge Rectifier . . . . .	13
2.5.2 Full-wave Bridge Rectifier . . . . .	13
2.5.3 Voltage Multipliers . . . . .	14
2.5.4 Active Rectification (Synchronous Rectification) . . . . .	14
2.6 Voltage Regulators . . . . .	15
2.6.1 Buck Converters . . . . .	15
LTC3588-1 . . . . .	16
2.6.2 Buck-boost Converters . . . . .	16
2.6.3 Linear Voltage Regulators . . . . .	17
2.7 3D Printing . . . . .	17
2.8 PCB Design . . . . .	18

---

<b>3 Choice of Components and Equipment</b>	<b>19</b>
3.1 Tools and Equipment . . . . .	19
3.2 System on a Chip . . . . .	20
3.2.1 nRF52832 . . . . .	20
nRF52 Clock Control . . . . .	20
nRF52 Internal Voltage Regulating . . . . .	20
3.3 Generators . . . . .	21
3.3.1 Piezoelectric Elements . . . . .	21
3.3.2 Electro-mechanical Generators . . . . .	21
3.4 Voltage Regulators . . . . .	22
3.4.1 LDO Regulators . . . . .	22
LDO Regulators Considered . . . . .	22
3.4.2 Buck Converters . . . . .	22
LTC3588-1 . . . . .	22
3.4.3 Buck-boost Converters . . . . .	23
3.5 Circuit Components . . . . .	23
3.5.1 Rectifiers . . . . .	23
Full-wave Bridge Rectifier . . . . .	23
Full-wave Voltage Multiplier . . . . .	23
3.5.2 Capacitors, Inductors and Diodes . . . . .	24
Capacitors . . . . .	24
Inductors . . . . .	25
Diodes . . . . .	25
3.5.3 Antenna . . . . .	25
<b>4 Method</b>	<b>27</b>
4.1 Firmware . . . . .	27
4.1.1 Preliminary Phase . . . . .	27
4.1.2 Firmware Development . . . . .	27
Stop Button . . . . .	28
Relayer . . . . .	29
Central . . . . .	30
System Flow Chart . . . . .	32
4.1.3 Energy Consumption . . . . .	33
Test Bench . . . . .	33
Measurements and Generated Results . . . . .	34
Calculations . . . . .	36
4.1.4 Troubleshooting . . . . .	42
System Test . . . . .	43
4.2 Hardware . . . . .	47
4.2.1 Preliminary Phase . . . . .	47
4.2.2 Design Phase . . . . .	47
Energy Source . . . . .	47
Rectifier Circuits and Initial Measurements . . . . .	48
Voltage Regulators . . . . .	49
PCB Design . . . . .	51
4.2.3 Production Phase . . . . .	60
Component and PCB Orders . . . . .	60
Soldering . . . . .	61
Troubleshooting . . . . .	61
4.3 Component Characterization . . . . .	62

4.3.1	AFIG-0007 . . . . .	62
4.3.2	LTC3588-1 . . . . .	64
	Simulations to Characterize the LTC3588-1 . . . . .	64
	Testing the LTC3588-1 in Different Configurations . . . . .	68
4.4	Energy Budget . . . . .	69
4.5	3D Modelling and Printing . . . . .	70
4.5.1	Central and Relayer Casings . . . . .	70
4.5.2	Stop Sign . . . . .	70
4.5.3	Designing and Printing Mechanical Parts . . . . .	71
4.5.4	Stop Button Casing . . . . .	72
<b>5</b>	<b>Results</b>	<b>75</b>
5.1	PCB Design and 3D printing . . . . .	75
5.1.1	Final Voltage Doubler (PCB Design and Schematics) . . . . .	75
	Final Voltage Doubler Solution PCB Design (Original Layout) . . . . .	76
	Final Voltage Doubler Solution PCB Design (Showcase Layout) . . . . .	77
5.1.2	Final LTC Solution (PCB Design and Schematics) . . . . .	78
	Final LTC Solution PCB Design (Original Layout) . . . . .	79
	Final LTC Solution PCB Design (Showcase Layout) . . . . .	80
5.1.3	3D Printing . . . . .	81
	Central and Relayer Casings . . . . .	81
	Stop Sign . . . . .	81
	Stop Button Casing . . . . .	82
5.2	BLE Event Statistics . . . . .	83
5.2.1	Final Voltage Doubler Solution . . . . .	84
5.2.2	Final LTC Solution, 2.5V Output Voltage . . . . .	84
5.2.3	Final LTC Solution, 1.8V Output Voltage . . . . .	85
5.3	Final System Field Tests . . . . .	85
5.3.1	Final Voltage Doubler Solution . . . . .	86
5.3.2	Final LTC Solution, 1.8V Output Voltage . . . . .	86
5.3.3	Final LTC Solution, 2.5V Output Voltage . . . . .	87
<b>6</b>	<b>Conclusion and Discussion</b>	<b>89</b>
6.1	Discussion . . . . .	89
6.1.1	Code . . . . .	89
6.1.2	Transmission Range . . . . .	90
6.1.3	Cost . . . . .	90
6.1.4	Final System Field Tests . . . . .	90
6.1.5	Circuit Design Choices . . . . .	91
6.1.6	Work Environment . . . . .	91
6.1.7	Simulations of the LTC3588-1 . . . . .	91
6.1.8	Energy Measurements . . . . .	92
6.2	Conclusion . . . . .	92
6.3	Further Work . . . . .	92
6.3.1	Synchronous Rectification . . . . .	92
6.3.2	Optimization of Code . . . . .	93
6.3.3	Mechanical Engineering . . . . .	93
6.3.4	Central and Relayer PCBs . . . . .	93
	<b>Bibliography</b>	<b>99</b>

<b>A Bill of Materials</b>	<b>103</b>
<b>B Datasheets</b>	<b>107</b>
<b>C Schematics</b>	<b>111</b>
C.1 nRF52 Development Kit and Stop Button Central Schematics . . . . .	111
C.2 Energy Harvesting Stop Button Schematics . . . . .	119
<b>D CODE: Relayer</b>	<b>123</b>
<b>E CODE: Stop button</b>	<b>125</b>
<b>F CODE: Central</b>	<b>127</b>
<b>G Energy Harvesting Stop Button Poster</b>	<b>131</b>

## Chapter 1

# Introduction

This chapter focuses on background material, and provides a basis for further understanding the assignment. The background [1.1] goes through the idea behind the product and asks the initial *why*. Defining the project scope [1.2] explains *what* has to be done, and the essential features and main aspects of the thesis is the outline [1.3], that asks *how*.

## 1.1 Background

A public transport bus has about 24 stop buttons that are intricately wired. This thesis will present an alternative, with wireless stop buttons using energy harvesting. This will remove the need to change batteries in current wireless alternatives, and potentially reduce the cost of installation and maintenance.

## 1.2 Project Scope

The fundamental problem to be solved is two-sided. On one hand it is to design and implement a power generator with the corresponding circuitry. The power generator must supply enough power to sustain a wireless transmitter with only a push of a button, converting mechanical energy to electrical energy. On the other hand, a code has to be developed, that is energy efficient, and compact enough to send as many data packets as possible in a restricted amount of time, with the available power. Even though the transmitter unit is the main task, the project group also has to design and build a working receiver that displays some sort of confirmation that the stop button signal is received.

To design and produce an EHSB system that is intended to be implemented in public transport, an array of challenges have to be addressed.

- Energy budget (operating voltage; peak, quiescent and average operating currents)
- Energy storage device (capacity, leakage, temperature performance, et cetera.)
- Energy harvesting circuits (capability, requirements, limitations, et cetera.)
- Microcontroller (processing performance, power efficiency, DSP, I/O, low-power modes, et cetera.)
- Power management devices (features, performance, et cetera.)
- Wireless connectivity (peak power, range, frequency, protocols, et cetera.)
- Mechanical construction (size, design)
- Production and assembly

- Long-term reliability

The power budget is a key part of the project. Without a power budget it is almost impossible to design a functional stop button of this kind. It is necessary to know how much energy is needed to run the SoC and for how long. And also how much energy is possible to attain from a given energy source. The nRF52 operates between voltages of 1.7 volts through 3.6 volts, which means the supply voltage has to be fairly accurate to safely operate it.

### **1.3 Outline**

To get a better understanding of the system, the firmware development has to be explained in fair detail, as it is how the system functions and is intertwined with the entire project. How the stop buttons radio is configured and how the system handles the different buttons identification is directly related to energy consumption. Means of redundancy needs to be taken into consideration. For example how to avoid collisions with other Bluetooth Low Energy systems.

The hardware part of the project revolves around how to actually supply the nRF52 with power. To harvest as much energy as possible, the regulator circuit is of primary importance and has to be energy efficient. Seeing as the regulator circuits main interaction is through the press of a button, the construction of the circuit and casing needs to be mechanically stable, so that it will be able to endure years of usage.

### **1.4 Disposition**

- Introduction
  - Introductory Pages
  - Background
  - Project Scope
  - Outline
- Main section
  - Theory
  - Choice of Components and Equipment
  - Method
- Results and Conclusion
  - Results
  - Discussion
  - Conclusion

## Chapter 2

# Theory

Chapter two will describe what theory has to be explained and understood before embarking on a project of covering so many subjects within electrical engineering. The theory chapters goal is to give the reader a brief, necessary understanding of every facet of this project.

### 2.1 Microcontrollers and System on a Chip

Microprocessors are used to perform a broad spectrum of tasks such as video rendering, data storage and data processing. To perform smaller, more specific tasks such as turning on a LED or sending a wireless signal, a simple, flexible and less powerful unit would seem preferable, such as an MCU. The MCU is basically a scaled down microprocessor with RAM and ROM in the same chip focused on pin control rather than processing power. MCUs are commonly produced for low cost and low power. The MCU has mostly fixed hardware built around a CPU, with the CPU controlling a range of peripherals, which may provide both digital and analog functions, such as timers and ADCs. MCUs include both volatile and non-volatile on board memory. In addition to the memory, the MCU has a clock source and I/O ports. The firmware on MCUs is written using programming languages such as C or C++ and the firmware is directly flashed to the MCUs hardware, enabling the MCU to run without additional support. See figure 2.1 for a basic visual representation of the basic components in an MCU. [7]

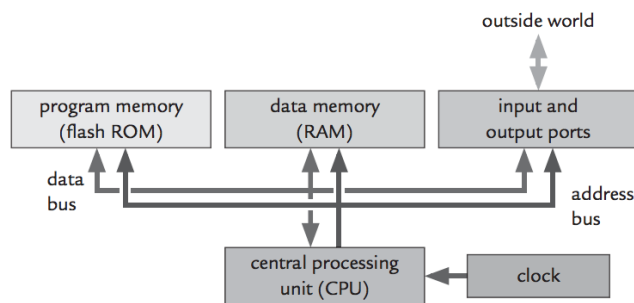


FIGURE 2.1: Basic MCU functional block diagram [7]

The SoC is an integrated circuit that implements most of, or all of the functions of a complete electronic system, all in one chip. An SoC is basically an MCU with additional hardware blocks. For example: Voltage regulators, RF modules and internal oscillators. Although MCUs and SoCs are based on the same components, SoCs often come with more processing power and flexibility, making it capable of more complex tasks. See figure 2.2 for a typical SoC block diagram, the nRF52. [6]

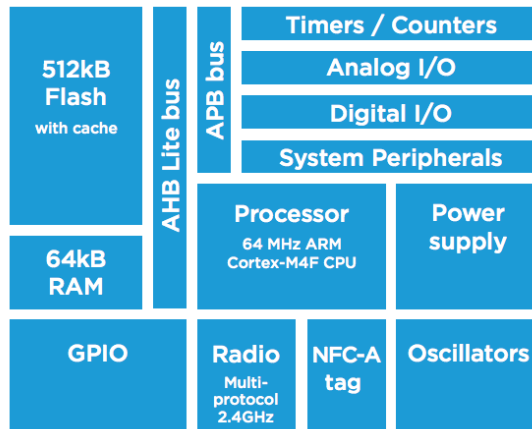


FIGURE 2.2: nRF52 SoC functional block diagram [6]

## 2.2 Bluetooth

Bluetooth or IEEE 802.15.1 is a wireless standard operating on the unlicensed 2.4GHz frequency band, more specifically 2.4GHz to 2.485GHz. The standard is designed to transfer data over short distances, typically under 100 meters and supports data rates up to 3Mbps. Bluetooth was invented by Ericsson in 1994 and is commonly found in short range communication devices such as wireless headsets and keyboards. In the Bluetooth core system the 2.4GHz to 2.485GHz frequency range is divided into 79 channels with 1MHz spacing. The standard supports 1 master and 7 slaves in a single network. Figure 2.3 illustrates typical Bluetooth topologies. [43]

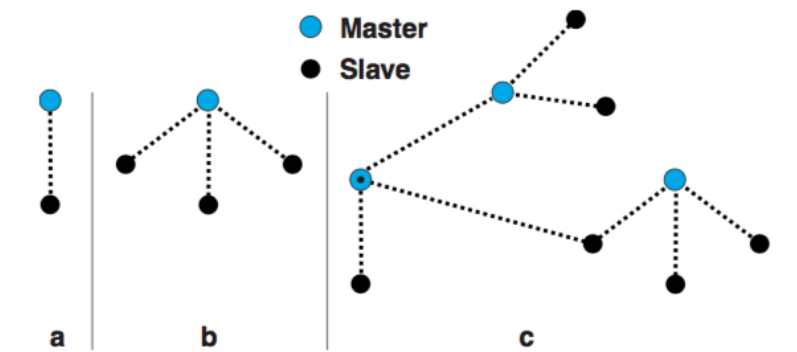


FIGURE 2.3: Bluetooth network topology

### 2.2.1 Bluetooth Low Energy (BLE)

BLE formerly known as BT SMART was added in BT version 4.0 in 2010. BLE is designed to operate within the smartphone environment and other applications that require a longer life span, than what can be sustained by the original Bluetooth specification. In BLE, power is conserved by operating at a reduced duty cycle, sleeping for a majority of the time, awakening only to process data transfers. BLE supports data transfers up to 2Mbps and ranges up to 100 meters. BLE uses the same frequency range as the Bluetooth core system, but uses 40 channels instead of 79 with 2MHz spacing. Channels 37 (2402MHz), 38 (2404MHz) and 39 (2406MHz) are used for advertising. These three specific channels were selected by SIG to avoid Wi-Fi interference. See figure 2.3. The yellow markings display Wi-Fi busy channels while the green markings shows the BLE advertising channels. [4] [43]

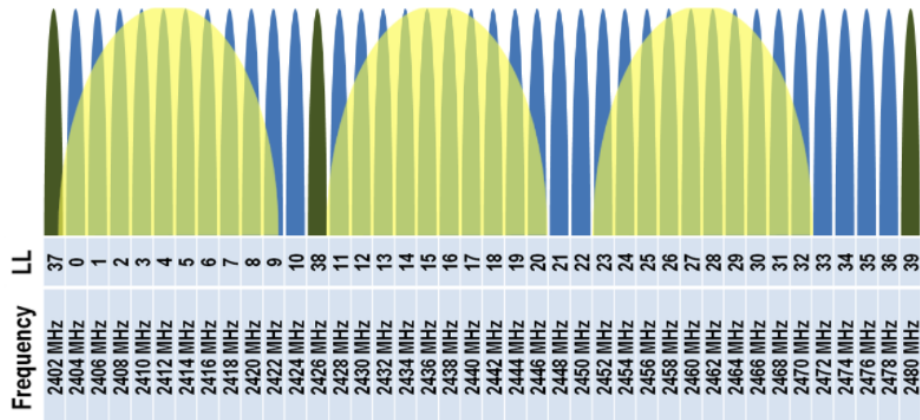


FIGURE 2.4: BLE channel overview[32]

### Bluetooth Low Energy Advertising Packet

The BLE advertising packet mainly consists of six different segments. These six segments total the actual information advertised by a BLE peripheral device. See figure 2.5 and 2.6.

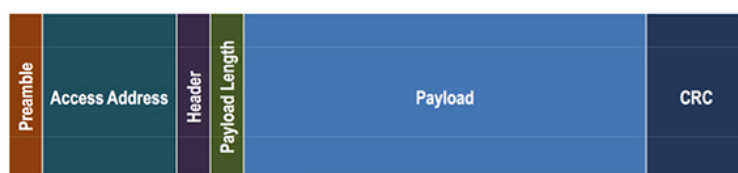


FIGURE 2.5: BLE advertising packet structure[10]

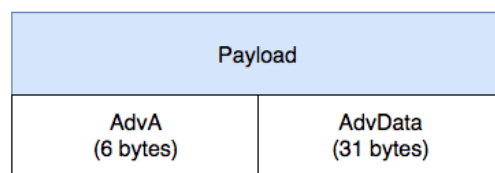


FIGURE 2.6: BLE advertising payload structure

**Preamble (1 byte)** : A consistent bit pattern that makes it easier for the radio to identify the beginning of a BLE packet. Often referred to as "synchword" in other protocols.

**Access Address (4 bytes)** : Hardware filters out non-relevant BLE packages based on the access address. All advertising packages have a predetermined access address.

**Header (1 byte)** : Meta-data which describes the content of a BLE packet such as length and type.

**Payload length (1 byte)** : Length of the payload.

**Payload (6 - 37 bytes)** : 0 - 31 bytes AdvData + 6 bytes AdvA. AdvData is user defined and can contain anything from manufacturer specific data to a 128-bit UUID while AdvA is always 6 bytes. AdvA functions just like an access address but on a higher level in the protocol stack. Payload is often referred to as TX payload.

**CRC (3 bytes)** : Error-detecting code commonly used to detect accidental changes to raw data.

For more information regarding packet format see Bluetooth specification version 5.0 | Vol 6, Part B. [42]

## 2.2.2 Generic Access Profile (GAP)

GAP controls connections and advertising in BLE. It basically sets the communication ramifications between two devices in form of minimum and maximum parameter limits. To stay within the BLE specification, application design must follow parameter limits set by GAP. In general two different roles are defined by GAP, these being peripheral and central devices. Peripheral devices are low power, resource constrained devices that often broadcasts or connects to central devices. Central devices are often much more powerful and complex devices that commonly controls several peripheral devices. [17]

## 2.2.3 Generic Attribute Profile (GATT)

Typically when a connection is established between a peripheral and central device the peripheral device will stop advertising and the central device will stop scanning. Further communication will happen via GATT Services and Characteristics. GATT makes use of a generic data protocol, ATT, which is used to store Services and Characteristics in a simple lookup table using 16-bits identifications for each entry in the table.

In GATT two roles are defined, server and client. The peripheral device is known as the server, holding the ATT lookup data and characteristic definitions while the central is known as the master, sending requests to the server. This is a master/slave relationship where the server acts as a slave and the client as a master.

When establishing a connection the peripheral device will suggest a connection interval to the central. Even though a connection interval is suggested, the central does not have to use the suggested parameter, this occurs often when the central is busy talking to other peripheral devices or when system resources are not available. See figure 2.7. [18]

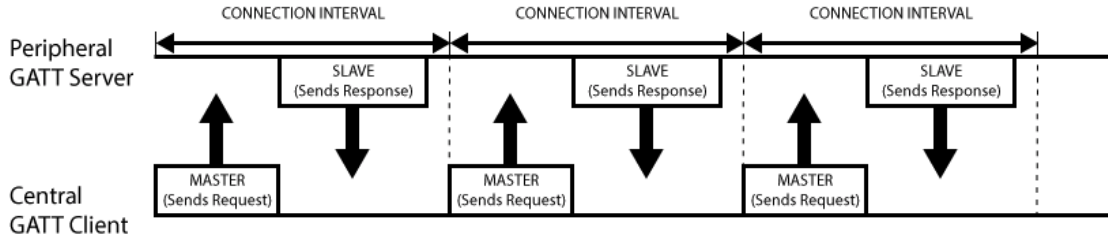


FIGURE 2.7: GATT data exchange process [18]

### Services and Characteristics

GATT transactions in BLE are based on high-level nested objects called Profiles, Services and Characteristics. See figure 2.8.

**Profile** - Pre-defined collection of Services that has been compiled by either the Bluetooth SIG or by the peripheral designers.

**Service** - Contains specific parts of data called Characteristics. A Service can have several Characteristics distinguishing themselves with a unique numeric identification called UUID. If the Service is fully adopted by Bluetooth SIG a 16-bit UUID is accepted, if not a 128-bit UUID is used.

**Characteristic** - The lowest level in a GATT transaction. A Characteristic can hold a single data point that can contain both specific values or arrays of related data. For example data from a XYZ accelerometer. When communicating with a BLE peripheral, Characteristics are the main point of interaction. It is possible to write to Characteristics making enabling the central to send data back to the BLE peripheral device.

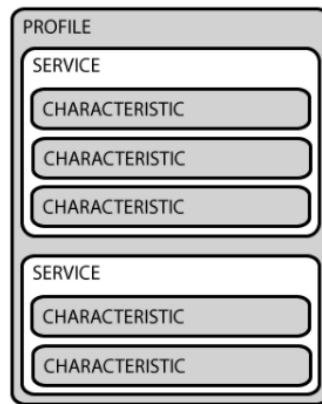


FIGURE 2.8: GATT Profile structure [18]

## 2.3 SoftDevice

A SoftDevice is a wireless protocol stack developed by Nordic Semiconductor for SoC solutions. It is essentially a fixed precompiled radio stack for ANT and BLE designed to run as a base for the application. Fixed meaning that the SoftDevice can not be altered during application development. All code alteration happens in the application. The SoftDevice is 100% event driven meaning that interaction with the SoftDevice happens via API calls

and events. The SoftDevice is located in a reserved memory space and ensures run time protection of memory and hardware resources. See figure 2.9. [39] [40]

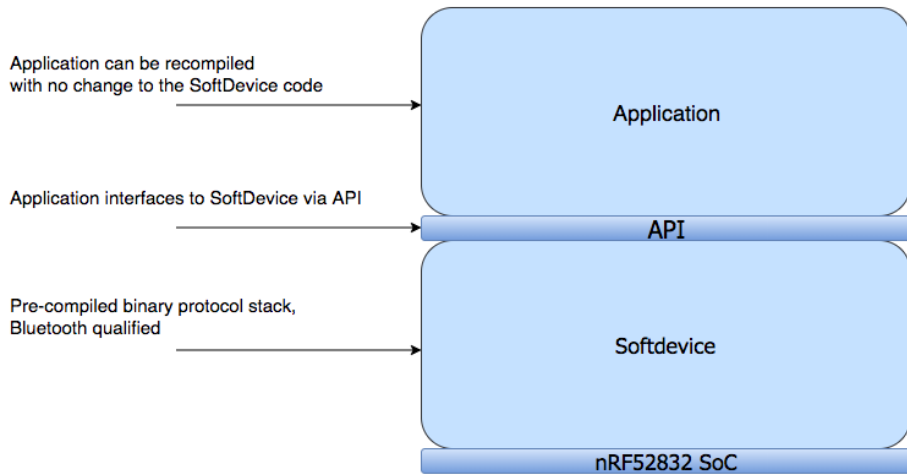


FIGURE 2.9: nRF52 software architecture

### 2.3.1 SoftDevice S132

The SoftDevice S132 is a wireless protocol stack solution for central and peripheral BLE applications. The protocol stack supports up to 20 connections with an additional observer and broadcaster role all running simultaneously. The SoftDevice has a built in API for GATT and GAP, giving the application access to BLE functionality. In other words the SoC can be set to sleep between events making the device more energy efficient. See figure 2.10.

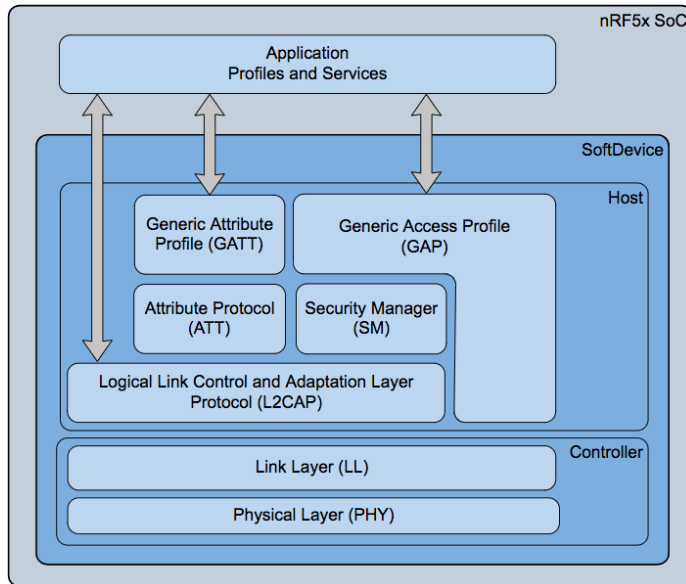


FIGURE 2.10: Detailed nRF52 software architecture [41]

## 2.4 Energy Harvesting

Energy harvesting is the phrase coined for the process of capturing energy through ambient background sources. Contrary to traditional large scale generators, energy harvesting modules or systems are primarily meant for low power appliances such as wireless sensor networks and wearable electronics. In theory self sustaining through external sources such as kinetic energy, solar energy, thermal energy, et cetera.

### 2.4.1 The General System of Energy Harvesting

As shown in figure 2.11, the general system of energy harvesting consists of six parts, excluding the source. Even though following this system is not a must, it gives a general outline and a step by step overview of most energy harvesting systems and circuits.

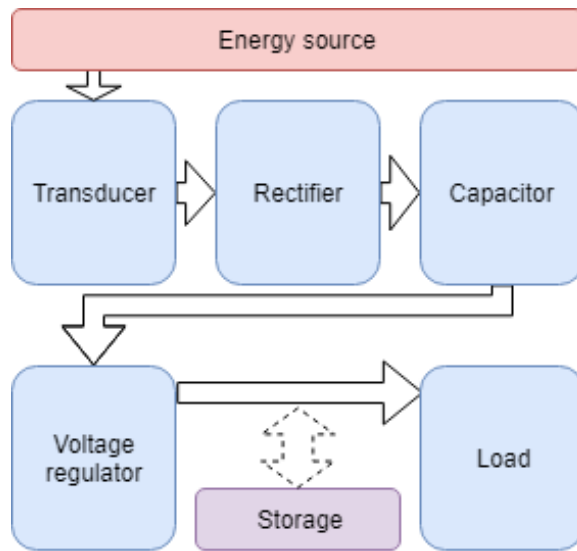


FIGURE 2.11: The general system of energy harvesting

**Energy source** - In energy harvesting the sources exploited are mainly ambient. Meaning they surround the harvesting system, and supply energy without any third party effort. Usually solar, thermal or mechanical, as they are the most available sources. Mechanical energy is usually either applied by a user or supplied by vibrations from the surroundings. Thermal energy can be harvested from any heat source or areas with temperature differences, and solar energy from sunlight.

**Transducer** - The transducers job is to convert applied energy to electrical energy. Different types of transducers include thermoelectric modules for heat, solar cells for sunlight, and piezoelectric crystals for vibrations [13].

**Rectifier** - The purpose of a rectifier is to change the current form from AC to DC. Rectifiers are generally based on certain diode configurations that only allow current to flow in one direction. The configuration seen in figure 2.17 is the most commonly used. Alternative configurations are categorized as single phase rectifiers, three phase rectifiers and voltage multiplier rectifiers. For more in-depth information regarding rectifiers, see section 2.5.

**Capacitor** - Together with the rectifier the capacitor smooths out rectified DC voltages. Making a close to constant DC voltage. Capacitors try to resist sudden changes in

voltage, leading to an elongated discharge time when the voltage is dropping. Even though the output voltage from the capacitor is not purely constant, it is constant enough for the voltage regulator to work with. The voltage output from the capacitor will be similar to the "regulator input" in figure 2.12.

**Voltage regulator** - The basic premise of voltage regulators is that they cut the voltage at a given point, leaving the remaining energy to be lost or stored in the meantime, as seen in figure 2.12.

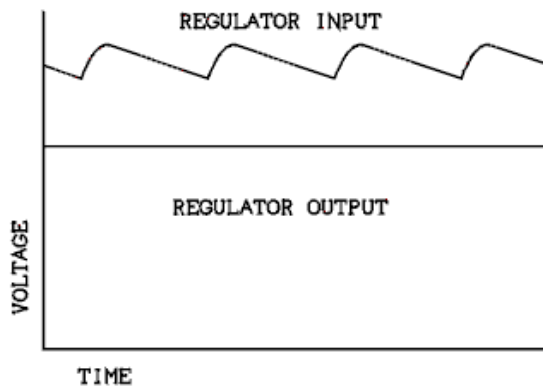


FIGURE 2.12: Voltage before and after regulation [15]

**Energy Storage** - Depending on what kind of energy is harvested or what kind of system is running on the supplied energy, an energy storage is usually added. Capacity, leakage and temperature performance are all variables that effect the choice of storage device, ranging from conventional batteries to solid state batteries and super capacitors. See figure 2.13 for some example energy storage options.

Conventional Batteries	Supercapacitors	Solid State Batteries
<ul style="list-style-type: none"> <li>+ High discharge current</li> <li>+ High energy density</li> <li>+ Inexpensive</li> <li>- Limited life</li> <li>- Replacement labor cost</li> <li>- Unsafe, polluting</li> <li>- Form factor</li> </ul>	<ul style="list-style-type: none"> <li>+ Peak power delivery</li> <li>+ Long life</li> <li>+ Inexpensive</li> <li>- High leakage</li> <li>- Very low energy density</li> <li>- High temperature degradation</li> <li>- Form factor</li> </ul>	<ul style="list-style-type: none"> <li>+ Moderate energy density</li> <li>+ Near zero leakage</li> <li>+ Long life / Permanent</li> <li>+ Low cost of ownership</li> <li>+ Form factor</li> <li>+ Safe / Eco-friendly</li> <li>+ Broader temp. range</li> </ul>

FIGURE 2.13: Comparison of types of energy storage devices. [44]

**Load** - The load meaning whatever system you intend to run on an energy harvesting circuit. The load is usually MCUs, sensors and/or actuators. Loads used with energy harvesting is usually low energy/high efficiency systems and sensors drawing average currents of microamps.

### 2.4.2 Electro-mechanical Generator (Inductive Transducer)

The inductive transducers work on the principle of the magnetic induction of magnetic material. Just as the resistance of the electric conductor depends on the number of factors, the induction of the magnetic material depends on a number of variables, like the number of turns of the coil on the material, the size of the magnetic material, and the permeability of the flux path. In the inductive transducers the magnetic materials are used in the flux path and there are usually one or more air gaps. The change in the air gap also results in change in the inductance of the circuit and in most of the inductive transducers it is used to make the instrument function. There are two common types of inductive transducers: Simple inductance and two-coil mutual inductance type. See figure 2.14. [25]

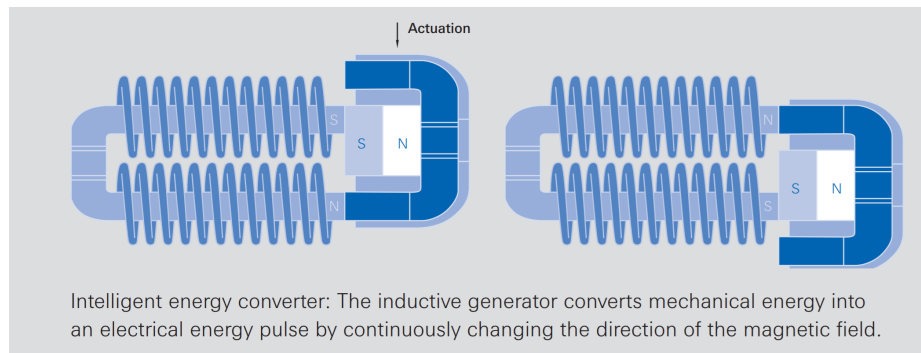


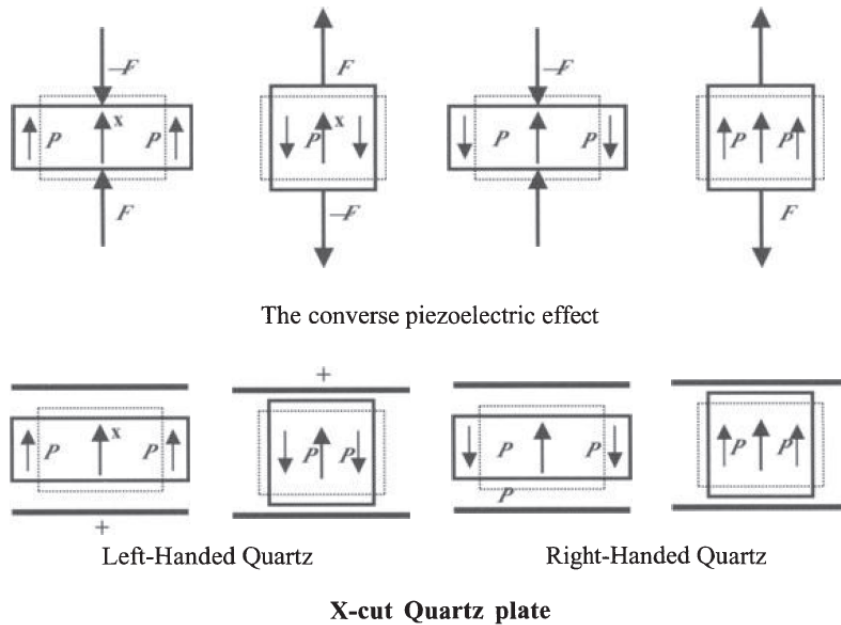
FIGURE 2.14: Inside the AFIG-0007s casing [50]

### 2.4.3 Piezoelectric Transducers

Piezoelectricity is understood as a linear electro-mechanical interaction between the mechanical and the electrical state in crystals without a center of symmetry. The direct piezoelectric effect is present when a mechanical deformation of the piezoelectric material produces a proportional change in the electric polarization of that material.

The piezoelectric effect can best be illustrated with a quartz plate cut normal to the crystallographic x-axis (X-quartz plate) as shown in figure 2.15. The acting force F deforms the quartz plate and produces through the piezoelectric effect its electric polarization P. In the converse piezoelectric effect the external electric field E between the electrodes induces the mechanical stress, which deforms the quartz plate.[19]

## The direct piezoelectric effect



### X-cut Quartz plate

In the conoscope, z-axis rings will *contract* when the eyepiece is rotated clockwise. In the polariscope, the analyzer must be rotated *countrerclockwise* to reestablish extinction.

In the conoscope, z-axis rings will *expand* when the eyepiece is rotated clockwise.  
In the polariscope, the analyzer must be rotated *clockwise* to reestablish extinction.

FIGURE 2.15: Schematic representation of the piezoelectric effect in an X-quartz plate. The polarities indicated follow IEEE Standards on Piezoelectricity [19].

## 2.5 Rectifier Topologies

Converting AC to DC is important when you have a system that uses components and circuitry designed for DC when you get the energy from an AC source. There is a variety of ways to do the conversion, and some of these solutions will be listed in the following section to highlight the importance of a proper way to rectify the source for optimal performance.

To get the energy pulse to last as long as possible, different options for an efficient circuit which prolonged the energy pulse long enough to power the nRF52 for the desired amount of time had to be considered. As the generator outputs two pulses, one positive and one negative, it seemed necessary to have a circuit where both pulses would be utilized to maximize the pulse duration, preferably converting the negative pulse to a positive one by means of a full-wave bridge rectifier or a full-wave voltage doubler. The difference between a half-wave and a full-wave pulse is illustrated in figure 2.16.

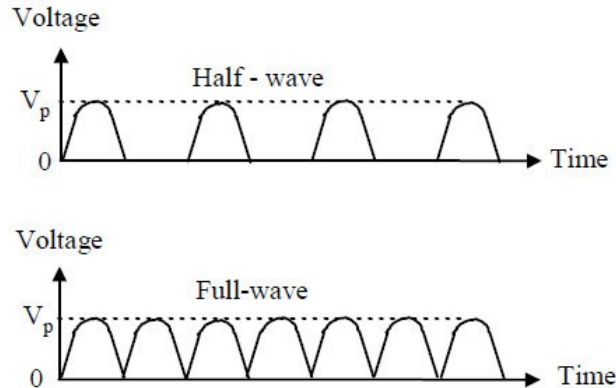


FIGURE 2.16: Comparison between half- and full-wave rectification [20]

### 2.5.1 Half-wave Bridge Rectifier

A half-wave bridge rectifier uses only the positive cycle of an AC input. The construct usually consisting of a single diode next to the source that controls the direction of the current. Even though this type of rectifier does its job to turn AC to DC, its highly inefficient as more than half the energy applied is lost. That includes 100% of negative pulses and whatever the forward voltage is on a given diode.

### 2.5.2 Full-wave Bridge Rectifier

A full-wave bridge rectifier uses both half cycles of an AC input and converts them to a DC output. This allows for a stable DC output when applying an AC voltage. This circuit basically consists of four diodes put together in such a way that both AC pulses output to the same point, alternating on being the output pulse. In figure 2.17 the diode configuration of a full-wave bridge rectifier is displayed.

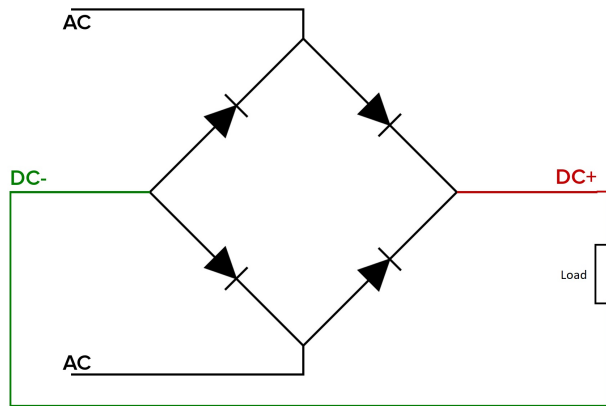


FIGURE 2.17: Full-wave bridge rectifier [16]

### 2.5.3 Voltage Multipliers

A voltage multiplier is a special type of diode rectifier circuit, which can produce an output voltage many times greater than the input, using diodes and capacitors. A half-wave voltage doubler is the simplest voltage multiplier circuit there is. In figure 2.18, the half-wave voltage doubler uses the positive half cycle of an AC input and applying it to capacitor C1, charging it up. When the negative AC cycle comes, the capacitor discharges itself, thus doubling the voltage through diode D1 compared to the source. A full-wave voltage doubler uses both pulses of a sinusoidal voltage to charge up two capacitors and double the AC input voltage, giving a DC output voltage that is effectively twice as big. See figure 2.18 for an illustration of a full-wave voltage doubler. Voltage multipliers that go higher builds on the same premise as the voltage doublers, adding more diodes and capacitors for each multiplier. [47]

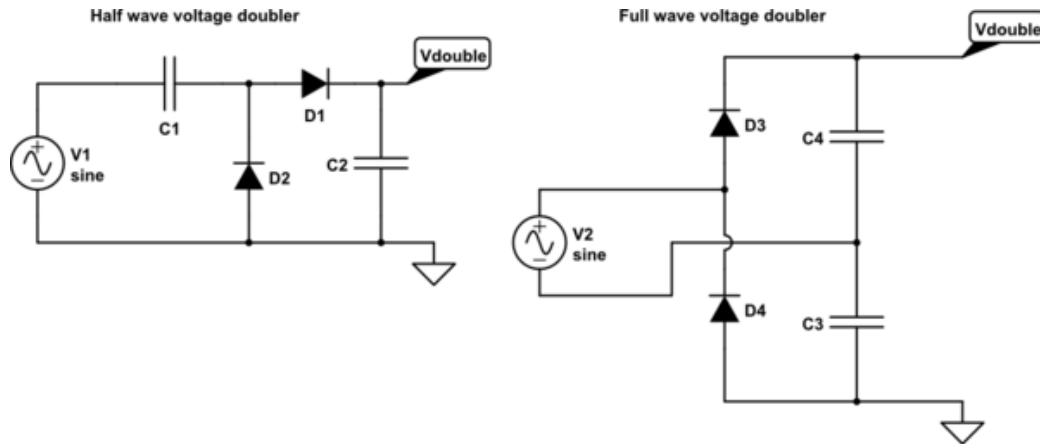


FIGURE 2.18: Schematics for both a half-wave and a full-wave voltage doubler [49]

### 2.5.4 Active Rectification (Synchronous Rectification)

The theory on synchronous rectification will be brief and only cover the absolute basics, as it is not used in the project, but thought of as a discussion piece for further work.

A synchronous rectifier is an electronic switch that improves power conversion efficiency by placing a low-resistance conduction path across the diode rectifier in a switched-mode regulator, and improves the efficiency of switched-mode power supplies, particularly in low-voltage low-power applications.

Synchronous rectification can increase the efficiency of a buck converter by replacing the Schottky diode with a low-side NMOS as illustrated in figure 2.19. The resulting voltage drop across the MOSFET is smaller than the forward voltage drop of the Schottky diode[1].

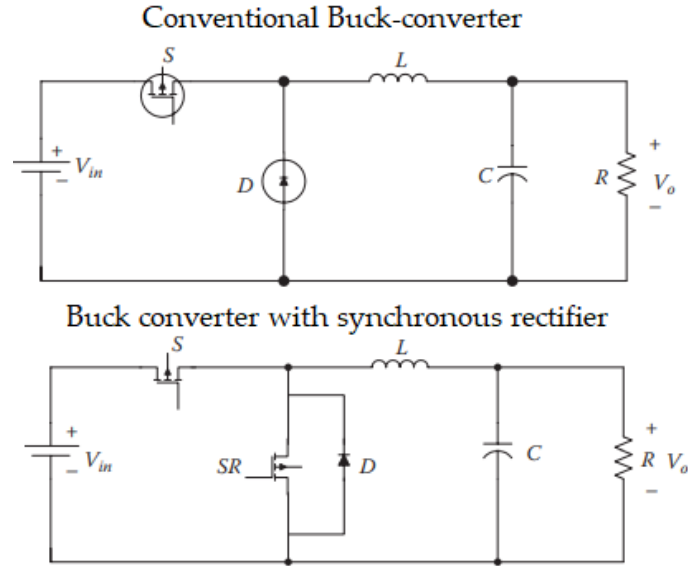


FIGURE 2.19: The difference between a normal step-down converter and a synchronous step-down converter.[1].

## 2.6 Voltage Regulators

This section will shed some light on the theory behind the regulators considered using in this project.

### 2.6.1 Buck Converters

A Buck converter, or step-down converter, is typically used in SMPS circuits where the DC output voltage has to be lower than the DC input. It is particularly useful where there is no need for electrical isolation between the switching circuit and the output. The buck converter consists of a switching transistor, a flywheel circuit, and a rectifier and reservoir capacitor. In figure 2.20 a buck converters components and its DC output graph is displayed. The transistor switches between high and low, creating a pulse that the flywheel circuit converts to a continuous DC output using the energy stored in inductor L1 for regulation. [3]

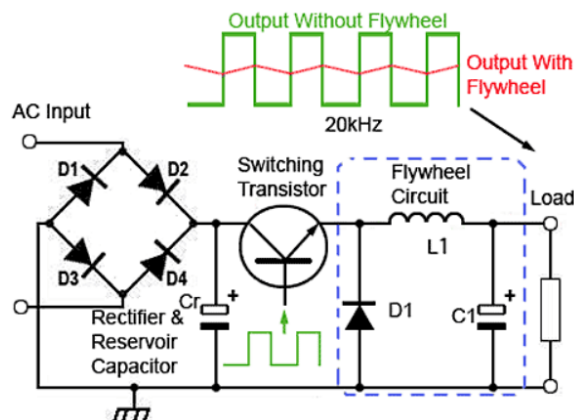


FIGURE 2.20: A full-wave bridge rectifier supplying a buck-converter with power and an illustration of the output over a load. [3]

### LTC3588-1

The LTC3588-1 is an IC designed for voltage regulating in energy harvesting circuits. It consists of a low-loss full-wave bridge rectifier and a highly efficient buck converter, see figure 2.21 for a complete look at the IC's components. These components forming a solution optimized for high output impedance energy sources like piezoelectric elements. An ultralow quiescent current undervoltage lockout mode with a wide hysteresis window allows charge to accumulate on an input capacitor until the buck converter can efficiently output the appropriate amount of stored energy. Pin selectable output voltages are also available on the D0 and D1 pins with four options, 1.8V, 2.5V, 3.3V and 3.6V, each with up to 100mA of continuous output current [46].

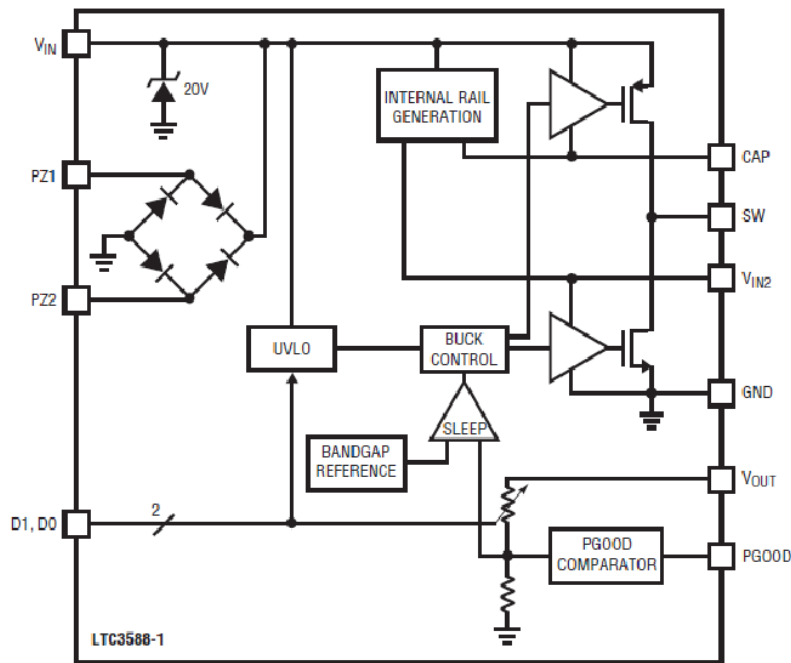


FIGURE 2.21: Block diagram of the LTC3588-1 [46]

### 2.6.2 Buck-boost Converters

A buck-boost converter is a type of switched mode power supply that combines the principles of the buck and boost converters into a single circuit. By combining the two regulator designs it is possible to have a regulator circuit that can cope with a wide range of input voltages both higher and lower than what is needed by the circuit. As both converters initially use similar components they just have to be re-arranged depending on the level of the input voltage. This is usually done by a manual switch, or a control unit that senses the level of input voltage, and then selects the appropriate circuit configuration. [2]

### 2.6.3 Linear Voltage Regulators

Linear voltage regulators use a closed feedback loop to bias a pass element to maintain constant voltage across output terminals. In practice, linear voltage regulators are step-down converters, meaning that the output voltage will always be lower than the input. In linear voltage regulators, there are a minimum voltage difference between  $V_{IN}$  and  $V_{OUT}$ , called the drop-out voltage. If the  $V_{OUT} > V_{IN} - V_{DROPOUT}$ , the linear voltage regulator can not regulate the output voltage to the desired level. The excess energy from the regulation process is wasted as heat, which in turn increases the regulators temperature. [24]

## 2.7 3D Printing

3D printing or additive manufacturing is a process of making three dimensional solid objects from a digital file. The creation of a 3D printed object is achieved using what is called an additive process. In an additive process an object is created by laying down successive layers of material until the object is created. Each of these layers can be seen as a thinly sliced horizontal cross-section of the eventual object. 3D printing is the opposite of subtractive manufacturing which is cutting out / hollowing out a piece of metal or plastic with for instance a milling machine.

3D printing enables you to produce complex (functional) shapes using less material than traditional manufacturing methods. [48]

- Clearance is important when designing mechanical parts for 3D printing.
- Parts have to be cleaned properly, and there must be space for this when printing designs with enclosed areas.
- Two surfaces (printed in the same orientation) that rub against each other cause more friction than one would expect due to the layer-wise production in 3D printing. This is called "hooking".
- Paint changes the mechanical properties of a 3D printed model.
- Manual correction of models with different tools is possible, but a cumbersome process.

This list is acquired from this [8] article on 3D printing.

## 2.8 PCB Design

A PCB is a multi-layered board that both mechanically supports and electrically connects a circuit. A PCB mainly consists of an isolating substrate, usually FR-4 (fiberglass), to make the board rigid and durable. Over the substrate, a thin layer of copper is laminated to the board, usually on both sides, as most PCBs today are double sided. On more advanced circuits the number of copper layers often go up to 16, and in certain instances, even higher. Above the copper there is the solder mask layer, which gives most PCBs their infamous green color. The solder mask layers main function is to insulate the copper traces from unintended contact with other conductive materials. It also makes soldering much easier, as solder sticks to the copper pads easier than to the solder mask. The outermost layer is the silkscreen layer, which is where letters and symbols usually are added to make it easier for people to see what components go where on the board. Figure 2.22 shows how a basic PCB is built up. [31]

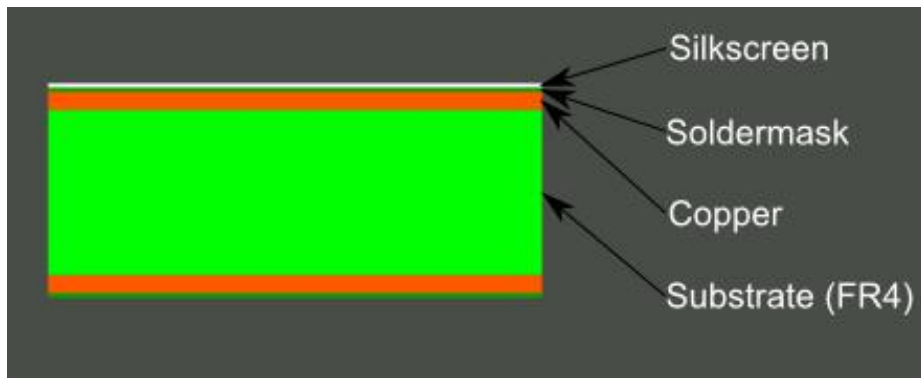


FIGURE 2.22: Basic PCB layers [5]

## Chapter 3

# Choice of Components and Equipment

This chapter will describe what components, tools and equipment were used during the project. Why all circuit components were chosen over other alternatives will also be thoroughly explained.

### 3.1 Tools and Equipment

TABLE 3.1: Tools and equipment necessary for this project

Necessary Tool	Used in This Project
3D modelling software	Fusion 360
3D Printer	Sketchup Free Ultimaker 2 Go Ultimaker Extended 2+
Application interface for the PPK	nRF Connect power profiler
BLE event current analyzer	Online power profiler
Data processing visualizer	LABview and Microsoft Excel
DC power analyzer	Keysight 1458A
IDE	Segger Embedded Studios
Impedance matching tool	Saturn PCB Design Toolkit
Multimeter	Fluke 289
Network protocol analyzer	Wireshark
Oscilloscope	Agilent InfiniiVision DSO-X 3102A oscilloscope
BLE packet sniffer	nrf-ble-sniffer-osx
PCB designer tool	Altium Designer 18
Power supply	Gwinstek GPD-3303S
Simulation tool for circuits	LTspice
Software development platform	GitHub
Soldering station	Tenma Soldering station Weller Soldering station Xytronic LF-389D
Tool for BLE communication	nrf Connect mobile application

## 3.2 System on a Chip

And seeing as this assignment was proposed by Nordic Semiconductor. It was clear that the assignment was meant to highlight their flagship SoC, the nRF52, and its power efficiency. Seeing as Nordic Semiconductor were able to provide nRF52s and nRF52DKs for free during this project, there was no reason to look at other options.

### 3.2.1 nRF52832

The nRF52 is a powerful, highly flexible ultra-low power multiprotocol SoC ideally suited for Bluetooth Low Energy, ANT and 2.4GHz ultra low-power wireless applications. The nRF52 SoC is built around a 32-bit ARM Cortex-M4F CPU with 512kB flash storage + 64kB RAM. The embedded 2.4GHz transceiver supports Bluetooth Low Energy, ANT and proprietary 2.4 GHz protocol stack [29]. The nRF52 being more than energy efficient enough to implement into this kind of circuit, it was an optimal SoC to use in this project.

#### nRF52 Clock Control

The SoftDevice uses a LFCLK to perform protocol timing and a HFCLK for main operations such as radio and CPU usage.

##### Low-frequency Clock Options

- Internal 32.768 kHz crystal oscillator (LFXO) controlled by an external 32.768 kHz crystal
- 32.768 kHz internal oscillator (LFRC)
- 32.768 kHz oscillator (LFSYNT) synthesised from the internal 64 MHz clock.

##### High-frequency Clock Options

- 64 MHz crystal oscillator controlled by an external 32 MHz crystal
- 64 MHz internal RC oscillator

#### nRF52 Internal Voltage Regulating

The nRF52 supports two internal power regulator alternatives, an LDO regulator and a DC/DC regulator. For regulator setup see figure 3.1.

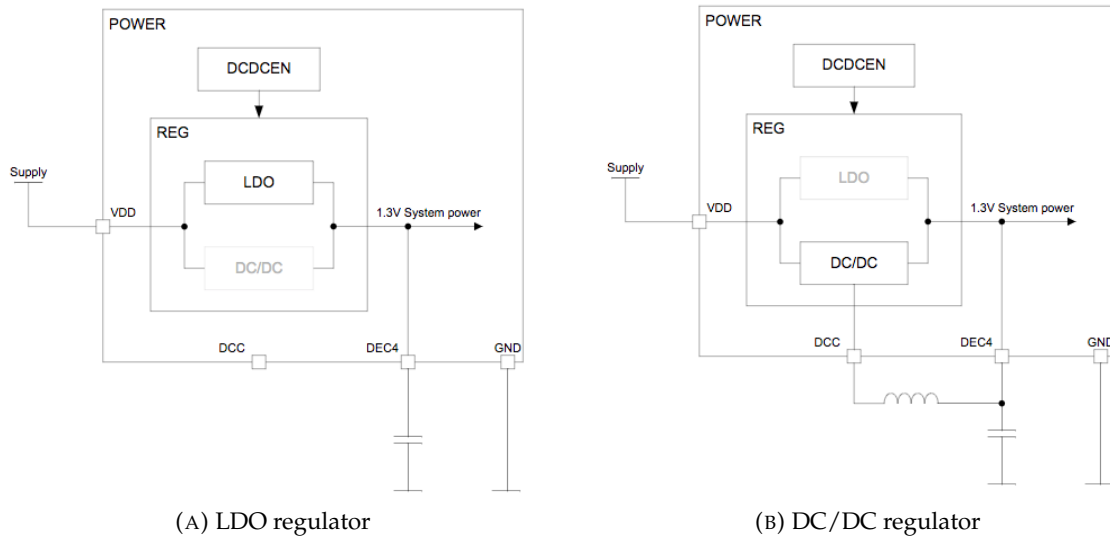


FIGURE 3.1: nRF52 internal regulator setup [34]

### 3.3 Generators

In the assignment text a piezoelectric element was proposed as the generator for the circuit, but as this was a mere proposal and not a requirement, other generator options had to be considered as well. One of the more prominent generators was shown during one of the first meetings with the supervisors. This was the electro-mechanical generator from ZF Electronics which was favoured due to its rigid and durable design, as piezoelectric elements proved to be too fragile to have the longevity planned for a finished stop button.

### 3.3.1 Piezoelectric Elements

Piezoelectric elements are widely used in a variety of energy harvesting technology, as their ability to convert mechanical stress applied to them into an electric charge makes it possible to store and output energy without the need of batteries or any other external power source. The elements are most reliable when exposed to vibrations and other sources of varying mechanical stress.

As the assignment proposed using a piezoelectric element, this was the initial choice of generator, but measurements showed that pressing the piezoelectric element like a button gave varying results depending on how hard and quickly one pressed. This, in conjunction with piezoelectric elements also being susceptible to vibrations that will likely occur while on a bus, made this option less appealing.

### 3.3.2 Electro-mechanical Generators

The ZF Electronics electro-mechanical generator harvests mechanical energy from an inductive generator, changing direction of its magnetic field when pushed, and converting it into an electrical energy pulse. See figure 2.14.

This generator, having a long maintenance-free mechanical life, capable of withstanding more than one million pushes, seemed like a reliable solution right out of the gate. Measurements on an oscilloscope proved to be very stable as well, further backing the decision to choose this generator. Ref. appendix B.



FIGURE 3.2: ZF Electronics energy harvesting generator [12]

## 3.4 Voltage Regulators

As the nRF52 can not handle more than its absolute maximum supply voltage of 3.9V, a reliable and efficient voltage regulator was needed to convert the high voltages provided by the chosen generator down to a voltage the nRF52 could handle. The regulator also had to be able to withstand voltages up to 20V, as this is how much the generator is able to output. Having a high voltage needed to be regulated down meant a boost-converter was out of the question, which is why it is not mentioned in this section.

### 3.4.1 LDO Regulators

An LDO regulator is a linear voltage regulator able to regulate output voltages very close to its supply voltage. This seemed like a viable option before any measurements were made, but as the supply voltage was likely to be up to 20V at maximum, none of the LDO regulators considered could handle it without having a rectifier circuit to lower the voltage applied to them, which was thought to cause too much of a voltage loss in conjunction with the fact that linear voltage regulators are inherently inefficient.

#### LDO Regulators Considered

- MP20043
- RT9032

### 3.4.2 Buck Converters

The reason no other buck converters are mentioned by name in this subsection, is that no other buck converters found while scouring various electronics websites had all the features that the LTC3588-1 had.

#### LTC3588-1

Linear Technologies had a variety of relevant regulators, and many of them were considered, but none stood out like the LTC3588-1, as it was the only circuit with a voltage operating range that seemed tailored for this exact project, being between 2.7V and 20V, which meant it could theoretically handle the generators supply voltage without having any components in between, which again meant minimal voltage loss. Another feature that the LTC3588-1 has, is that it has a hysteresis on the input, which gives it the ability to run all the way down to its absolute minimum input voltage while still giving a stable

output voltage. As the goal was to have a stable DC output for as long as possible the trade-off of having hysteresis seemed irrelevant, because the generator used will provide a high voltage that decreases over time. The LTC3588-1s output voltages are within the parameters of what the nRF52 can handle, which alongside its other capabilities made the LTC3588-1 a suitable option for this particular project.

### 3.4.3 Buck-boost Converters

A buck-boost converter seemed like a good choice for this project, as the potential to have a stable output voltage despite the input voltage being a pulse seemed promising. But after the first measurements were done of what the generators pulse would look like, the amount of time the "boost" element of the converter was needed was too low to justify having a buck-boost converter as the efficiency loss would be too significant.

## 3.5 Circuit Components

This section explains all minor components and ideas used in the energy harvesting circuit throughout the project.

### 3.5.1 Rectifiers

When looking at rectifiers, two archetypes were researched, these being bridge rectifiers and voltage multipliers. The main reason no other rectifier topologies were properly researched and tested, was due to the fact that the literature and previous similar projects did not mention any other topologies working very well with energy harvesting. The half-wave versions of both the bridge rectifier and the voltage multiplier was briefly tested, but as none of them use the negative pulse from the input voltage, they were not efficient enough to use as it was apparent early on that half of a button push would not suffice.

#### Full-wave Bridge Rectifier

Seeing as the bridge rectifier is such a safe way of rectifying an AC signal into a constant DC signal using both negative and positive pulses, this seemed like a good solution. Using it in conjunction with a capacitor for energy storage seemed very promising indeed. One thing to have in mind though, is that the voltage loss is bigger the more separate components in a circuit. In the end this circuit showed too ineffective to use in the final product.

#### Full-wave Voltage Multiplier

The full-wave voltage doubler circuit particularly was researched and tested thoroughly during this project. As the required voltages were met, there was no point in multiplying the voltage any higher than what a voltage doubler did. This seemed like a relevant circuit to go forth with, as several other energy harvesting circuits also opt for a voltage doubler. The voltage doubler was ultimately chosen due to its capability of outputting the desired voltage without too much loss and it being an affordable option.

### 3.5.2 Capacitors, Inductors and Diodes

#### Capacitors

As the vision was to have a small circuit, the initial idea was to have nothing but surface mounted capacitors. For the nRF52 reference design all capacitor sizes were either 0603 or 0402, and all values were predetermined. As for the capacitors needed in the LTC3588-1 circuit the values needed were first tested in simulations using LTspice, to find the theoretically best values. When a working circuit were up and running, tests with various capacitor values were made to ensure that the simulated results were correct. The values ultimately used can be seen in figure 3.3.

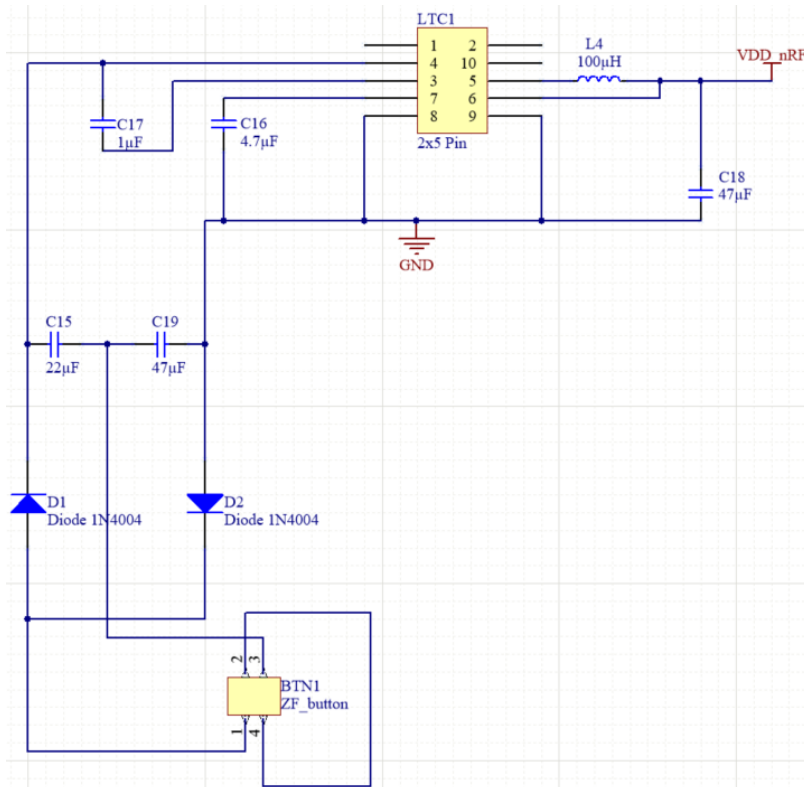


FIGURE 3.3: Schematics that show the most efficient capacitor and inductor values for the LTC3588-1 and its voltage doubler

Having two solutions, both containing the voltage doubler circuit, with one connected directly to the nRF52, and one connected to the LTC3588-1s pin 4 ( $V_{in}$ ). The instance where the connection is directly between the rectifier circuit and the nRF52, the capacitors had to be large enough to keep the voltage under the maximum voltage input for the nRF52, which is 3.9V absolute maximum. The process to find the correct capacitors where done mainly through trial and error. This is described better in section 4.2.2. What ultimately gave the best results is shown in figure 3.4.

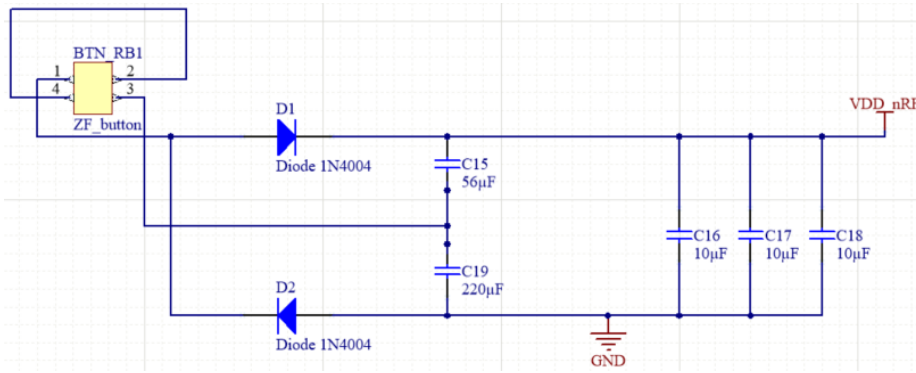


FIGURE 3.4: Schematics that show the most efficient capacitor values for the voltage doubler circuit

## Inductors

Seeing as the inductors used in the nRF52 reference design and the antenna are already optimized, the only inductor value necessary to find was the one used in the LTC3588-1s reference design. Its datasheet [46] suggests using either  $10\mu\text{H}$  or  $100\mu\text{H}$  for the inductor. The datasheet says  $100\mu\text{H}$  is the most efficient inductor value for the output voltages 1.8V and 2.5V. The efficiency was also tested in practice with an additional inductor value of  $22\mu\text{H}$ , just to be thorough. Yet no surprises occurred as the  $100\mu\text{H}$  inductor was the more efficient option, and the  $22\mu\text{H}$  inductor was very similar in efficiency to the  $10\mu\text{H}$  inductor. The inductor used is shown in the schematics in figure 3.3.

## Diodes

The diodes used in the voltage doubler circuit are schottky barrier diodes with the package format DB3X209K0L. They use the footprint type SOT23-N. Although this footprint has three pads only pin 1 and 3 are to be connected. These diodes were chosen because of their voltage rating (20V reverse voltage, and 0.3V forward voltage) that were perfect for the buttons output characteristics, and that they have the least voltage loss of all surface mounted diodes found. The only real trade-off being the package, which takes up a bit extra space with the extra pad. But with the components being as small as they are, they seemed reasonable to use. The diodes datasheet can be found at [30]

### 3.5.3 Antenna

Having limited experience with antenna theory, the supervisors recommended choosing a chip antenna from the company Johanson Techonology. Using their antenna selection guide [45] it was easy finding the optimal antenna. Their ultra-low profile corner mount chip antenna, 2450AT18A100, was ultimately chosen.

As any other antenna, the 2450AT18A100 set some criteria to the PCB design to make it to work properly. To work optimally the antenna needs certain areas and spaces around it to reduce noise. It needs two inductors and a capacitor to get tuned correctly, and lastly the feed line that is connected from the nRF52 to the antenna must be impedance matched to  $50\Omega$ . [45]



## Chapter 4

# Method

Having answered what theory and key components are relevant for this project, this chapter will explain how the project as a whole was executed. All work that is done, and how that work was carried out, is described in detail throughout the chapter.

### 4.1 Firmware

This section enlightens the different processes explored during firmware development. A substantial amount of time of the project has consisted of troubleshooting, testing and measuring the nRF52 system, optimizing its parameters and specifications as much as possible within the given time frame.

#### 4.1.1 Preliminary Phase

To get a brief but necessary understanding of Nordic Semiconductors system and programming of BLE applications in general, the first period of this project was entirely focused on researching BLE and practising code development. This was done via tutorials and forum posts mostly provided by Nordic Semiconductor and some by reading different scientific articles about BLE and the ramifications the BLE specification sets. In addition, an annual course held by Nordic Semiconductor at NTNU was attended. This course provided in-depth information about their system that accelerated the learning process. The two most important factors regarding developing the actual application firmware, was code efficiency and that the end product would fit the BLE specification. The actual firmware development was in small parts done during the preliminary phase but was not entirely focused on until Nordic Semiconductors available application code and API could be addressed with confidence. All firmware development was done using Nordic Semiconductors preferred IDE, Segger Embedded Studios [27].

#### 4.1.2 Firmware Development

This section highlights the most important code additions and alterations in the overall system. For a complete and functional firmware code for all three devices, go to [EHSB GitHub](#).

## Stop Button

In Nordic Semiconductors SDK different example applications are provided, with the `ble_app_beacon` example resembling the desired stop button application the most. The `ble_app_beacon` example is a non-connectable broadcasting application that advertises a 128-bit UUID alongside manufacturer specific data such as device type, company identifier, reference RSSI at one meter, and major/minor values used to identify different beacons. Ref. appendix (E). The first step towards an energy efficient application was to remove all unnecessary elements advertised by the application, thus making the advertising packet smaller. All other elements except the 128-bit UUID and a mandatory advertising flag defined by GAP, required by the BLE specification, was removed. Ref. appendix (E). The reason why the 128-bit UUID was kept, is because the central needs to identify the stop button in order for it to set the stop signal. Using a 128-bit UUID also serves the purpose of redundancy since it is close to impossible that two 128-bit UUIDs collide. Only stop button UUIDs whitelisted by the central will set the stop signal.

The initial code removal reduced the TX payload from 30 to 21 bytes, as shown in figure 4.1. The data was accessed using Nordic Semiconductors mobile application nRF Connect. The nRF Connect essentially turns any smartphone into a BLE central, allowing it to scan, connect and interact with BLE peripheral devices.

Raw data:		
0x0201041AFF59000215011223344556 6778899AABBCCDDEEFF001020304C3		

Details:		
LEN.	TYPE	VALUE
2	0x01	0x04
26	0xFF	0x590002150112233445566778899AABBCCDDEEFF001020304C3

LEN. - length of EIR packet (Type + Data) in bytes,  
TYPE - the data type as in <https://www.bluetooth.org/en-us/specification/assigned-numbers/generic-access-profile>

Raw data:		
0x02010411079FCADC240EE5A9E093F 3A3B50100406E		

Details:		
LEN.	TYPE	VALUE
2	0x01	0x04
17	0x07	0x9FCADC240EE5A9E093F3A3B50100406E

LEN. - length of EIR packet (Type + Data) in bytes,  
TYPE - the data type as in <https://www.bluetooth.org/en-us/specification/assigned-numbers/generic-access-profile>

OK

OK

(A) 30 bytes raw data/TX payload

(B) 21 bytes raw data/TX payload

FIGURE 4.1: One BLE packet before and after code reduction displayed in the nRF Connect application

BLE requires different advertising parameters defined by GAP. The relevant parameters used in the application is an advertising interval of 20ms and non-connectable undirected advertisement. Knowing that the device sleeps between advertising events, the lowest possible advertising interval for undirected advertisement was chosen, 20ms defined by GAP. Directed advertising can have a lower advertising interval but directed advertising does not carry any TX payload, which in this case is needed to carry a UUID. Even though sleeping consumes very little energy, approximately  $1.9\mu\text{A}$  [35] in system on mode, it is a waste of energy to have the stop button in sleep mode more than necessary. The advertising type tells the SoftDevice that no device can connect to the stop button and that the advertisement is undirected. This setting also saves energy because the SoC does not have to listen for any packets from centrals, hence disabling the radio between advertising events.

In addition the `ble_app_beacon` example toggled an LED every second to indicate that the beacon was advertising. Since there was no need for advertising indication in the final application, and energy consumption was of great importance, both LED initialization and enabling was removed. The nRF52s logging module was also turned off because it is mainly used for debugging purposes and consumes additional energy. Application name `ehsb_nordic_b`

#### `ehsb_nordic_b` key parameters:

- Advertising interval: 20ms
- TX payload: 21 bytes
- TX power: 0dBm
- DC/DC regulator enabled

Even though the advertising interval is set to 20ms, the SoftDevice adds up to 10ms randomly between each event. This is to prevent collision between two devices advertising at the same time with the same interval or that advertising always occurs between scan windows when trying to connect to a central. See figure 4.2.

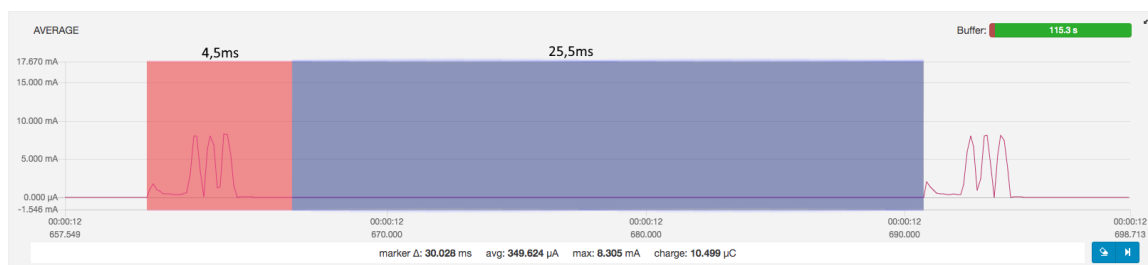


FIGURE 4.2: `ehsb_nordic_b` application BLE advertising event. The three current peaks in the red area is the nRF52 advertising on channels 37, 38 and 39.

The internal DC/DC regulator was enabled because of its low power consumption compared to the internal LDO regulator.

#### Relayer

The firmware code for the central and relayer were based on the UART examples `ble_app_uart_c` and `ble_app_uart` located in Nordic Semiconductors SDK. For more information about the Nordic UART Service, see reference [33].

When the relayer scans for advertising packets the SoftDevice generates an event called **BLE\_GAP\_EVT\_ADV\_REPORT**. This event is generated when a scan has been performed and data collected from the BLE advertising channels is available. With the relayer it was desired to forward all eligible UUIDs to the central. To do so a global variable called **adv\_rep\_uuid** was created. The **adv\_rep\_uuid** is an empty 8-bit, two dimensional array with 16 positions that exactly fits a 128-bit UUID. Ref. appendix D.

To check if one or more of the advertising packets carries an eligible UUID, an if statement was added under the **BLE\_GAP\_EVT\_ADV\_REPORT** in the BLE event handler. The BLE event handler handles events generated by the SoftDevice. Ref. appendix D.

The if statement checks two conditions. It checks if the advertising flag of each packet is BR/EDR not supported, 0x04 in position two and if the advertising packet carries a complete 128-bit UUID, 0x07 in position four. When both conditions are true the **adv\_rep\_uuid** variable gets overwritten with the UUID located in positions 5 through 16 in the advertising packet. When the overwrite has been performed a wireless UART string containing the **adv\_rep\_uuid** is sent to the central. Every time the **BLE\_GAP\_EVT\_ADV\_REPORT** event is generated the process will repeat itself. Ref. appendix D. For LED mapping see figure 4.3. Application name **ehsb\_nordic\_r**.

LED	Function
1	Toggles when advertising
2	Set when connected to central
3	Toggles when scanning
4	Not used

FIGURE 4.3: LED mapping relayer

## Central

On start-up the central will start scanning for peripherals, and if no stop buttons have been added to the system it will only react to advertising packets from the relayer. The two-dimensional array whitelist was created to store UUIDs of stop buttons added to the system by the user. Ref. appendix F. The fstorage library, delivered by Nordic Semiconductor, is utilized to write the whitelist to flash. On start-up an instance of fstorage is defined and initialized. Ref. appendix F.

When the central starts up, after initializing fstorage, it calls a function called **read\_flash** to check if any UUIDs have been saved to the flash memory, and retrieve them if that is the case. First, **read\_flash** gets a value indicating the next available slot in the whitelist, and saves it in an 8-bit unsigned integer called **uuid\_number**. The value of **uuid\_number** is then checked, and since an empty flash memory consists of only ones, it means that if **uuid\_number** equals to 255 no UUIDs have been stored in the flash memory, and **uuid\_number** is set to 0. For the case where the whitelist has been stored in the flash memory, a for-loop is used to read out as many UUIDs as indicated by **uuid\_number** and store them in the whitelist. Ref. appendix F.

Administration of the whitelist is done by using buttons, when buttons are either pushed or released the button handler function is called. Button number two is used for adding new UUIDs to the centrals whitelist. When it is pushed a timer indicating that the central

is waiting to receive a new UUID is started and a boolean variable `add_uuid` is set to true. Releasing the button stops the aforementioned timer and sets `add_uuid` to false, meaning that button two has to be held while a UUID is added to the whitelist. Erasing all added UUIDs from flash is done by holding button number three for four seconds. From button-press to flash-erase all LEDs on the central are toggled on and off every 250ms to indicate what is about to happen. Ref. appendix F.

When a user wants to add a new stop button UUID to the system, button two on the central must be held down while powering the stop button in question. While the button on the central is held `add_uuid` will be true and advertisement packets picked up by the central will be checked for crucial elements like RSSI (-35dBm), flag and UUID-type. This is to ensure that the UUID found is that of a stop button that belongs in the system. Then, if the UUID is not already present in the whitelist it is added and also written to flash. Ref. appendix F.

During normal operation the central will scan for advertisement packets and compare found UUIDs to the entries that are put in the whitelist by the user. Advertising flag and UUID-type are checked before comparing. This is to avoid going through the process for every advertisement packet, and thereby reducing workload on the central. When a registered stop button is found this is indicated by setting a GPIO pin connected to a stop sign. Ref. appendix F. For button layout and LED mapping see figure 4.4. Application name `ehsb_nordic_c`.

Button	Function	LED	Function
1	Reset stop signal	1	Toggles when scanning
2	Add new UUID to whitelist by RSSI	2	Set when observed UUID is in whitelist
3	Clear whitelist	3	Set when connected to relay
4	Not used	4	Set when relay has sent UUID that is in whitelist

FIGURE 4.4: Button layout and LED mapping central

## System Flow Chart

This section contains a flowchart illustrating the different processes happening in the central and relayer application. See figure 4.5.

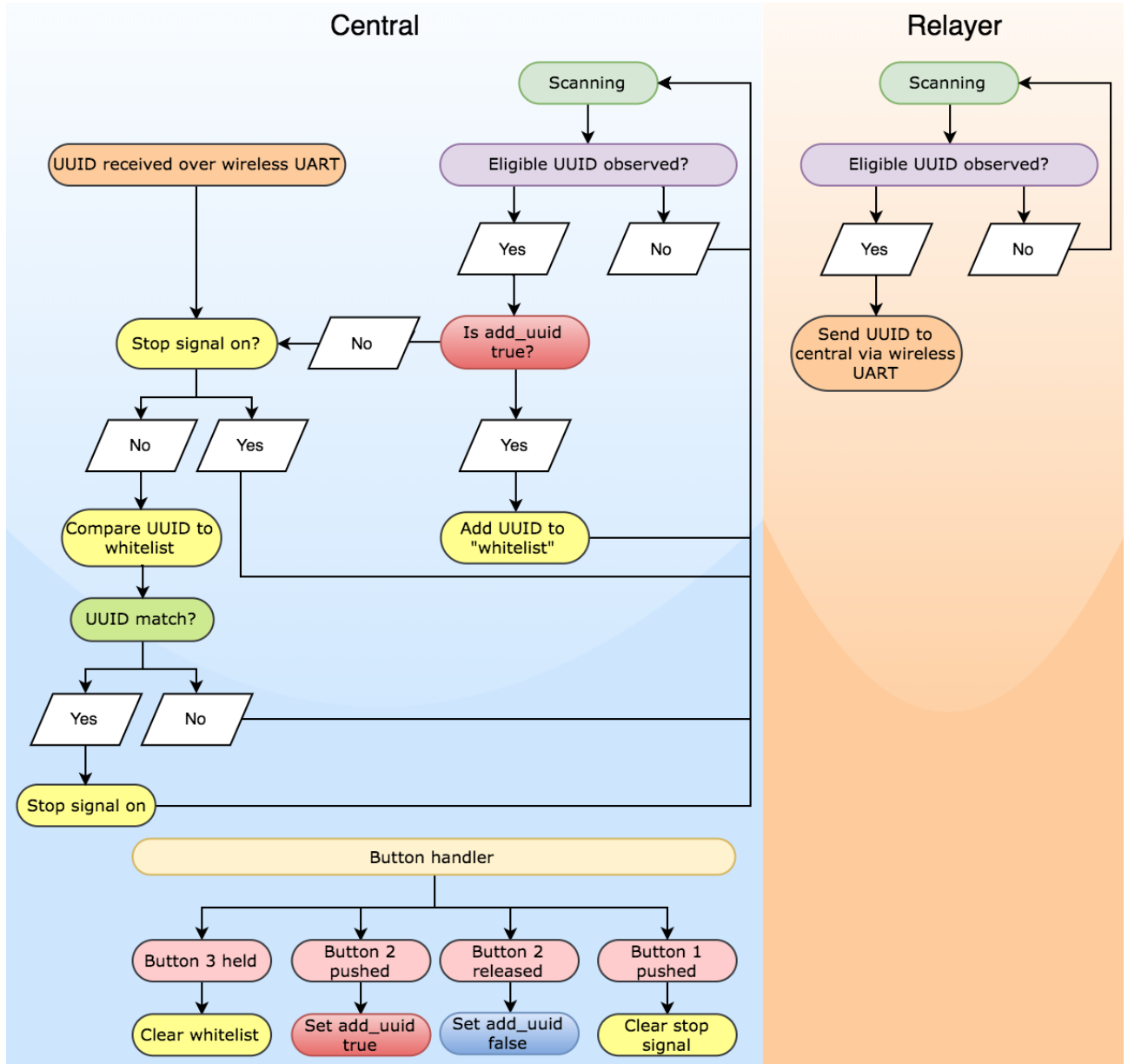


FIGURE 4.5: Flowchart central and relayer application code

### 4.1.3 Energy Consumption

The main goal was to send as many advertising packets as possible with the available energy. Therefore it was necessary to estimate the energy consumption of the stop button, which was heavily dependent on its application code, `ehsb_nordic_b`. The measurements were done with Nordic Semiconductors OPP [36] and PPK. The data generated by the PPK was accessed using Nordic Semiconductors nRF Connect power profiler computer software.

#### Test Bench

The PPK is designed to sit on top of the nRF52DK just like an Arduino shield framework measuring the average current of the nRF52. See figure 4.6 [37].

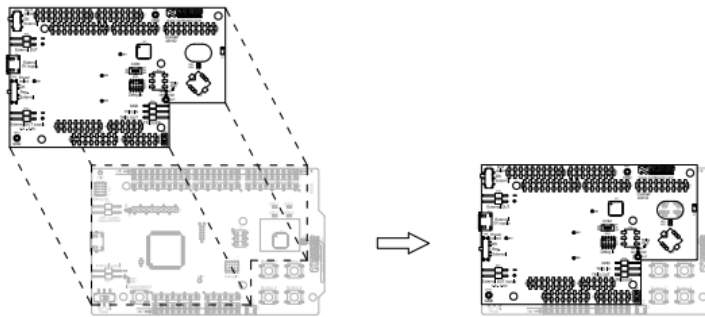


FIGURE 4.6: PPK mounting

To measure the average current on the nRF52DK, a simple modification had to be done. The solder bridge SB9 on the nRF52DK was cut setting pin 1 (VDD\_nRF) and pin 2 (VDD) on pin header P20 in series with the nRF52 on the nRF52DK. Ref. appendix C.1. The PPK uses these pins for current measurement. To measure as exact as possible the PPK user guide stated that the voltage had to match the nRF52DK voltage, measured at approximately 2.85V when supplied via USB. See figure 4.7. For PPK test setup, see figure 4.8.

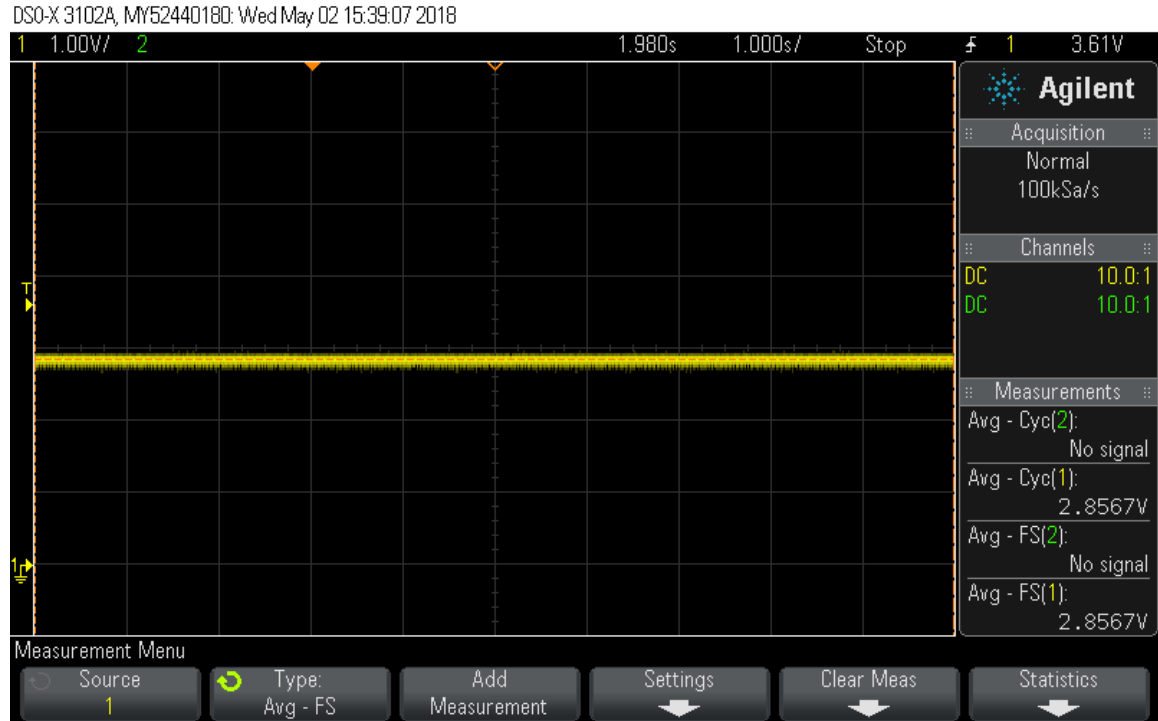


FIGURE 4.7: nRF52DK voltage with PPK mounted on top

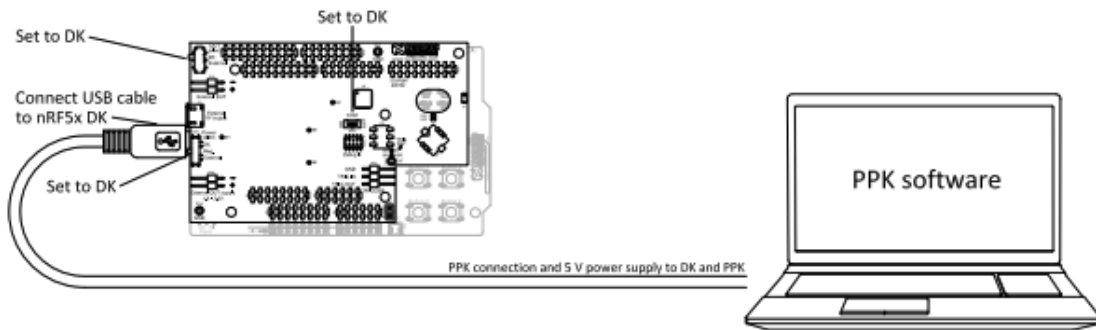


FIGURE 4.8: PPK test setup [37]

### Measurements and Generated Results

The [ehsb\\_nordic\\_b](#) application was measured with two different LFCLKs, LFXO and LFRC. Bear in mind that the OPP is only a general indication of expected energy consumption and does not apply to all applications. Measurements concerning the [ehsb\\_nordic\\_b](#) application were done with the PPK. See figure 4.9 for OPP generated results and figures 4.10, 4.11, 4.12 and 4.13 for PPK measurements.

Voltage	Time (ms)	Average current ( $\mu$ A)	Energy ( $\mu$ Ws)
1.8	25	713	32.1
1.9	25	684	32.5
2.0	25	661	33.1
2.1	25	640	36.6
2.2	25	621	34.2
2.3	25	603	34.7
2.4	25	586	35.2
2.5	25	570	35.6
2.6	25	555	36.1
2.7	25	542	36.6
2.8	25	530	37.1
2.85	25	524	37.3
2.9	25	519	37.6
3.0	25	508	38.1
3.1	25	497	38.5
3.2	25	585	38.8
3.3	25	478	39.4
3.4	25	471	40.0
3.5	25	465	40.7
3.6	25	460	41.4

FIGURE 4.9: OPP generated results across different voltage levels, one BLE event

Voltage	Time (ms)	Average current ( $\mu$ A)	Energy ( $\mu$ Ws)
2.85	511	69	100.5

FIGURE 4.10: PPK - LFXO - **startup + one BLE event**

Voltage	Time (ms)	Average current ( $\mu$ A)	Energy ( $\mu$ Ws)
2.85	32	1082	98.7

FIGURE 4.11: PPK - LFRC - **startup + one BLE event**

Voltage	Time (ms)	Average current ( $\mu$ A)	Energy ( $\mu$ Ws)
2.85	24	398	27.2

FIGURE 4.12: PPK - LFXO - **one BLE event**

Voltage	Time (ms)	Average current ( $\mu$ A)	Energy ( $\mu$ Ws)
2.85	24	395	27.0

FIGURE 4.13: PPK - LFRC - **one BLE event**

## Calculations

To calculate the energy consumption a basic formula for Watt-seconds was used. See equation (4.1).

$$\text{Energy} = \text{Ws} = U \times I \times s = 1.8\text{V} \times 713\mu\text{A} \times 25\text{ms} = \underline{\underline{32.1\mu\text{Ws}}} \quad (4.1)$$

The generated data from the OPP disclosed 1.8V as the voltage level with the lowest energy consumption. See figure 4.9. Since the `ehsb_nordic_b` application code could only be measured at 2.85V with the PPK, values for 1.8V had to be estimated based on the OPPs 2.85V to 1.8V percent difference. See equation (4.2).

$$\text{Percent difference } 2.85\text{V to } 1.8\text{V} = 100\% - \frac{32.1\mu\text{Ws} \times 100}{37.2\mu\text{Ws}} = \underline{\underline{14\%}} \quad (4.2)$$

The energy consumption of one BLE event is  $\approx 14\%$  more effective at 1.8V than 2.85V. This percent difference will later be used to calculate the energy consumption at 1.8V.

Start-up energy is the energy consumption before the first advertising event occurs. Therefore, the energy from one BLE event had to be subtracted from the (startup + one BLE event) energy measurements. This probably seems unnecessary, but was done because the nRF52 consumes additional energy during its first sleep cycle. See figure 4.14 and 4.15.

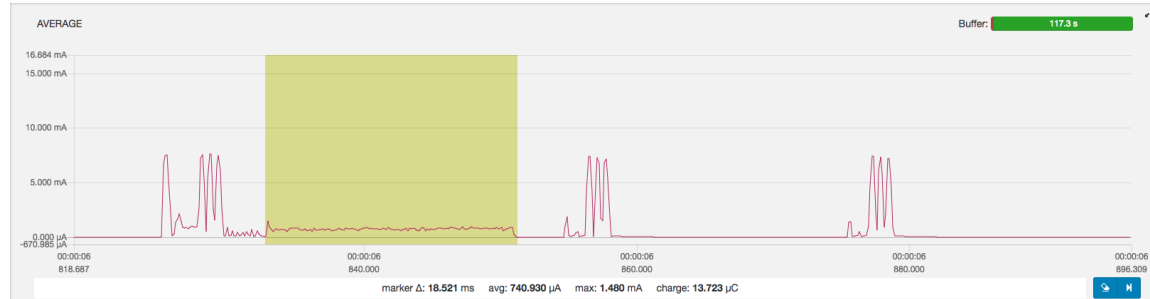


FIGURE 4.14: Startup LFXO at 2.85V

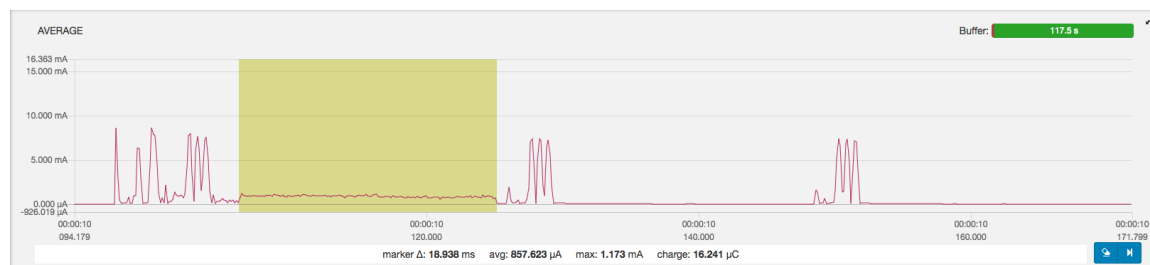


FIGURE 4.15: Startup LFRC at 2.85V

See figure 4.16 for a comparison of an RC calibration event at start-up and 0.5 seconds later when the LFRC calibration event is isolated from the start-up procedure. Figure 4.16 (A) displays the start-up of the nRF52 where the current consumption can be  $\approx 1.5\text{mA}$  over 20ms. Figure 4.16 (B) displays the energy consumption of an LFRC calibration event that is  $\approx 600\mu\text{A}$  over 10ms. Even though the LFRC takes up a good portion of the start-up energy, the rest of the energy consumption is an unknown factor.

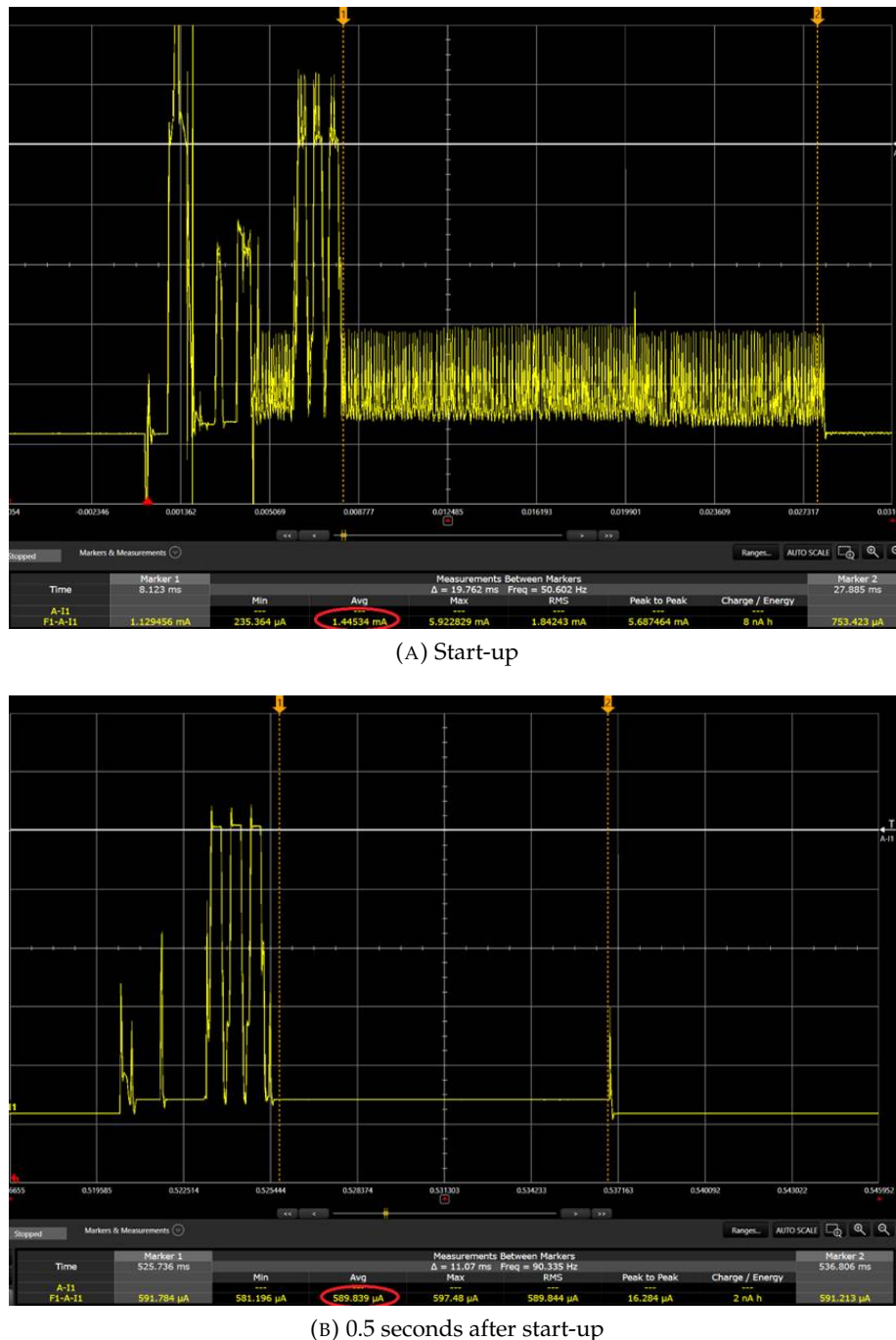


FIGURE 4.16: DC Power Analyzer measuring current consumption of an LFRC calibration event. The LFRC calibration takes place between the cursors in both figures.

**nRF52s Startup Energy Consumption. See equation (4.3) and (4.4).**

$$\text{Energy (LFXO, start-up, 2.85V)} = 100.5\mu\text{Ws} - 27.2\mu\text{Ws} = \underline{\underline{73.3\mu\text{Ws}}} \quad (4.3)$$

$$\text{Energy (LFRC, start-up, 2.85V)} = 98.7\mu\text{Ws} - 27.0\mu\text{Ws} = \underline{\underline{71.7\mu\text{Ws}}} \quad (4.4)$$

**Energy Consumption at 1.8V. See equations (4.5), (4.7), (4.6) and (4.8).**

$$\text{Energy (LFXO, start-up, 1.8V)} = 73.3\mu\text{Ws} \times 86\% = \underline{\underline{63.0\mu\text{Ws}}} \quad (4.5)$$

$$\text{Energy (LFRC, start-up, 1.8V)} = 71.7\mu\text{Ws} \times 86\% = \underline{\underline{61.7\mu\text{Ws}}} \quad (4.6)$$

$$\text{Energy (LFXO, event, 1.8V)} = 27.2\mu\text{Ws} \times 86\% = \underline{\underline{23.4\mu\text{Ws}}} \quad (4.7)$$

$$\text{Energy (LFRC, event, 1.8V)} = 27.0\mu\text{Ws} \times 86\% = \underline{\underline{23.2\mu\text{Ws}}} \quad (4.8)$$

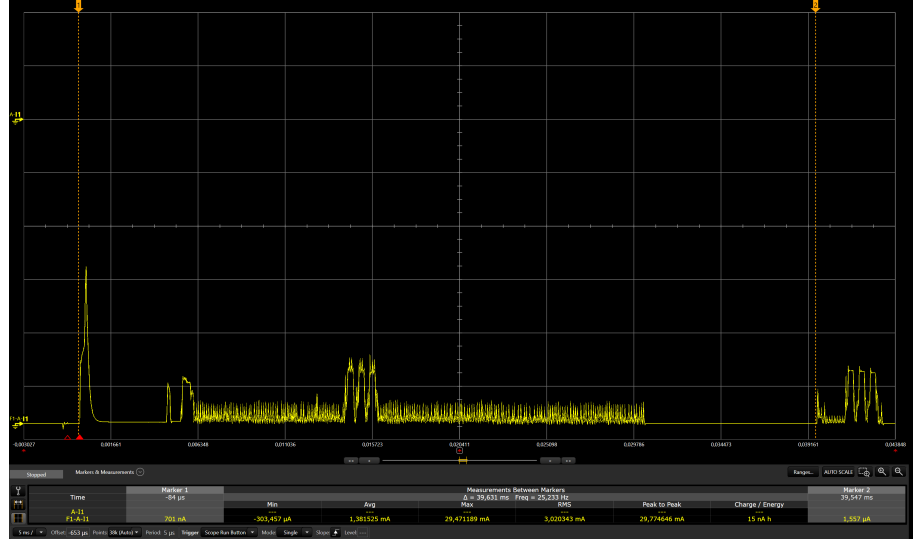
**Start-up Time in LFXO and LFRC. See equations (4.9) and (4.10).**

$$\text{Start-up time LFXO} = 511ms - 24ms = \underline{\underline{487ms}} \quad (4.9)$$

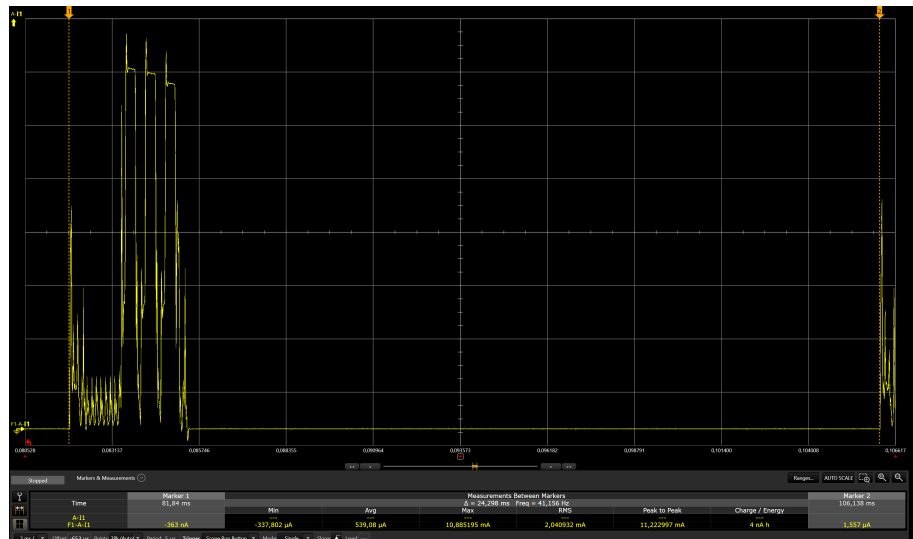
$$\text{Start-up time LFRC} = 32ms - 24ms = \underline{\underline{8ms}} \quad (4.10)$$

### PPK and DC power analyzer data comparison

To verify the measurements and calculations, a DC power analyzer was used to analyze the power consumption of the `ehsb_nordic_b` application at 1.8V with the LFRC clock enabled. See figure 4.17, and equations (4.11), (4.12) and (4.13).



(A) Start-up



(B) BLE event

FIGURE 4.17: DC Power Analyzer measuring current consumption on the nRF52 at 1.8V

$$\text{Energy (RC, event, 1.8V)} = 1.8V \times 24ms \times 539\mu A = \underline{\underline{23.3\mu Ws}} \quad (4.11)$$

$$\text{Energy (RC, start-up, 1.8V)} = 1.8V \times 40ms \times 1382\mu A - 23.3\mu Ws = \underline{\underline{76.2\mu Ws}} \quad (4.12)$$

$$\Delta T(\text{RC, start-up}) = 40ms - 24ms = \underline{\underline{16ms}} \quad (4.13)$$

In figure 4.18 data from the PPK and DC power analyzer is compared. The energy consumption is very much the same when it comes to the advertising cycle, but not in start-up time and energy consumption. As stated before all advertising events occur at a set time interval +(0-10ms) with the first advertising event occurring somewhere in the start-up procedure during the LFRC calibration. The randomized time interval explains the difference in start-up time as 8ms (PPK) and 16ms (DC power analyzer) are within 10ms of each other. See figure 4.19 and figure 4.20 for measurements of the additional energy consumption during the nRF52s start up procedure.

Method	Start-up energy	Start-up time	BLE event energy	BLE event time
DC analyzer	76.2 $\mu$ Ws	16ms	23.3 $\mu$ Ws	24ms
PPK	61.7 $\mu$ Ws	8ms	23.2 $\mu$ Ws	24ms

FIGURE 4.18: PPK and DC power analyzer data comparison

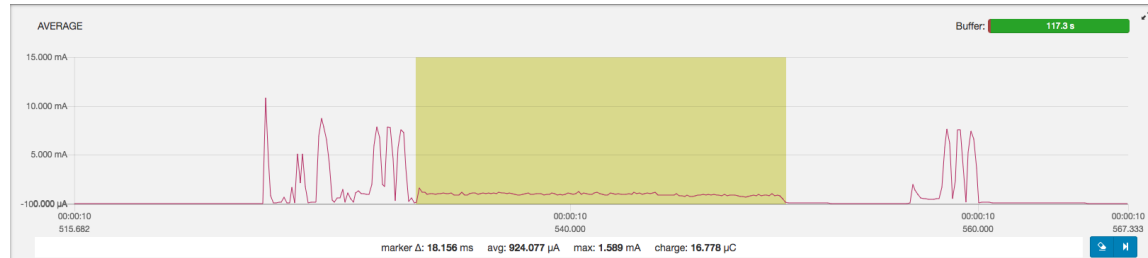


FIGURE 4.19: PPK measuring the additional current consumption

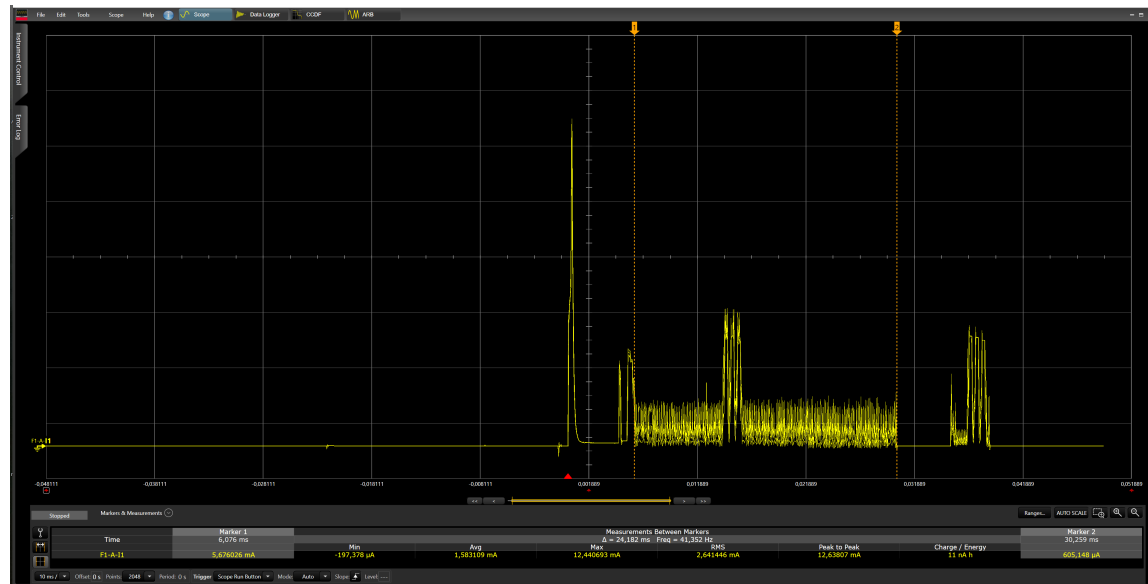


FIGURE 4.20: DC power analyzer measuring the additional current consumption

$$\text{Energy (PPK)} = 2.85V * 18.2ms \times 924\mu A \times 86\% = \underline{\underline{41.2\mu Ws}} \quad (4.14)$$

$$\text{Energy (DC analyzer)} = 1.8V \times (24.2ms \times 1.58mA - 1.9ms \times 6.8mA) = \underline{\underline{45.6\mu Ws}} \quad (4.15)$$

In equation (4.15) the energy consumption during the actual advertisement was subtracted from the total energy consumption in the marked period of time. This is to get an accurate comparison.

The additional energy consumptions were similar. An indication that the two measuring methods were performed similarly. It should be mentioned that the DC power analyzer is overall a more reliable tool that enables current measurements across different voltages on the nRF52DK, in contrast to the PPK that only can measure at DK voltages to get acceptable results. The downside with the DC power analyzer was that it was not available at all times since it was only available through the project supervisors at Nordic Semiconductor.

Considering measurements, calculations and comparisons it is safe to say that the LFRC clock source is the best option for the application. The most distinguishable difference between the two clock sources is start-up time where the LFRC is about half a second faster than the LFXO. This is because the LFXO relies on an external crystal that uses a fair amount of time to gain the accuracy needed for it to be used by the nRF52. See equations (4.9) and (4.10).

#### **DC/DC Regulator vs LDO Regulator, see equation (4.16) and (4.17)**

All of the measurements were performed with the internal DC/DC regulator enabled. This is because the LDO regulator is a lot less energy efficient than the DC/DC in the particular application at the desired voltage level. See equations (4.16) and (4.17).

$$\text{Energy(RC, event, 1.8V, LDO)} = 2.85 \times 26.9ms \times 568\mu A \times 0.86 = \underline{\underline{37.4\mu Ws}} \quad (4.16)$$

$$\text{Percent difference DCDC/LDO at } 1.8V = 100\% - \frac{23.2\mu Ws \times 100}{37.4\mu Ws} = \underline{\underline{38\%}} \quad (4.17)$$

In the case of the stop button application, the DC/DC regulator is approximately 38% more effective than the LDO regulator.

#### **Average resistance start-up + three events, see equation (4.18)**

$$R_{avg} = \frac{\frac{V^2}{W_{start-up}} + \frac{V^2}{W_{event}} \times 3}{4} = \frac{\frac{1.8V^2}{61.7\mu Ws} + \frac{1.8V^2}{23.2\mu Ws} \times 3}{4} \approx \underline{\underline{2620\Omega}} \quad (4.18)$$

The average nRF52 resistance value of start-up + three advertising events is used as an estimated load in the hardware simulations when characterizing the LTC3588-1, see section 4.3.2.

#### 4.1.4 Troubleshooting

When all the devices in the system had a complete and functional code running on nRF52DKs, it was important to stress test the system to uncover possible system bugs. The system test was performed on a regular transport bus ranging approximately 10 meters in length.

The `ehsb_beacon_b` application was temporary modified to advertise five events at three packets each. This was done to emulate the final stop button which was going to advertise a limited amount of packets. See figure 4.21 for PPK measurement of the modified `ehsb_nordic_b` application. Note that the LFXO clock source is used in the modified example, giving a longer start-up time than what is expected in the final stop button.

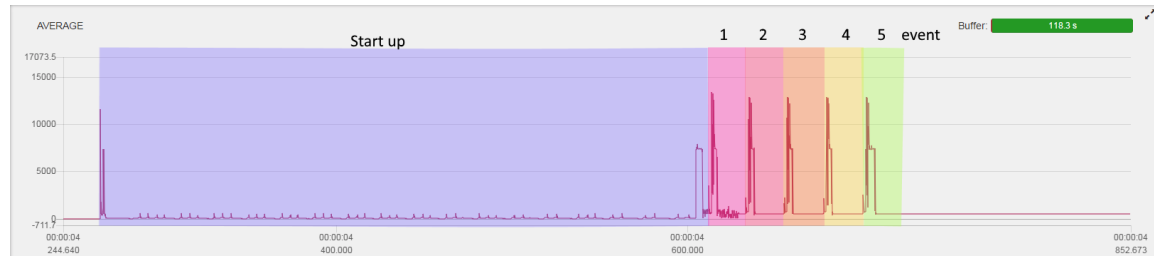


FIGURE 4.21: Stop button advertising 5 events, LFXO

**The following scan and connection parameters for the central and relay were used:**

- Scan interval: 70ms
- Scan window: 60ms
- Connection interval: 20ms to 75ms

By setting the scan parameters in each device to a 70ms scan interval and a 60ms scan window, a stop button advertising at 20ms advertising interval (5ms actual advertising and 20ms sleep in total 25ms per cycle) would be detected by both devices even when only two advertising events were sent. See figure 4.22 and 4.23.

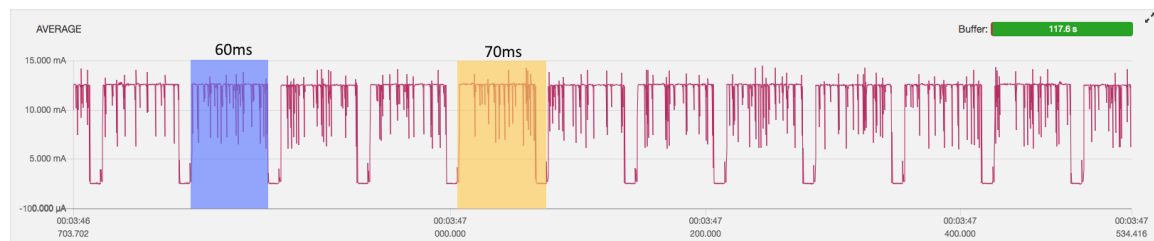


FIGURE 4.22: Current consumption of scanning central

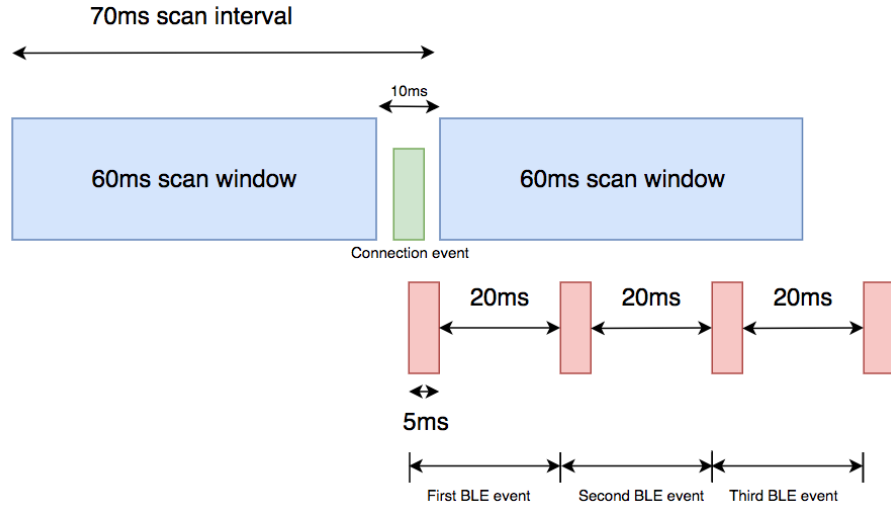


FIGURE 4.23: Scan parameters in relation to advertising and connection events

### System Test

The system was tested in two situations. See figure 4.24 and figure 4.25.

**Situation one** - The stop button was detected by the central 40 out of 40 times. 100% observation rate.



FIGURE 4.24: Central in front and stop button in back

**Situation two** - The stop button was detected by either the central or relayer 22 out of 30 times. 73% observation rate.

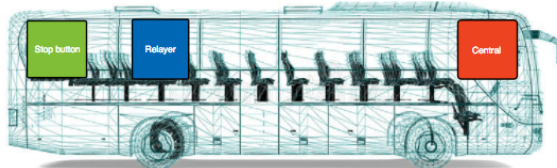


FIGURE 4.25: Central in front, relayer in back/middle and stop button in back

In situation one the stop button was observed by the central 100% of the times. In situation two the observation rate dropped drastically, to 73%. Considering the results it was safe to say to say that the communication between the central and relayer was not optimal. Further analysis with the PPK uncovered what was happening in the two devices. See figure 4.26.



FIGURE 4.26: Relayer current consumption when scanning and communicating with the central.

The PPK measurement showed the relayer having a very inconsistent scan/connection plan, sleeping for the majority of the time. Both devices should be alternating between scan and connection events, and sleep only for the minimal amount of time possible. This is to enhance the chance of observing the stop buttons UUID. So the reason why the observation rate drastically dropped in situation two of the system test was simply a matter of SoftDevice scheduling.

The relayer and central use the same type of LFCLK, LFXO. The accuracy of LFXO is set to  $\pm 20\text{ppm}$  ( $\pm 0.66\text{Hz}$ ) [23], which means that protocol timing in both devices does not happen exactly at the same time, even when exchanging connection events. Connection events are requested by the central essentially forcing the relayer to act on two clocks. Its own for scanning, and the central's clock for connection events. In other terms, the two functions (scanning and exchanging connection events) slowly went out of synchronization, halting scan events in favour of maintaining the connection interval.

To counteract the synchronization problem, additional code was added to the relayer making it restart the scan function after a scan timeout of 120s. The restart synchronized the two clocks avoiding collision between the two functions. Ref. appendix D.

After further testing and troubleshooting the parameters had been optimized to:

#### Central optimized parameters

- Scan interval: 100ms
- Scan window: 90ms
- Connection interval: 100ms

#### Relayer optimized parameters

- Scan interval: 100ms
- Scan window: 90ms
- Connection interval: 100ms
- Scan timeout: 120s

The scan window and scan interval in both devices were extended to ensure greater redundancy. See figure 4.27. To prove that the optimized parameters worked, the PPK was used to measure the devices current consumption. See figure 4.28, figure 4.29 and figure 4.30.

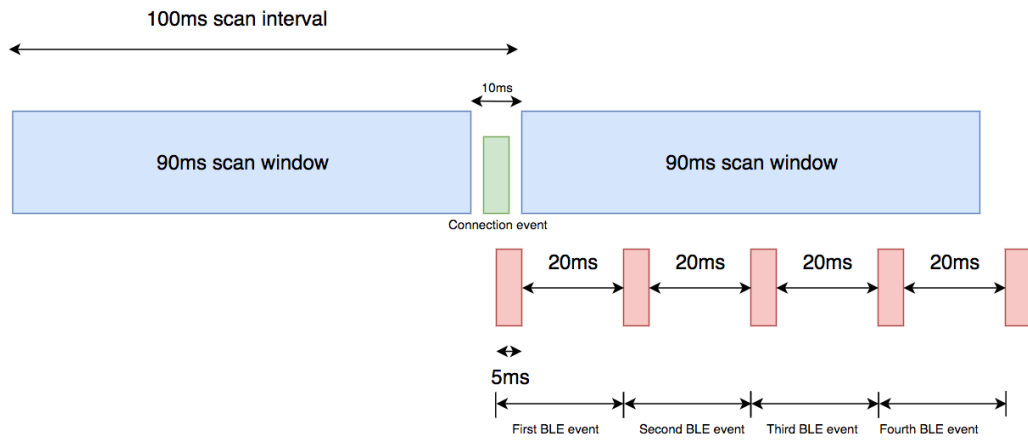


FIGURE 4.27: Scan parameters in relation to advertising and connection events

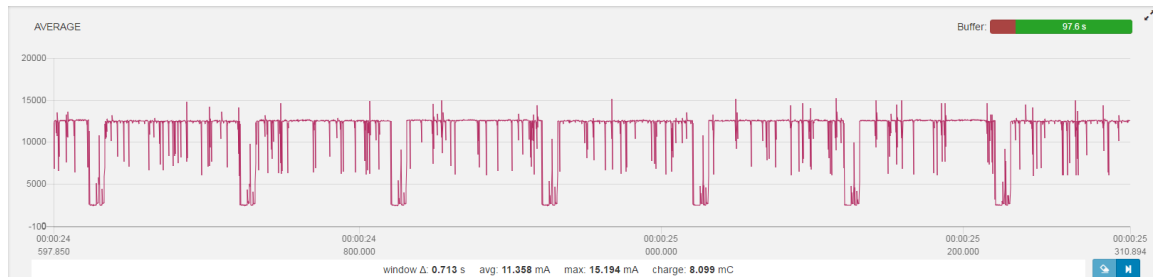


FIGURE 4.28: Central current consumption, new parameters

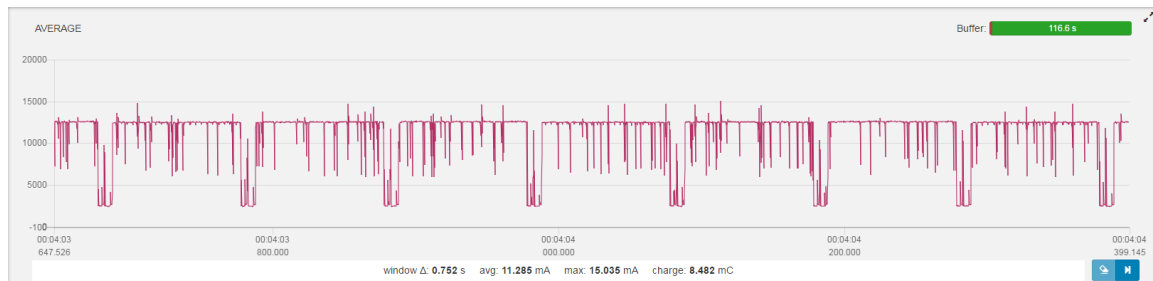


FIGURE 4.29: Relayer current consumption, new parameters

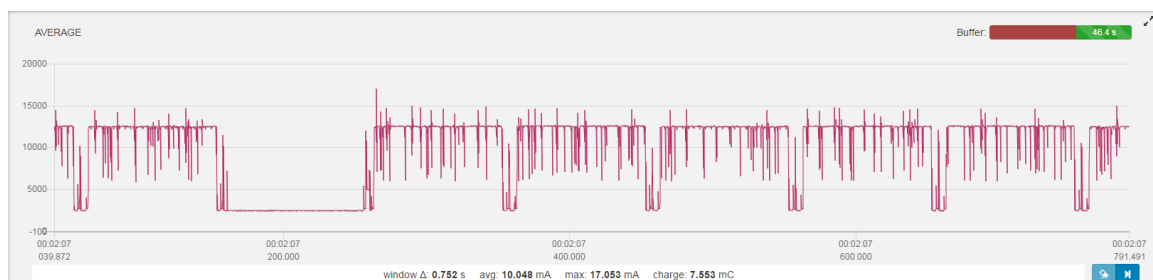


FIGURE 4.30: Relayer current consumption, new parameters, scan timeout at 120s

## Flashing the nRF52

All firmware in this project was either flashed via USB to the nRF52DK or via the nRF52s ISP header on the final designs. The nRF52DKs debugger MCU was used as an external debugger to flash the nRF52 on the final designs. See figure 4.31 for the setup that was used.

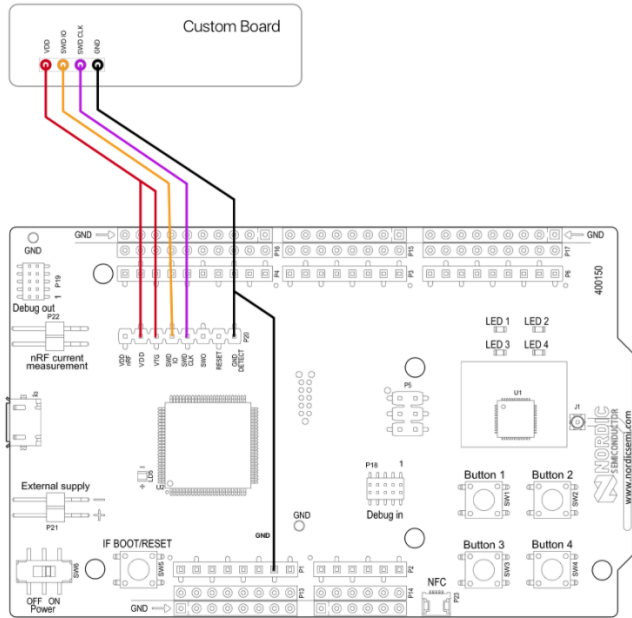


FIGURE 4.31: nRF52 debug out setup [26]

## 4.2 Hardware

The second main segment in this project is the hardware section, which contains the functional and mechanical aspect of the method chapter, and describes the process of how hardware design and production was done. This includes the design and component decisions in the PCB design, and the process of producing the final designs.

### 4.2.1 Preliminary Phase

The assignment was not specific on requirements for the circuit, only stating that it was to harvest energy and be able to send a wireless signal using the nRF52. It was proposed using a piezoelectric element, although other similar sources would also be welcome.

The decision was made to have a custom PCB for the energy harvesting circuit with an nRF52 SoC, as the thought was to fit the stop button circuitry into a casing with the size of a typical stop button found on a bus. This meant reading up on both energy harvesting circuits and PCB design. Before being able to find the optimal electrical components, and designing an efficient PCB, it was necessary to create a working test circuit that was able to power the nRF52. This part of the report will shed some light on the process of making this circuit, and whether the set milestones, goals and stretch goals were met or not.

The first six or so weeks of the project period consisted mainly of research on energy harvesting circuits. The process began with piezoelectric elements and their use in energy harvesting, as this was the energy source proposed in the assignment. Various literature were found mainly online, and some were recommended by professors at NTNU [14] [28]. The process of picking out what was, and was not relevant turned out to be a tedious task, as there is a hefty amount of literature published on energy harvesting [11] [13] [22] [44]. The texts all pointed towards two main segments that were vital to most energy harvesting circuits. A rectifier of some sort, to get the most out of the generators energy pulses. And a voltage regulator, to convert a given input voltage into the desired output voltage. At the first meeting with supervisors from Nordic Semiconductor, they suggested taking a look at ZF Electronics' electro-mechanical generators, or buttons for future reference. This generator also seemed like a viable source to test and compare to piezoelectric elements.

The preliminary phase also consisted of learning how to use the PCB design tool Altium Designer 18. And as none of the group members had any prior experience with the program, the learning curve was steep, as Altium is an intricate program. And since Altium Designer 18 was released 15 Dec. 2017, example projects and tutorials for the new version were scarce, and it took about a month of practice and completing various tutorials to feel comfortable making schematics and PCB designs from scratch.

### 4.2.2 Design Phase

The design phase was the biggest part of this project. Everything from testing out the first component to the final draft of the finished PCB design was done during this phase, and lasted from mid February through to mid May.

#### Energy Source

The first milestone set, was to order up a variety of generators (Piezoelectric elements and the aforementioned buttons). Nordic Semiconductor, regularly ordering components from <https://www.digikey.com/>, mentioned that they could take care of the orders as

long as they got a "cart share" link from Digikey. The decision was made to order various of the larger piezoelectric elements found in Digikeys catalogue, as well as a couple of buttons from ZF Electronics. A little mishap occurred due to inexperience, as no one thought of adding spares for any of the piezoelectric components. This led to some trouble as they were difficult to solder wires to, breaking due to the temperatures before the wires set properly to the piezoelectric elements. As the button was easier to get a repeatable measurement from, the decision was made to move forward with it, leaving the piezoelectric elements somewhat behind. Measurements of a working piezoelectric element versus measurements on the button are illustrated in figure 4.32.



FIGURE 4.32: Piezoelectric elements were hard to get repetitive results on compared to the button, which gives the same output every time

### Rectifier Circuits and Initial Measurements

After ordering the first batch of energy sources, research on various energy harvesting circuits began. First looking at rectifier circuits, as it was desired to have a circuit ready for testing as soon as the generators were delivered. The first circuit that came to mind was the full-wave bridge rectifier, as there would most likely be generated both a positive and a negative pulse from the various energy sources. Further research showed that a full-wave voltage doubler often was used in energy harvesting circuits, due to its ability to give higher output than input voltages and being more efficient due to less diodes. As these two rectifier alternatives seemed the most likely to provide good measurements the group decided to make a few of these circuits in to the lab at Elektra, using breadboards and components found there. As there was some time to spare before the generators arrived, a half-wave voltage doubler was thrown together for good measure, in case that would somehow work better than one operating with both positive and negative pulses.

The ordered parts arrived the following week and tests could begin with the rectifier circuits. Both circuits seemed promising when testing with the button, and as expected the piezoelectric elements gave varying results. To get the desired output voltage needed to power the nRF52, testing with various components on both circuits with  $2.2\text{k}\Omega$  as a load, as this was the load value representing a running nRF52 advertising three BLE events. This was calculations made early on in the process, but more recent calculations proved  $2.6\text{k}\Omega$  to be more accurate 4.18. After a great deal of trial and error, a definitive value and number of capacitors in both rectifier circuits were found. For the full-wave bridge rectifier, one single capacitor at  $100\mu\text{F}$  gave the most efficient output voltage. See figure 4.33

As for the full-wave voltage doubler, two capacitors are required. To test all possible combinations with relevant capacitors would prove time consuming, and was done during the

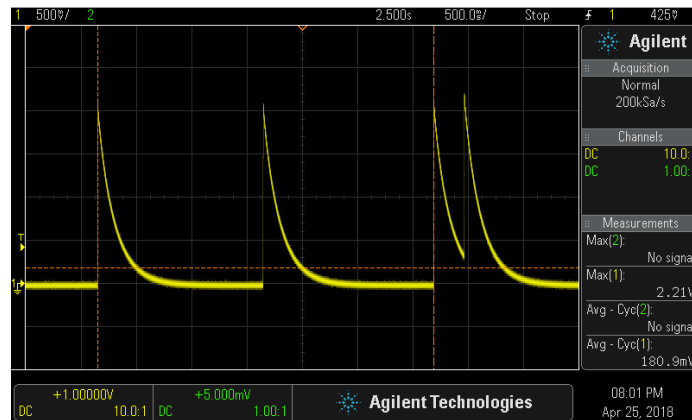


FIGURE 4.33: Single pulses first. Then the complete pulse, which is able to power the nRF52 for 40ms

entirety of the design phase. The discovery of the most efficient circuit was not made until the later phases of the project, as no one thought of using two capacitors with imbalanced values to maximize efficiency in the energy harvesting process 4.2.2. Initially, the option that gave the most efficient output voltage with two identical capacitors was the circuit with two capacitors at  $82\mu\text{F}$ , which figure 4.34 shows.

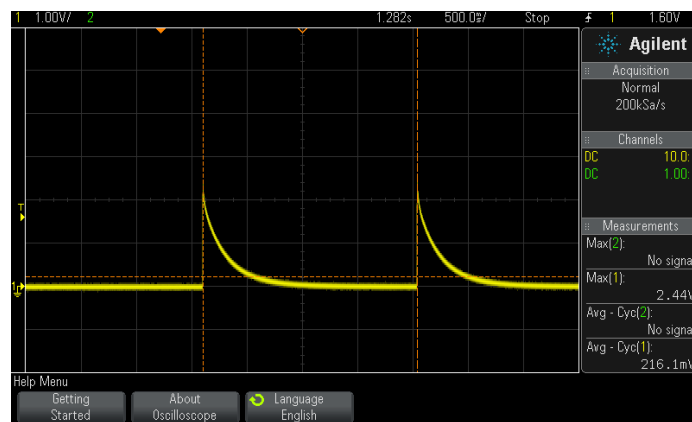


FIGURE 4.34: Holds a voltage able to power the nRF52 for 62ms

As the voltage doubler was able to, according to measurements and calculations, sustain the nRF52 for 22ms or about 1 more advertising event, than what the bridge rectifier was able to provide. This made the decision to venture on with it, as opposed to a bridge rectifier.

### Voltage Regulators

Next, the circuit would need a regulator, to prevent any possible transient voltage spikes from damaging or potentially destroying the nRF52. Thorough research was done to find potential regulators, although not too many buck- or buck/boost-converters could handle both the extreme low and high input voltages the considered generators provides. At first, various LDO regulators were considered, as they were able to output the needed voltage even at low input voltages. Unfortunately, these would likely be exposed to too high input voltages to use without danger of overloading, and in turn damaging them. As this was a foreseen problem, the plan was to place them in series with a rectifier circuit, both to

maximize the input voltage for the regulators and to keep the maximum voltage from exceeding the regulators thresholds. An issue here, was that a lot of energy presumably would be lost to the various components.

When discovering the LTC3588-1, the initial thought was that this IC, which already had a rectifier circuit and a buck-converter in one single chip, would be a good all-in-one package solution. It would also be the most secure option, as it has a defined maximum voltage input of 20V, which meant the button would not damage the IC, which in turn with its set output voltages would not damage the nRF52. This led to ordering some LTC3588-1 ICs, and the most promising of the LDO regulators, the ADP5090. The ADP5090 was never actually tested, as too much time went into making the LTC3588-1 work properly.

### Using the Voltage Doubler as a Passive Regulator

Even though the thought of regulating the voltage without an LDO regulator had been shelved for a while, it was given another go. The issue the standard way to use a voltage doubler presented was that the time window where the generator had to be pressed and released was so short that the two voltage pulses did not overlap, and the results gave two separate rectified pulses which meant the nRF52 powered down between the pulses. Usually one or two spikes giving an active time between 10-20ms each. The solution was to use two capacitors with different values, contrary to the general model. Doing so meant having the capacitor that is charged first to be oversized, with a value between 100 and  $330\mu\text{F}$ . The first pulse not reaching the needed voltage level to run the nRF52, but the time it supplied a voltage was extended a significant amount. The first pulse now working as a kind of DC offset gave the second pulse a higher starting point and resulting in a longer period of time within the nRF52's active voltage range, between 60 and 85ms. The second capacitor being in the range of  $22\text{-}68\mu\text{F}$ . Removing the focus from increasing the efficiency of two pulses to rather using the energy of the first pulse to boost the second one provided approximately one extra advertising event. This distinction is illustrated in figure 4.35.

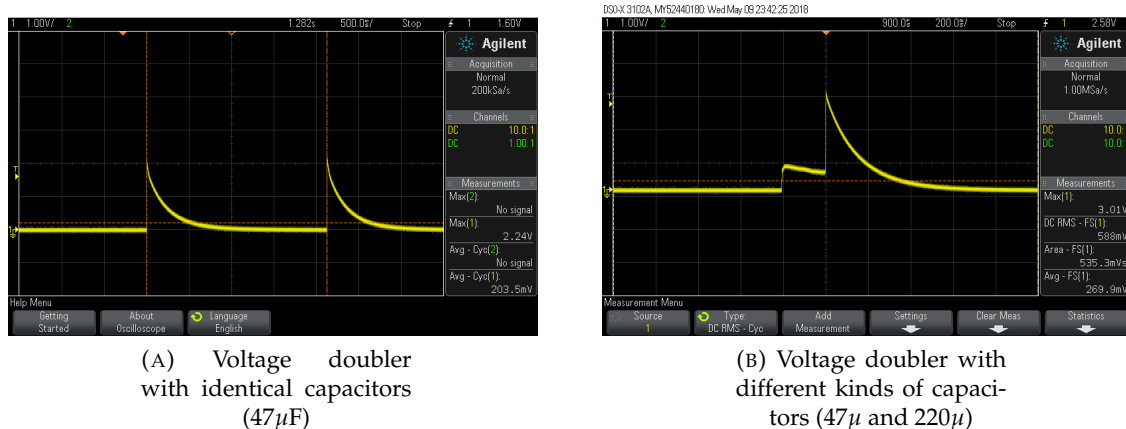


FIGURE 4.35: The two voltage doubler solutions put up against each other.  
Both measured over a  $2.2\text{k}\Omega$  resistor

Now remained choosing capacitors that in this configuration would not allow the voltage to exceed the maximum voltage input of the nRF52, a sort of passive voltage regulating, while still providing an output time long enough to send the required amount of packages. This process is described in section 4.2.2 under "Final Voltage Doubler Solution".

## PCB Design

As the voltage regulators and other SMDs were ordered, a simple breadboard would no longer suffice for testing, and a PCB design would be required to easier solder components together into a working circuit. All PCB designs made during this project were made in Altium Designer 18, all soldering done by hand at NTNUs facilities, and manufacture orders were sent to NTNUs electronics and prototype laboratory for early PCB designs, and to <https://jlcpcb.com/> for later prototypes and final designs.

The process had a slow start, as making PCB designs were a learning experience from start to finish. Starting with making multiple different break-out boards with pin headers, allowing swapping out capacitors and diodes to test which combinations would be more efficient. Three different break-out boards were made, a regulator circuit using the LTC3588-1, one using the reference design for the nRF52, and one having both the bridge rectifier and the voltage doubler. Figures 4.36, 4.37, 4.38, 4.39, 4.41 and 4.42 shows the three first PCB designs made.

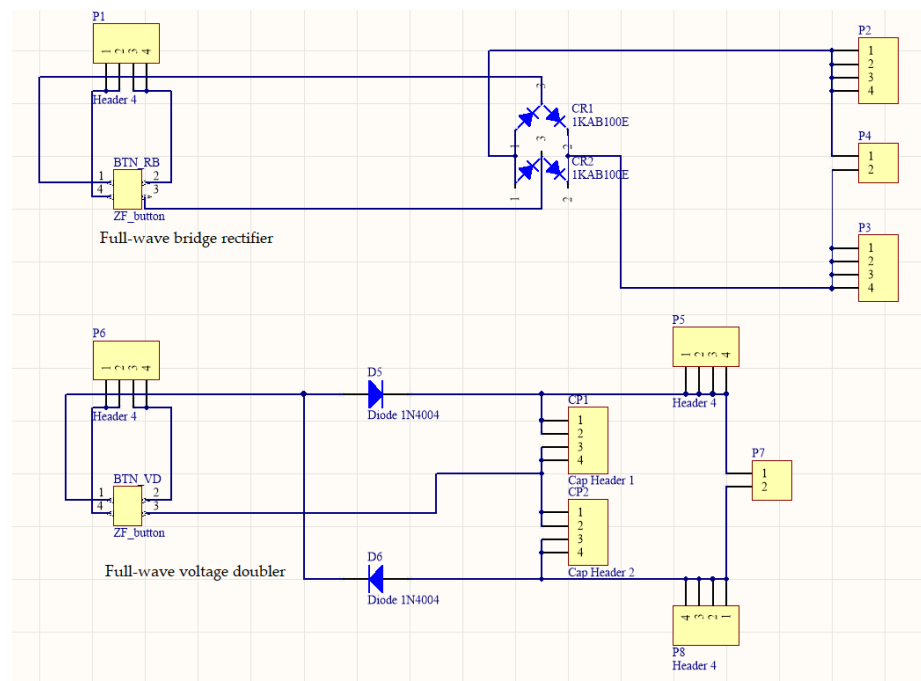


FIGURE 4.36: Schematics for the two rectifier circuits

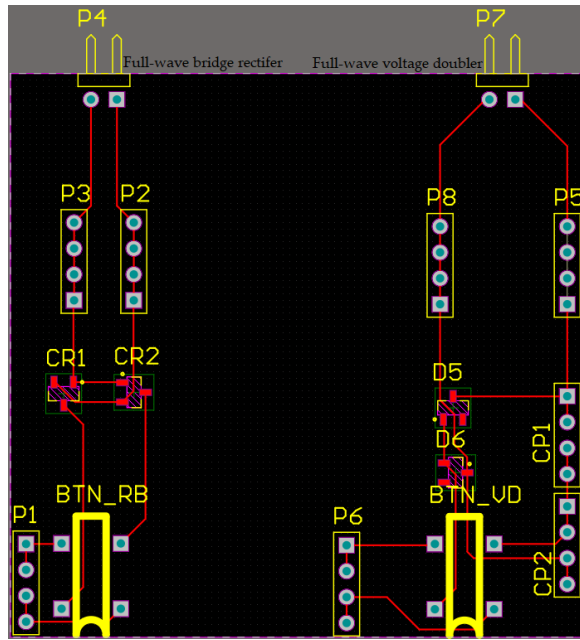


FIGURE 4.37: PCB design for the two rectifier circuits

These first circuits, figures 4.36 and 4.37, are two simple circuits with nothing but the button, two diodes, and pin headers for various capacitors and measurements. The first thing to do was making footprints and schematic components for the button, as there was no such thing in the data sheets from ZF Electronics. This was done using Altium's "Footprint Wizard" for the footprint in the PCB design, and "Component Wizard" for the schematic component. These "wizards" are easy to understand and use, as the only thing to do is feed them with data from the data sheets, and the software will make the footprint with the correct dimensions and placement of pins. B. The next step was making schematic components for the diodes, as the footprint SOT\_23\_N already existed in Altium's libraries. The diodes for both the voltage doubler and the full-wave bridge rectifier used the same footprint, although they needed different schematic components because of the fact that the voltage doubler only uses two of the pins (pins 1 and 3), and the bridge rectifier uses all three. For the voltage doubler a regular diode component could be used, but the bridge rectifier needed its own component to successfully mimic a bridge rectifier in Altium.

The main concern during PCB design, was to study the proof of concept, and there is likely room for improvement. The main goal was to test the circuits and not for them to be aesthetically pleasing. This made for a slightly confusing design as the PCB print at NTNU was not able to provide a top overlay explaining what components went where, which meant a computer with Altium was needed when soldering the components to the board. There is not a ground layer in this PCB design, which is why it looks so different compared to future PCB designs in this project, as that was deemed unnecessary in this particular circuit. Ultimately, these circuits were not used, as it proved faster and easier to use breadboards and through-hole components for simple break-out boards like these. The LTC3588-1s datasheet [46] provides a reference design when using it for regulating the power going into a MCU, and therefore this next break-out board is based on that design. Pin headers were used instead of where the energy source (pin header P1) and microchip (pin header P2) goes in the reference design, as these components would be on other PCBs during this phase. The pin header, P3, is there to allow swapping between the output voltages using jumper pins to set pins eight and nine on the LTC3588-1 high or

low. The last pin header, P4, was initially put in just to measure the voltage over the two capacitors C1 and C3. A second use for it was discovered later, where using pin header P4 to bypass the internal rectifier in the LTC3588-1 and applying the input voltage directly to pin 4 ( $V_{IN}$ ), made it possible to test other rectifier circuits, which could potentially enhance the circuits efficiency. See figures 4.38 and 4.39

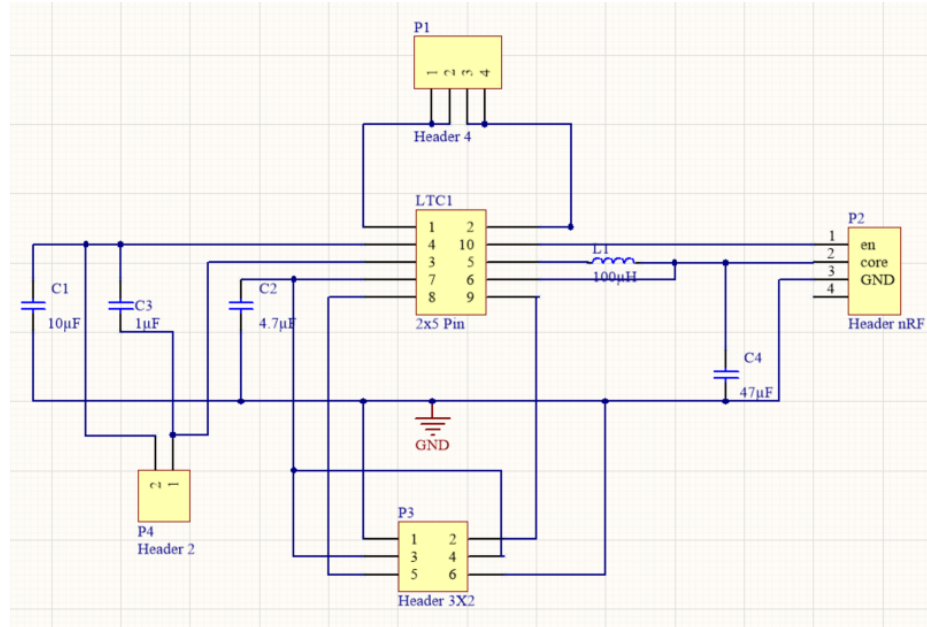


FIGURE 4.38: Schematics for the first LTC3588-1 circuit with its reference design and pins to configure the output voltage.

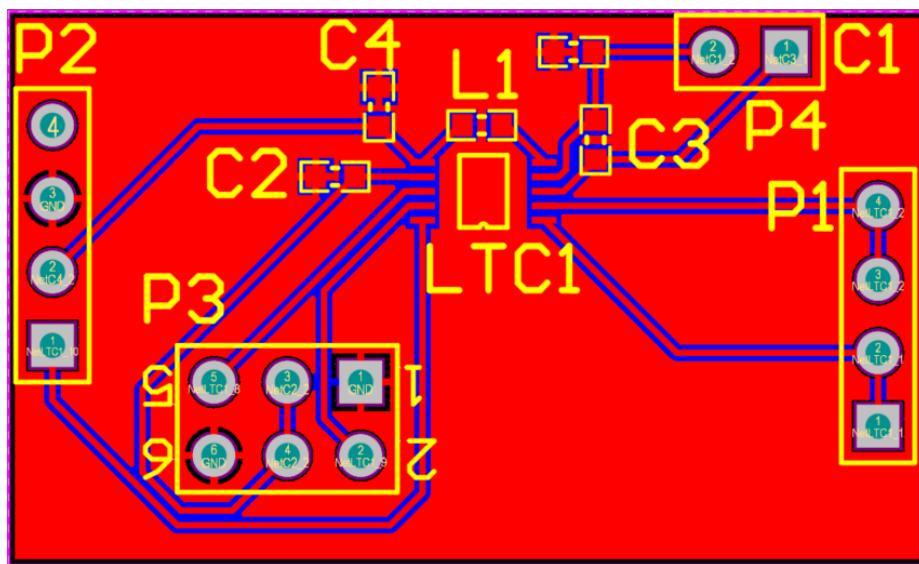


FIGURE 4.39: PCB for the first LTC3588-1 circuit with its reference design and pin headers to configure the output voltage and measure voltages between C1 and C3.

This circuit mainly uses footprints that already existed in Altium's libraries, and the only necessary change was to modify an MSOP-10 footprint to have the correct widths between pins and a ground plane underneath like the LTC3588-1 IC has. All capacitors and the one coil uses a standard 0603 SMD footprint.

When printing the LTC3588-1 circuit at NTNUs facilities, there were some complications, as the boards did not have a solder mask protecting the copper layers from repeated soldering sessions. This led to the circuit boards both getting damaged and damaging the LTC3588-1s when soldering on and off components. This problem persisted through multiple of these boards and a conclusion was made to order the LTC3588-1 break-out board from <https://jlcpcb.com/>. This provided the solder masks that were likely to solve the problem. Even though these circuit boards were more expensive than the ones provided by NTNUs, the LTC3588-1 was too promising to give up on.

Once these circuit boards arrived, the problem was proven to be the lack of solder masks, as there were nothing but steady results from the LTC3588-1 when mounted on a circuit board with solder masks. This type of circuit board slightly reduced the soldering time as well. Figure 4.40 shows one of these circuit boards.

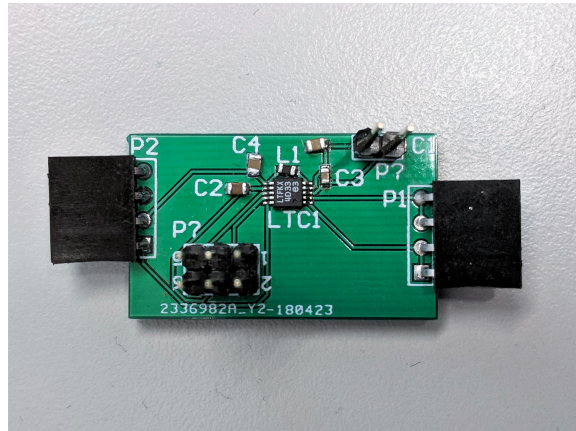


FIGURE 4.40: An LTC3588-1 break-out board from <https://jlcpcb.com/> with all components mounted.

As for the nRF52, no new footprints or schematic components were required as the reference design is downloadable with its own PCB library. The changes made compared to the reference design is that the pin header P1 was added for GPIO pins and an analogue input pin, as these were recommended by the supervisors to install for the possibility to test if the nRF52 was working and programmed correctly. Pin header P2 was added to have voltage input from the previous circuits. Pin header P3 is connected to the SWDIO and SWCLK pins which are necessary for programming the nRF52. The last addition, that was not in the reference design from Nordic Semiconductor is the copper antenna, (the ANT net in the figure 4.42), which was copied from the nRF52 development kit, to easily get a usable range on the signals bound to be sent from it.

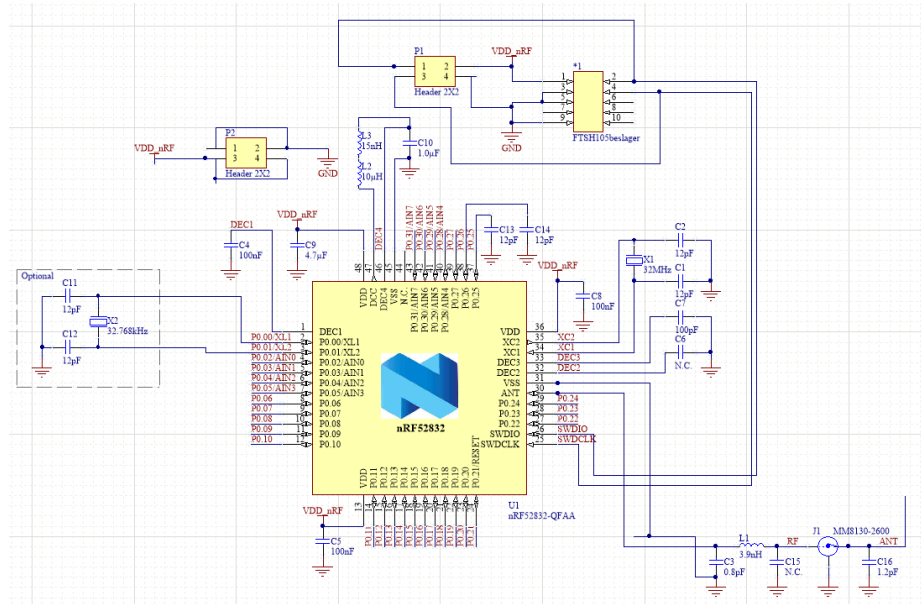


FIGURE 4.41: Schematics for the nRF52s reference design with additional pin headers for making measurements and programming the SoC.

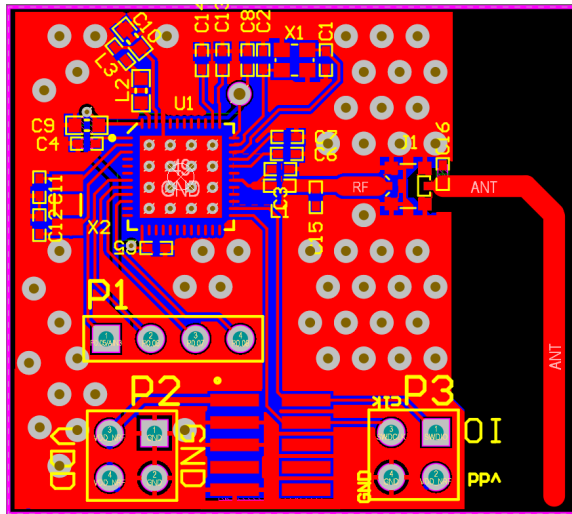


FIGURE 4.42: PCB for the nRF52s reference design with additional pin headers for making measurements and programming the SoC.

Although these first PCB designs are simple break-out boards, they were designed with the intention of later combining them into one final PCB. Test results from these break-out boards, would clearly show which configuration of components would yield the best result.

#### What to Consider When Completing a PCB Design

When all the components are placed in correct position and the design is starting to reach its final form, there are usually some final steps to consider.

**Via stitching** - The process of via stitching is quite simple, and Altium also has a via stitching function available. A via is a hole that connects one plane to another. As both planes on all the designed PCB in this thesis functioned as ground planes, multiple vias are placed around every board to connect both ground planes with each other.

The shorter the distance from each component to ground, the shorter the return loops are. Via stitching also help maintain a low impedance. The process of stitching contains placing multiple vias all over any area that can fit it. It is also normal to put vias as close to decoupling capacitors as possible to ensure short return loops. The via stitching and shielding can be seen in figure 4.43, the vias being the small dark circles spread around.

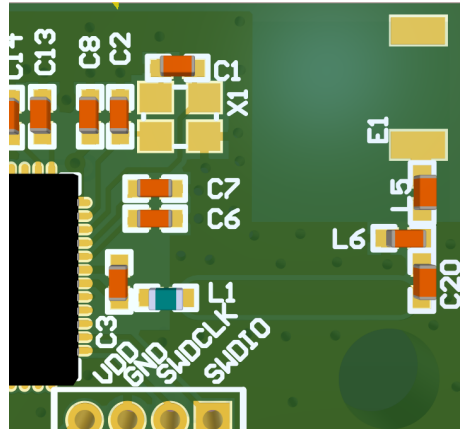


FIGURE 4.43: Via stitching and shielding can be seen as small dark spots

**Via shielding/fencing** - Similar to via stitching via fencing consists of placing vias around on the ground planes. This time vias are placed closely to each other on each side alongside a signal trace. This is to isolate the said signal trace from any noises or disturbances. This is usually also done along the edge of the whole PCB, especially around the antenna section. As seen in figure 4.43 along the line between L1 and C20

**Removing "fingers"** - Fingers is a term used for parts of the ground plane that is separated partly or altogether from the rest of the plane. These emerge in tight areas where the plane can not reach. These fingers can cause interference as they can develop antenna like tendencies. The fingers can be removed by one of two options; if the finger can be via stitched close to or at the edge of the finger, or remove it all together. See figure 4.44 for finger removal.

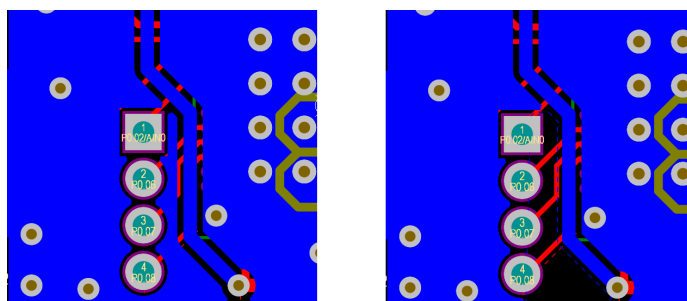


FIGURE 4.44: A so called finger before(left) and after removal(right)

**Spacing** - Even though the spacing distances between traces and/or components are preset in the Altium rules, certain components need to be kept away from each other even further, to prevent disturbances. This can be seen in figure 4.43 around the antenna labeled E1. As specified in the antennas data sheet [45], the antenna needs to be a given distance away from ground on both planes. It is usually mentioned in a given components data sheet if this has to be considered.

**Rule check** - Lastly and and maybe most importantly a rule check should be executed.

PCB design software as Altium usually has a rule check function. Rules can be set as width between traces and components, trace width, via sizes et cetera. The user has the option to set rules the PCB design has to follow, and by performing a rule check, mishaps can be discovered and fixed.

**Antenna Tuning** Antenna tuning was the final task in the PCB design phase. As time grew scarce during the last weeks of the project, the amount of time and work put into antenna tuning was limited. This was somewhat expected as antenna tuning was set as a stretch goal, and never a primary objective. The goal of tuning an antenna is using capacitors, inductors and correct trace width compared to the PCB design to prevent power to be reflected from the antenna to the radio module, while also utilizing the most of given power and decreasing efficiency loss. The necessary inductors and capacitors being stated in nRF52s QFAX reference design [38], and the antenna 2450AT18A100's datasheet as seen in appendix [45]. This left choosing the correct RF trace width to be determined based on the rest of the PCB.

Having chosen the antenna 2450AT18A100, it was necessary to impedance match the RF trace to  $50\Omega$ . The RF trace is the trace going from the nRF52 out to the antenna, made to transfer the radio frequencies. The supervisors suggested using the antenna tuning calculators found online at [eeweb.com](#) [9] or [multi-circuit-boards.eu](#)[21]. The factors both of these calculators use are the following; what frequency the antenna will be working on, PCB height, trace width, width between traces, trace height, and the dielectric constant of the material the PCB is made of. Mostly basing the values on what the PCB (at this point) was set as, the following values were chosen; 2.4GHz frequency, 1.2mm PCB height, 0.16mm width between traces, and the standard values of trace height of 1oz, and the dielectric constant of FR4, fiberglass, which is 4.3. This left choosing trace width by using the calculators.

By using the calculator at [multi-circuit-boards.eu](#) , the trace width was set at 1.466mm. Thinking that antenna tuning was now completed, the first sets of final PCBs, were ordered. Not long after the orders were made, it was discovered that the trace widths suggested by [multi-circuit-boards.eu](#) and [eeweb.com](#) did not match. The supervisors then suggested using the software Saturn PCB Design Toolkit to do this, as the web pages apparently were not reliable. As seen in figure 4.45 the RF trace width was ultimately set at 1.035mm for the second batch of PCB designs.

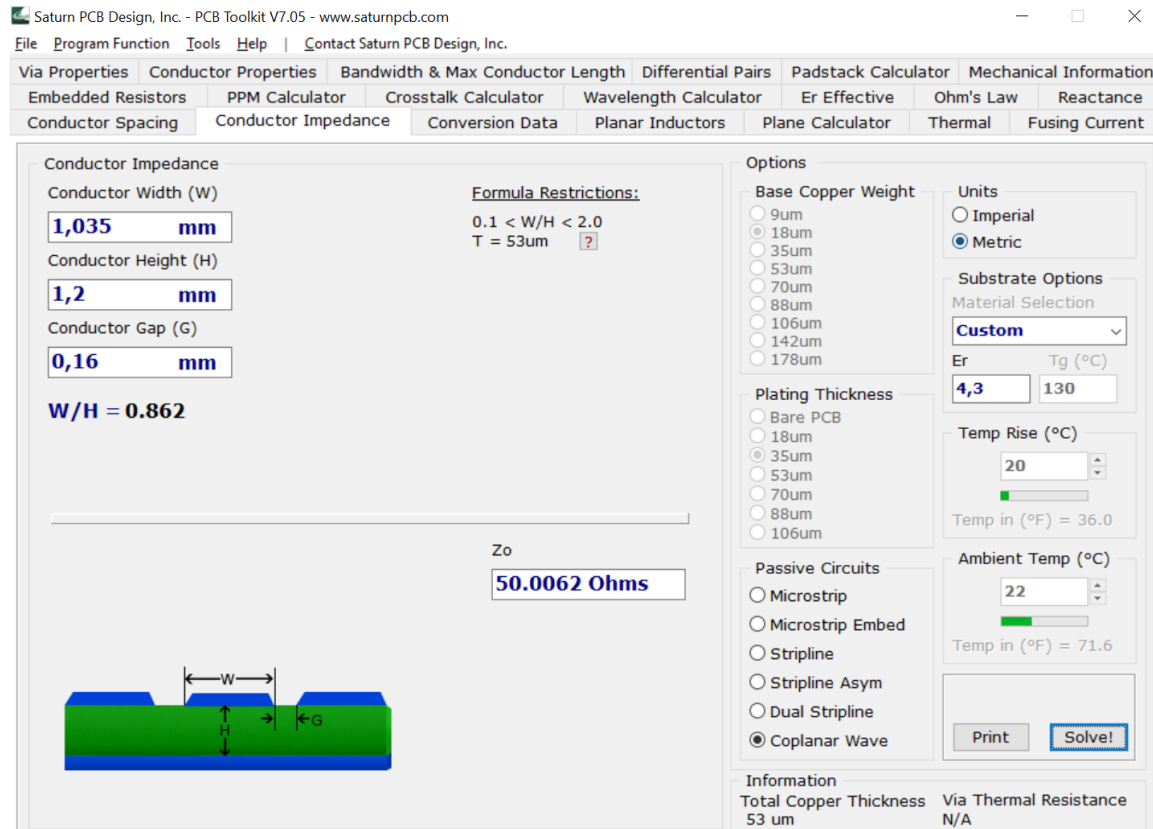


FIGURE 4.45: Saturn PCB Design Toolkit with the key values set

As mentioned above the antenna tuning is not a crucial part to make the system work, but a safeguard to prevent power to bounce into the radio, and to make the antenna as efficient as possible. This meaning that the PCBs ordered with the RF trace width of 1.466mm still were more than capable of doing its job. Having to remake the PCB layout with a different sized RF trace also made it possible to have multiple versions and compare results. While remaking the PCBs a new way to position the components were also discovered. This resulting in a new smaller and sleeker design that now easily fit inside a bus stop button. More about the new designs in the following sections.

### Final Voltage Doubler Solution

When the time came to design the PCBs it was decided on making multiple designs. The decision was made based on the thought that the LTC3588-1 still at this time gave inconsistent results. This design is based on the voltage doubler described in section 4.2.2. Even though the design based on the voltage doubler gave consistent results, the design had no upper limit or regulator to stop the voltage to surpass the upper limit of the nRF52, given a user pressing the button multiple times within a short period of time. Though it must be said that to exceed this limit the user has to press the button frantically, multiple times.

The voltage doubler-based design consisted of a voltage doubler with decoupling capacitors in parallel to prevent transients from damaging the nRF52 put onto the same circuit board as the nRF52 reference design with slight layout modifications to utilize the space in the best way possible. The capacitor values found to be the most efficient for the energy harvesting circuit were:  $220\mu\text{F}$  for the energy storage, allowing it to hold on to the voltage for the desired amount of time.  $56\mu\text{F}$  for the second capacitor that provides the pulse that

can power the nRF52, but not so high that it can damage it.  $33\mu\text{F}$  as a decoupling capacitor to avoid transients. This solution gave an average output voltage above 1.7V for 82ms when using the nRF52 as load with. As the nRF52 has a start-up time of approximately 10ms with each BLE event lasting for 25ms, the circuit in theory should be able to consistently send three full BLE events. No component values that originally were in the nRF52 reference design have been altered.

### Final LTC Solution

The second solution, was a "hybrid", mentioned briefly earlier in this chapter, between the voltage doubler circuit and the LTC3588-1s reference layout. As there was some trouble getting the LTC3588-1 to work properly when using its reference design in conjunction with the button. An idea to connect the button directly to the LTC3588-1s pin 4 ( $V_{IN}$ ), using a custom made rectifier circuit instead of the internal full-wave bridge rectifier came to mind, as the internal rectifier was not suspected to handle the buttons energy pulses optimally. A rectifier between the button and pin 4 ( $V_{IN}$ ) would be necessary as the LTC3588-1 was likely to be overloaded and/or damaged if the input voltage was too high when directly applied to pin 4, as some of the LTC-circuit would not be used in this instance. See figures 4.46 and 4.47 for a visual representation of this solution.

The component values measured to be the most efficient in this circuit, were  $47\mu\text{F}$  for the energy storage capacitor, and  $22\mu\text{F}$  for the capacitor pushing the voltage to a level where the nRF52 can operate. All other capacitors have the values recommended in the LTC3588-1 reference design when connected to an MCU. The inductor in the LTC3588-1 was measured to be most efficient at  $100\mu\text{H}$ . No component values originally in the nRF52 reference design have been altered.

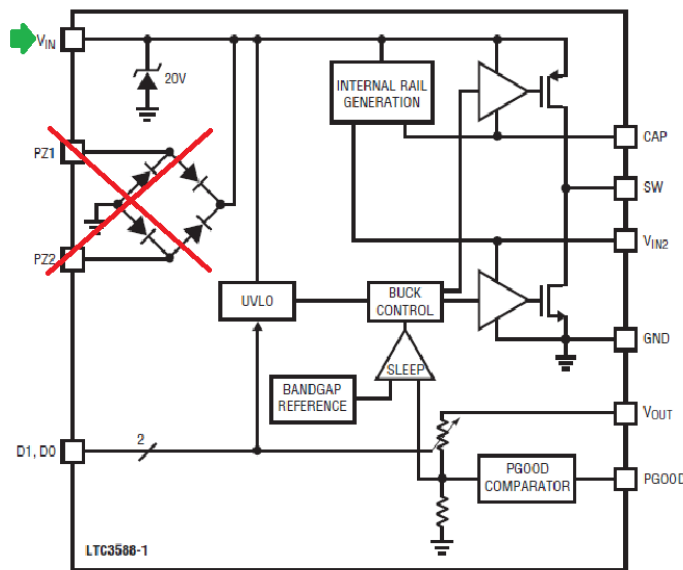


FIGURE 4.46: LTC3588-1 block diagram, where instead of the current going in on pins PZ1 and PZ2, an already rectified signal goes directly into the  $V_{IN}$  pin.

Images of both solutions final "showcase" circuit boards can be found in figures 5.4 and 5.10 in the next chapter.

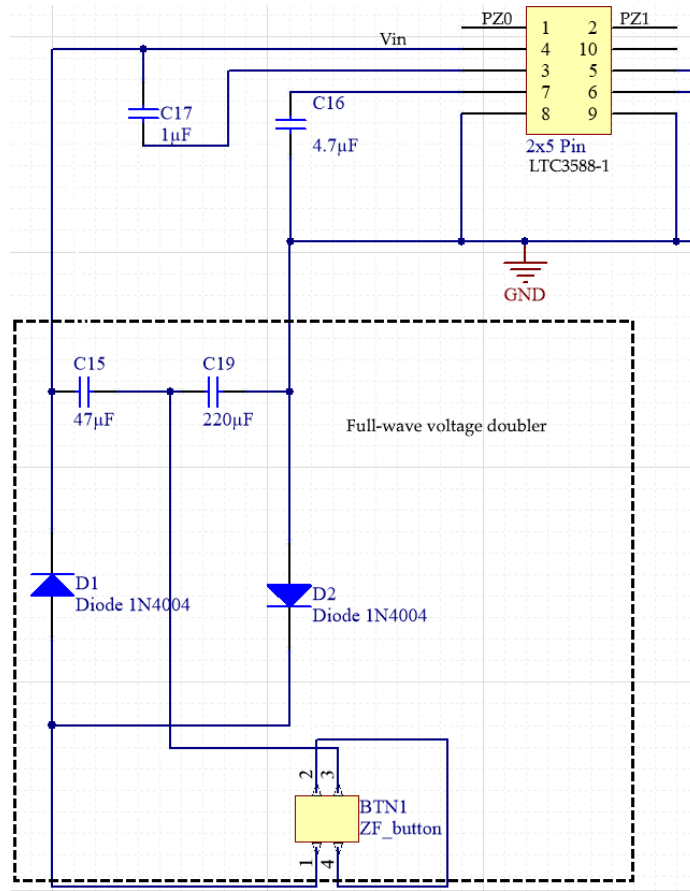


FIGURE 4.47: Schematics of the circuit in Altium, where the full-wave voltage doubler rectifies the energy from the button and sends it directly to pin 4 on the LTC3588-1. Pins 1 and 2 (PZ0 and PZ1) are not connected as the source connects directly to  $V_{IN}$ . Note: component values here are not final.

#### 4.2.3 Production Phase

The production phase will describe the processes of final component and PCB orders, soldering and troubleshooting the final product. The challenges they provided and how they were overcome will also be explained in this section.

##### Component and PCB Orders

As already mentioned all components, except the nRF52 which Nordic Semiconductor supplied, were ordered from <https://www.digikey.com/> via Nordic Semiconductor. A full shopping list can be seen in the bill of materials (A). The orders made are, in conjunction with leftovers from previous orders, enough to produce four finished boards.

The final PCB designs were ordered from <https://jlcpcb.com/>. In the end four different designs were ordered. Two for the "final voltage doubler solution", and two for the "final LTC solution". The reasoning behind having two different designs of each solution was primarily because the first batch were incorrectly impedance matched. This led to having one original layout, which put all components on one side, and made them easy to handle while soldering. The other design, the showcase layout, was made to fit into a custom 3D-printed bus stop button chassis, that would be used when presenting the project. Having two solutions and two layouts were also a great way of attaining a high chance of success.

Especially since one layout was not antenna tuned properly, and other possible errors on the PCB designs not yet discovered. In this instance more is better and this will ensure having at least one solution that works in the end.

### Soldering

Although soldering of components went on through the entirety of the process, this section will only cover the soldering process of the final circuit boards, as the soldering of the early iterations of the stop button circuit was mostly trial and error. Any challenges that arose and how they were tackled will also be presented in this section.

As most of the components to be soldered to the circuit board, like the capacitors and inductors, were in the size of 0603(1.6mm\*0.8mm) or 0402(1.0mm\*0.5mm). Soldering all the components to a PCB less than the size of a thumb( $\approx 34\text{mm}^*14\text{mm}$ ) took both patience and planning. To get all the components properly soldered on and to minimize the risk of damaging components, the soldering was done in a very particular order. First, all 0603 and 0402 sized components going onto the top side of the circuit board were soldered fast, as the larger components might be in the way of soldering these smaller components. Then the larger ICs, diodes, and SoCs were fastened using hot air soldering, as this is the safest way to make sure all pins are soldered to their footprint on components with multiple pins. Finally, the pin headers and generator were soldered on, as these take up the most space. On all components except the LTC3588-1 and nRF52, a soldering iron was used.

Using solder paste for the majority of the components including SoCs and ICs as the preferred material to use when soldering. The solder masks on the PCB makes it easier to solder as the solder paste does not flow away from the pads when melting. Using flux while soldering to distribute heat and improve the chance of a successful solder. The flux prevents the solder paste from oxidizing. Any problems with the finished were solved by re-flowing the faulty connections with a soldering iron or hot air solderer.

### Troubleshooting

This section will describe the troubleshooting process of the final PCB designs, what other problems occurred, and if they were or were not solved.

### Original Layouts

There were some connectivity issues when first testing the two solutions after soldering. Somewhat caused by the antenna not being properly impedance matched in these PCB designs, but also because all components were not properly soldered to the board. Some components, specifically a few nRF52s and some LTC3588-1s, did not work properly after soldering. A likely cause is that they were exposed to small ESDs, as the environment where all soldering took place, is not properly secured against ESDs. There is also the possibility that either of these components were damaged during soldering. The impedance matching was hard to do anything about, except wait for the showcase layouts, which were likely both correctly impedance matched. The soldering however, was fixed after finding out what components did not stick and soldering them so that they properly stuck to the circuit board. The faulty components were replaced as there were enough spare parts to take from.

## Showcase Layouts

The showcase layouts arrived a few days later than the original layout ones, and at the time of their arrival a number of the original layouts had already been soldered, which made soldering these circuit boards go quicker as the soldering now was more of a fine-tuned process than with the earlier iterations. When testing, there were no further issues with these PCB designs, as they worked as intended. Although when fitting them into the 3D-printed stop button chassis, one capacitor did not fit and had to be re-soldered.

## 4.3 Component Characterization

The components characterized in this project were the AFIG-0007, and the LTC3588-1. The AFIG-0007 was characterized using oscilloscope measurements. The characterization of the LTC3588-1 proved to be a problematic task due to inexperience, and several issues with the LTC3588-1 itself, that resulted in characterization of the LTC3588-1 was done mainly by means of simulations in Linear Technologies' simulation tool, LTspice.

### 4.3.1 AFIG-0007

The AFIG-0007 was measured over connection points P1 and P3 in figure 4.48, which displays the circuit diagram of the AFIG-0007. The measurements were carried out using different load resistors R1. The internal inductor resistance of the generator is  $51\Omega$ .

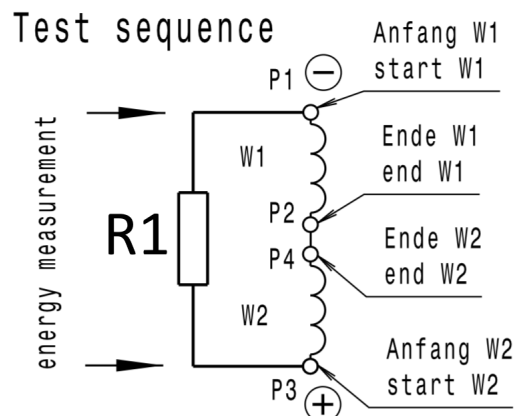


FIGURE 4.48: AFIG-0007 circuit diagram (B)

### Push

R1 ( $\Omega$ )	Total generator resistance ( $\Omega$ )	Time (ms)	DC RMS (V)	Energy (mWs)
100	33.77	10	2.17	0.13944
300	43.84	10	3.19	0.20418
2200	49.58	10	3.88	0.34533
2600	50.00	10	4.01	0.32160

FIGURE 4.49: Push

### Release

R1 ( $\Omega$ )	Total generator resistance ( $\Omega$ )	Time (ms)	DC RMS (V)	Energy (mWs)
100	33.77	10	2.12	0.13309
300	43.84	10	3.11	0.19406
2200	49.58	10	3.98	0.36348
2600	50.0	10	3.89	0.30264

FIGURE 4.50: Release

### Total energy push and release

Load resistance ( $\Omega$ )	Total generator resistance ( $\Omega$ )	Total energy (mWs)
100	33.77	0.27253
300	43.84	0.39824
2200	49.58	0.70892
2600	50.0	0.62422

FIGURE 4.51: Total energy across different R1

The AFIG-0007s datasheet stated that with a load resistance R1 set at  $100\Omega$  a total of 0.33mWs could be harvested. Ref. appendix (B). When comparing the total energy from the measurements with the same load resistance, the two values are in close proximity to each other, 0.27mWs compared to 0.33mWs. See figure 4.52 for measurements done with an oscilloscope.

FIGURE 4.52: Measurements of the AFIG-0007 pulse over a total resistance of  $33.77\Omega$ ,  $R1 = 100\Omega$

### 4.3.2 LTC3588-1

Characterizing of the LTC3588-1 was done by simulations, because producing multiple LTC-circuits with different component values would be a time-consuming and expensive process. The sampled data from the AFIG-0007s energy pulse was imported to the simulation tool LTspice from the oscilloscope, by means of a .csv-file. The pulse extrapolated from the oscilloscope is shown in figure 4.53. This way the same pulse could be replicated and used in each desired LTC3588-1 component and voltage configuration. The simulated results would then give a good indication of the combination of components and voltage output level to go for, which would then be the optimal setup in a final, real life LTC-circuit. The AFIG-0007s energy pulse was sampled with an output load resistance R1 at  $2.6\text{k}\Omega$ , which replaces the nRF52 advertising three full BLE events. Calculations for the average resistance value over three BLE events can be found in section 4.18.



FIGURE 4.53: The single button pulse used as the voltage source in simulations. R1 set at  $2.6\text{k}\Omega$

### Simulations to Characterize the LTC3588-1

In figure 4.54 the current drawn from the different voltage configurations are depicted with a constant voltage supply of 10V. This simulation is used to make an efficiency diagram. In figure 4.55 the efficiency diagram from the LTCs datasheet is replicated using simulations in LTspice. The results show similar behavior to the efficiency diagram presented in the LTC3588-1s datasheet [46]. The efficiency percentages however, are not matched to what the datasheet shows, this is likely due to the datasheet not presenting what component values were used when making the efficiency diagram.

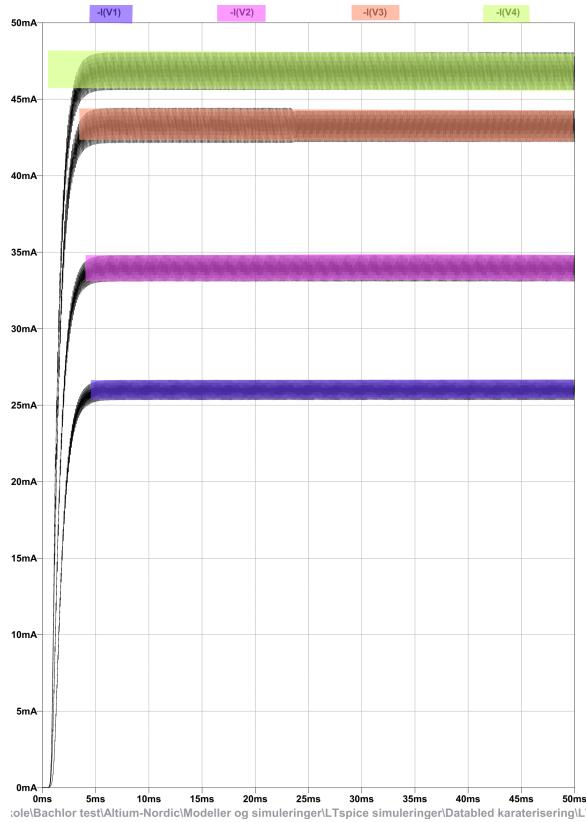


FIGURE 4.54: Current drawn by the LTC3588-1 at 10V DC input. The four configurations are all based on the same load, set to 100mA.  $V_1 = 1.8V$ ,  $V_2 = 2.5V$ ,  $V_3 = 3.3V$  and  $V_4 = 3.6V$

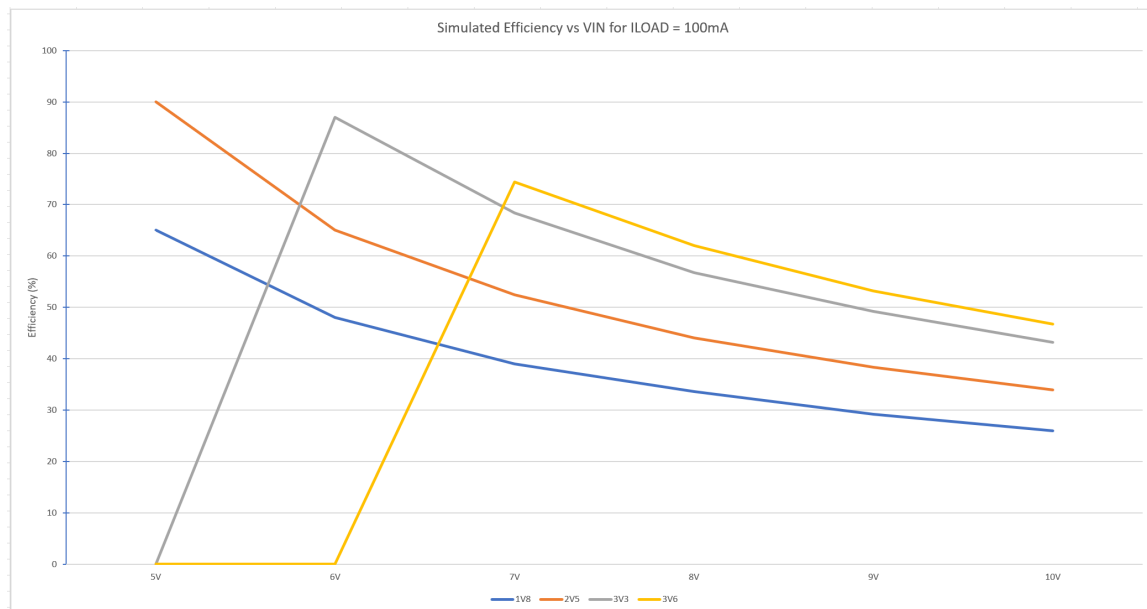


FIGURE 4.55: Efficiency diagram simulated in LTspice, of the LTC3588-1s output efficiency at its four  $V_{OUT}$  settings

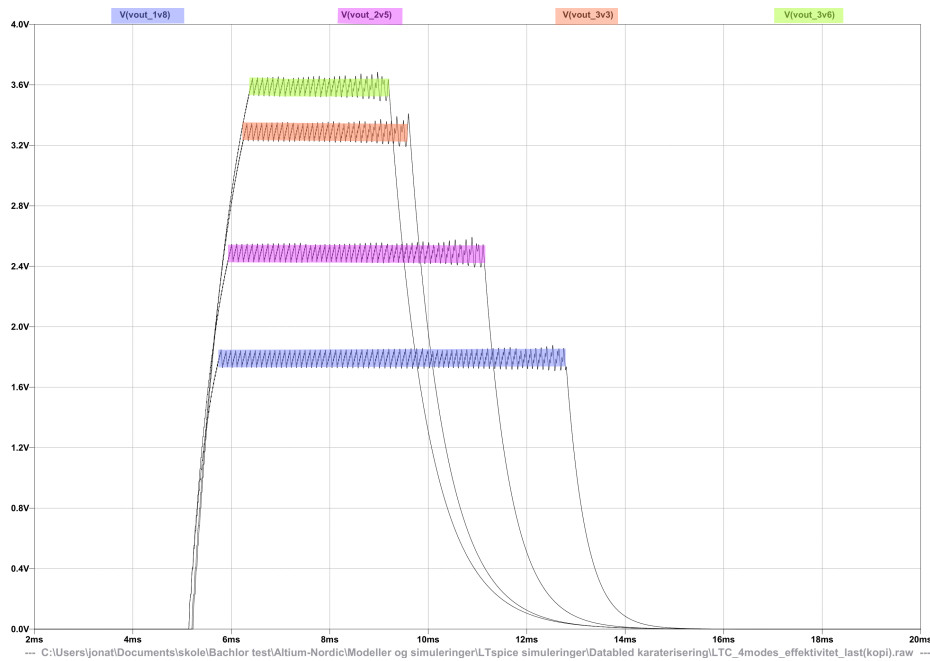
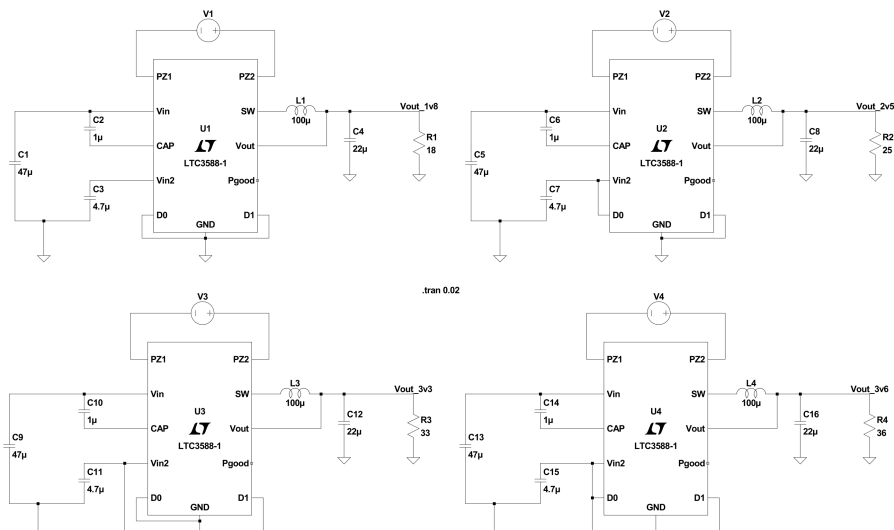


FIGURE 4.56: The LTC3588-1s  $V_{OUT}$  simulations over time for the four  $V_{OUT}$  configurations with the same load of 100mA and an inductor value of  $100\mu\text{H}$

Figure 4.56 shows simulations of the duration the LTC3588-1 will be able to sustain a voltage output in its four voltage output configurations from a single button pulse. The results clearly indicates that the 1.8V option is the most efficient as it lasts noticeably longer than the other configurations. The schematics for the circuits used in these simulations are displayed in figure 4.57.



... C:\Users\jonat\Documents\skole\Bachelor test\Altium-Nordic\Modeller og simuleringer\LTspice simuleringer\Datasheets karakterisering\LTC\_4modes\_effektivitet\_last(kopi).asc ...

FIGURE 4.57: Circuit schematics in LTspice of the four LTC3588-1  $V_{OUT}$  configurations. Simulations are based on these schematics with an input load of 100mA.

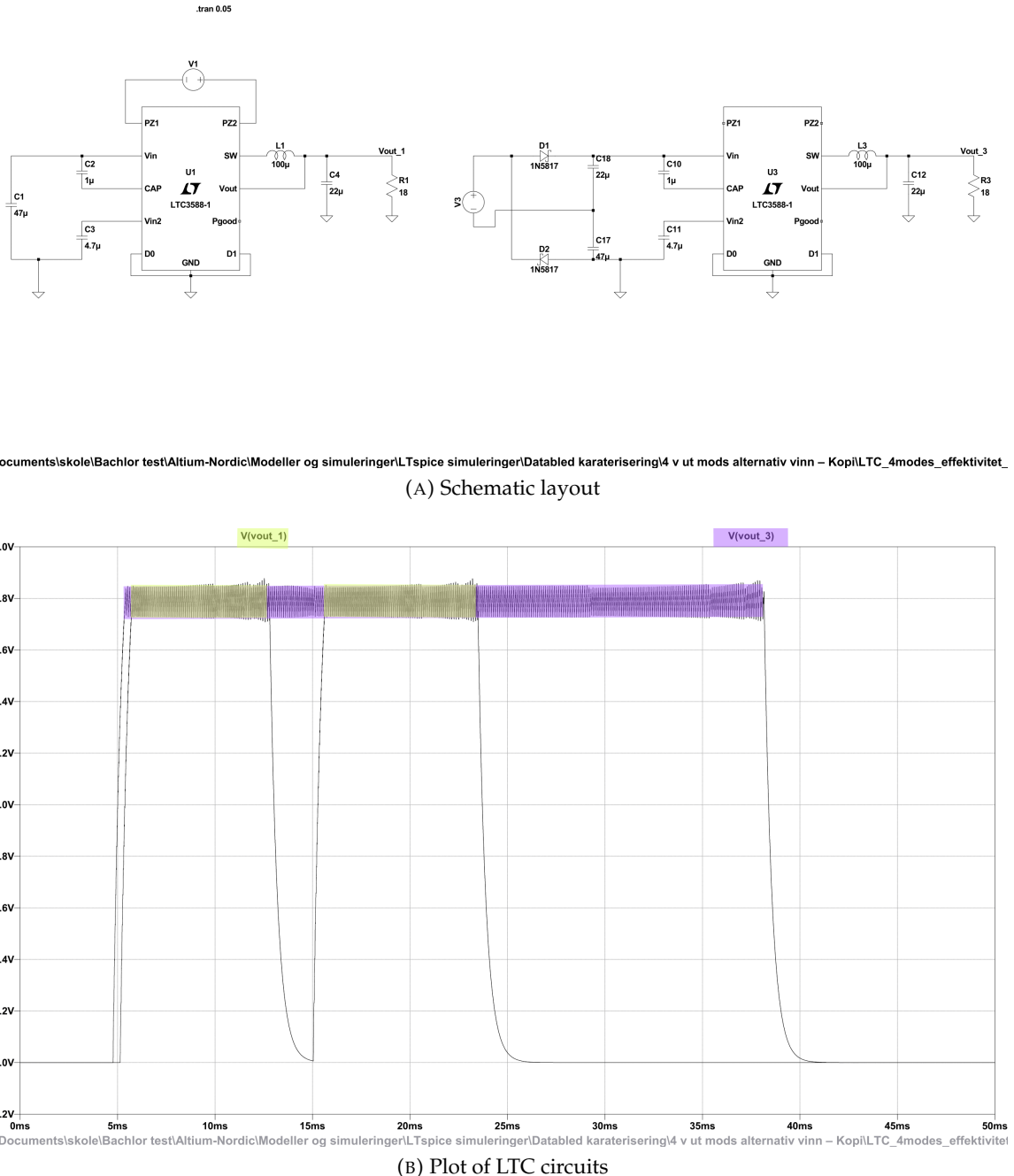


FIGURE 4.58: LTC3588-1 with different rectifying circuits, the diagram displays the energy harvested from both push and release, with the output configuration set at 1.8V and a constant load of 100mA.

Figure 4.58 displays the time of the 1.8V regulated output signal from the LTC3588-1 with different rectifier circuits. The yellow graph represents the LTC3588-1 using the internal rectifier circuit, which outputs two separate signals, one for push and one for release. The purple graph represent the internal rectifier being bypassed in favor for an external

voltage doubler with imbalanced capacitors, as used in the final designs. Even though the time perspective in the simulation can not be trusted fully due to the constant load. It still displays that the voltage doubler circuit gives one elongated output signal instead of two shorter ones, which matches real life observations.

### Testing the LTC3588-1 in Different Configurations

In this test the LTC3588-1 breakout board was used to compare the different voltage output levels of the LTC3588-1. The test displays the duration of the output signal as well as the number of events advertised by the nRF52. The circuit was shorted between each button push, making sure that no voltage was stored in the capacitors from the previous pushes. See figure 4.59 for the schematic of the circuit that was used when measuring values for the 1.8V output. The pins 8 and 9 where set high accordingly to test for the other voltage configurations [46].

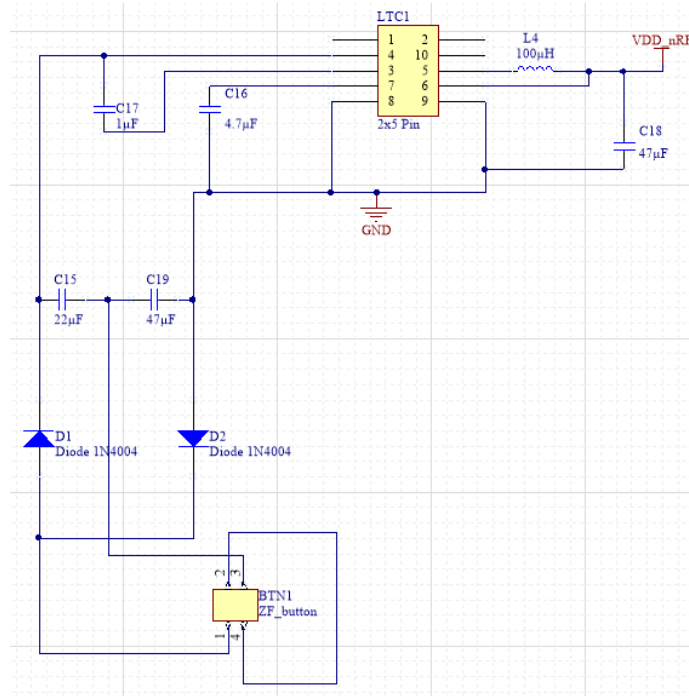


FIGURE 4.59: Schematic for test setup of the LTC3588-1

LTC 3588-1 Test Data							
1.8V		2.5V		3.3V		3.6V	
Packets	Time (ms)	Packets	Time (ms)	Packets	Time (ms)	Packets	Time (ms)
3	63	3	58	2	43	1	36
3	80	3	55	2	33	2	36
3	63	2	58	2	45	2	29
3	80	2	55	2	50	1	35
2	92	2	61	2	50	1	36
2	37	2	52	2	50	1	33
2	65	2	54	2	51	1	35
4	87	2	52	2	53	2	33
3	61	2	55	2	56	2	34
3	86	3	58	2	37	2	34
2.8	71.4	2.3	55.8	2	46.8	1.5	34.1

TABLE 4.1: Results when testing the LTC in its different  $V_{OUT}$  configurations.

The test disclosed a clear coherence between the number of advertised events, duration of the output signal and output voltage configurations of the LTC3588-1. The 1.8V output configuration gave the best results with an average of 2.9 advertised events over a duration of 71ms. These results confirm the previous simulations and calculations. Another interesting observation of the test is that a different number of events is advertised at the same amount of time. This proves the SoftDevice adds up to ten ms randomly between each advertising event, mentioned in section 4.1.2.

## 4.4 Energy Budget

In the energy budget the total theoretical amount of advertising events is calculated based on the total output energy of the electro-mechanical generator and the nRF52s energy consumption, with the stop button firmware code. The efficiency rates of the LTC3588-1 and the nRF52 is also compared, to find the optimal voltage to run the nRF52 on.

### PPK Measurements (4.1.3)

- Start-up energy  $61.7\mu\text{Ws}$  at 1.8V for 8ms
- one BLE event energy  $23.2\mu\text{Ws}$  at 1.8V for 24ms

### AFIG-0007 Measurements (4.3.1)

- 0.14 mWs push
- 0.13 mWs release
- 0.27 mWs push and release

**Theoretical number of advertising events if the regulator circuit has no efficiency loss.**  
See equations (4.19) and (4.20)

$$\text{Start-up} + \text{one BLE event} \times \text{number of packages} = \text{Generator total energy} \quad (4.19)$$

$$\frac{0.27\text{mWs} - 61.7\mu\text{Ws}}{23.2\mu\text{Ws}} \approx \underline{\underline{9 \text{ BLE events}}} \quad (4.20)$$

The AFIG-0007 generator should be able to sustain the nRF52 even when factoring in the efficiency loss in the regulator circuit. It is highly improbable that the final circuit will be upwards to 80% ineffective, which would total 0 packages advertised.

## 4.5 3D Modelling and Printing

SketchUp Free is an easy tool to model simple designs and quick to learn. Designs for the different development kit casings, stop sign and early stages of the button were all modelled in SketchUp to get familiar with 3D-printing and testing out different design ideas.

### 4.5.1 Central and Relayer Casings

When designing the casings for central and relayer it was a simple task of following the nRF52 development kit dimensions. The lid was made so that there was access to the buttons used on the development kit and with holes to put LEDs in the same configuration as on the development kits. See figure 4.60.

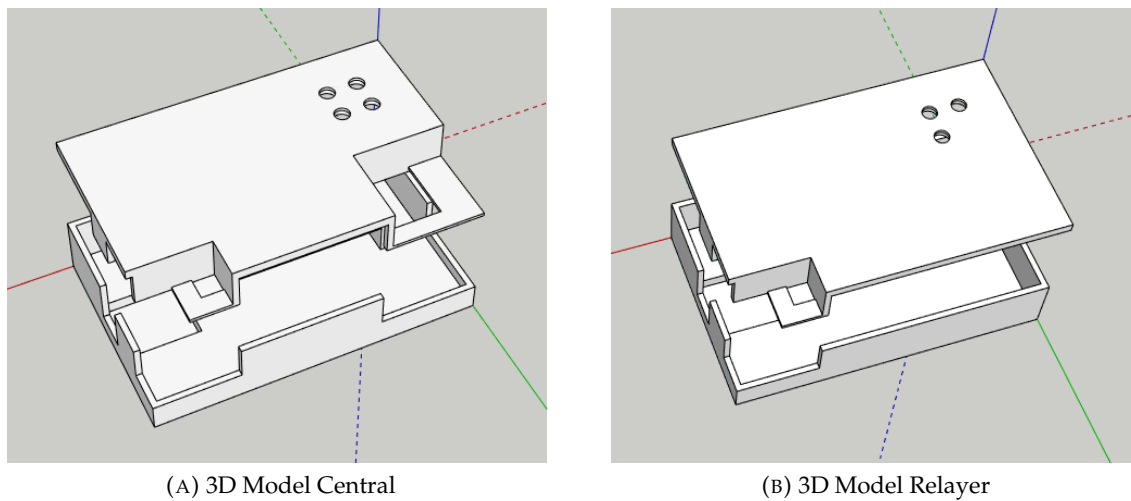


FIGURE 4.60: Central and relay casing modelled in SketchUp

### 4.5.2 Stop Sign

The stop sign was made as a way to showcase the final product and have a visual indication that the stop button works. The idea was to make a simple box with the word "STOP" written on one side and have it be much thinner than the surrounding wall. Then, when a light source is put inside the box, "STOP" lights up. See figures 4.61 and 4.62.

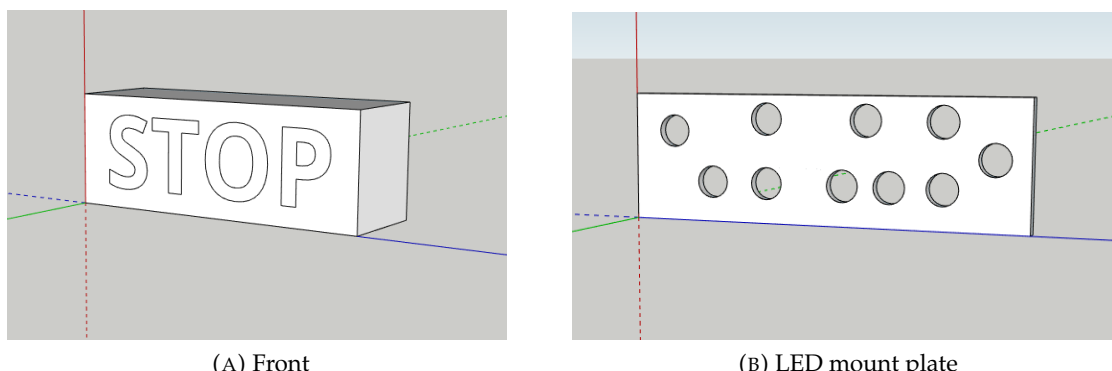


FIGURE 4.61: Stop sign modelled in SketchUp, front and middle part

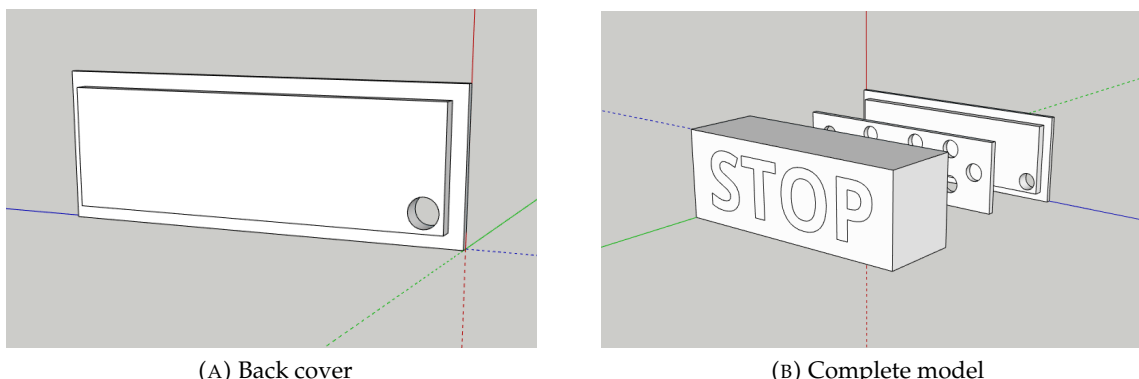


FIGURE 4.62: Stop sign modelled in SketchUp, back plate and complete model

#### 4.5.3 Designing and Printing Mechanical Parts

To get some exercise in printing designs with moving parts, a simple button was made. See figure 4.63. Although this design was not intended to be a part of the final product, it was a good way to understand the considerations needed when designing something like this.

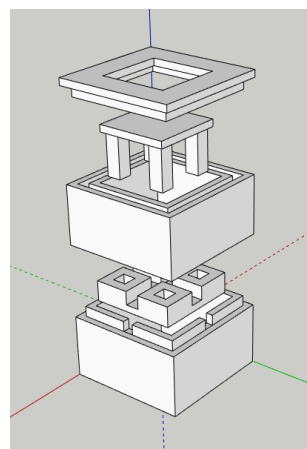


FIGURE 4.63: Button with moving parts

The design in figure 4.63 was made to be spring-loaded, and that in and of itself makes the size of the button bigger than desired for a final product. Since the generator used, already has its own spring, a quick solution was to just use this as a way to have the button return after pressing it. See figure 4.64 for a simple design used for testing if this would suffice.

Another suggested solution was to make a sort of snap-back function where the generator returns to its starting position without having to release the button. See figure 4.65. An advantage with this is that it makes for a more equal push of the button every time. The only problem with this solution was that little experience made it hard to design and print a satisfactory product within the time limits of the project.

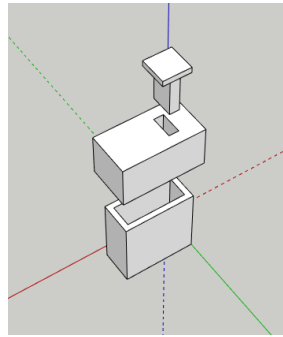


FIGURE 4.64: Test using spring present on the generator

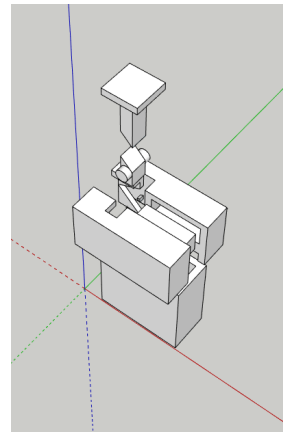


FIGURE 4.65: Trying to implement a snap-back function

#### 4.5.4 Stop Button Casing

Modelling more intricate shapes in the free version of SketchUp can be quite the project, so when a final stop button casing was to be modelled, a new program was needed, and Fusion 360 with a student license seemed like a viable option. Designing a button to replace existing solutions which are present in today's buses may prove to be a very comprehensive task, and so for the purpose of this project, button design is restricted to a prototype that looks and functions in a similar fashion. A simple button can be designed in numerous different ways, but to get a good result there needs to be a set of rules and conditions at the core of the design. Important factors to consider are reliability, longevity and ease of use. The first iteration of the stop button casing was made mainly to get a sense of sizes and make further modelling easier. See figure 4.66.



FIGURE 4.66: First iteration of the stop button casing modelled in fusion 360

After printing the first iteration it became clear that some changes had to be made. Some measurements needed altering as the PCB did not fit in the casing as expected. The actual moving part of the design was also changed to make it more sturdy. See figure 4.67.



FIGURE 4.67: Second iteration of the stop button casing modeled in fusion 360



# Chapter 5

## Results

Chapter five will present what was accomplished during this project. This includes, PCB designs, 3D models, BLE event statistics, and results of system tests done in an articulated bus. Each section has elaborate figures covering both circuit solutions and layouts.

## 5.1 PCB Design and 3D printing

A total of three solutions, each in the form of two PCB designs were finalized as working prototypes. Excluding the fact that the original layout PCB designs have not fully impedance matched antennas, and that some of the capacitor values throughout the PCB designs are not optimized. Finished 3D-modelled products are also displayed in figures in this section.

### 5.1.1 Final Voltage Doubler (PCB Design and Schematics)

The finalized schematics for the voltage doubler solution with correct component values are shown in figure 5.1. In the showcase layout, an additional capacitor, C21, was added with a value of  $10\mu\text{F}$  in order to get as close as possible to the optimal value of  $56\mu\text{F}$ . This additional capacitor was placed in parallel with capacitor C15 which has a value of  $47\mu\text{F}$ . This was done because there was no space for two 1210-sized capacitors in this design.

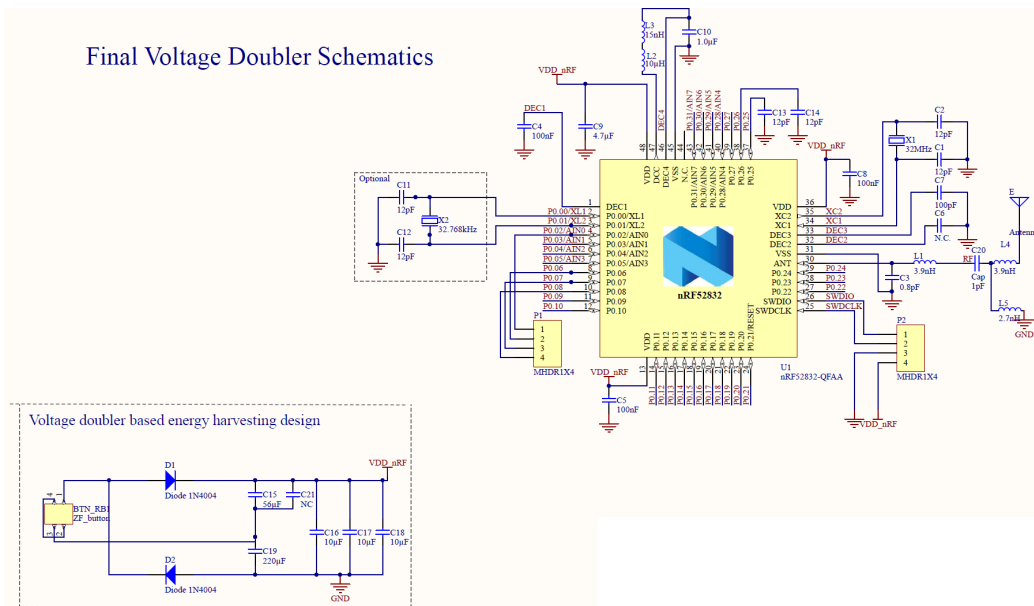


FIGURE 5.1: The finalized schematics for the optimized voltage doubler solution

### Final Voltage Doubler Solution PCB Design (Original Layout)

The final PCB design, Altium Designer file in figure 5.2, and real life photo of the circuit after soldering in figure 5.3. These figures show the final voltage doubler solution in its original layout.

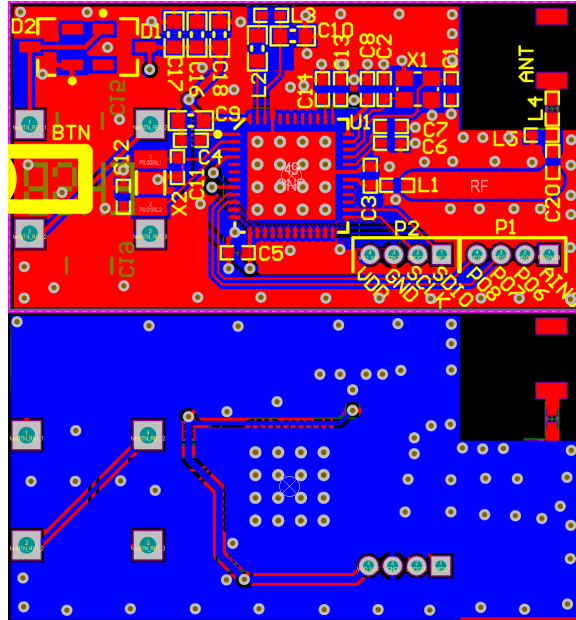


FIGURE 5.2: The original layout PCB design for the voltage doubler solution, measured to be 30.43mm x 16.49mm. The red part being the top layer and the blue part being the bottom layer



FIGURE 5.3: End product of the original layout for the voltage doubler solution

### Final Voltage Doubler Solution PCB Design (Showcase Layout)

The showcase PCB design, Altium Designer file in figure 5.4, and real life photo of the circuit after soldering in figure 5.5. These figures show the final voltage doubler solution in its showcase layout. The via holes in the top-left and bottom-right corners are there to fasten the circuit board inside the stop button chassis.

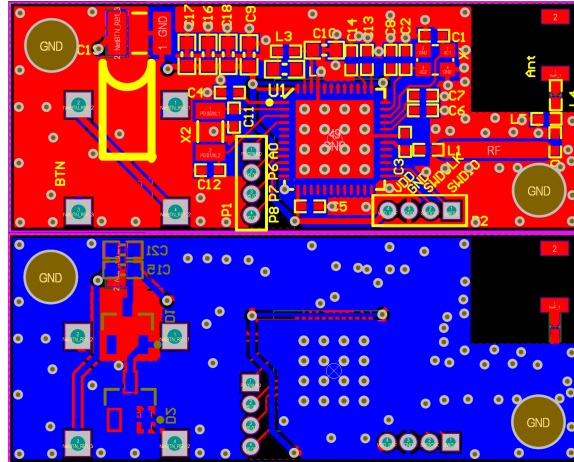


FIGURE 5.4: The showcase PCB design for the voltage doubler solution, measured to be 34.19mm x 13.79mm. The red part being the top layer and the blue part being the bottom layer

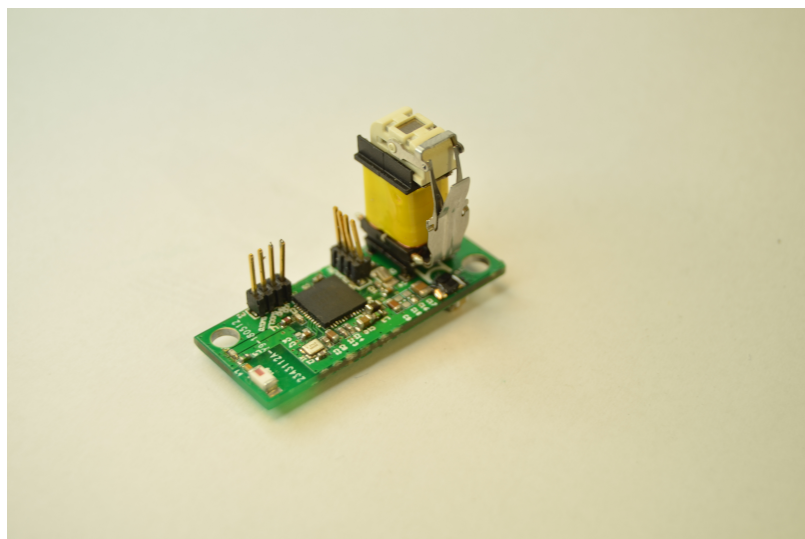


FIGURE 5.5: End product of the showcase layout for the voltage doubler solution

### 5.1.2 Final LTC Solution (PCB Design and Schematics)

The finalized schematics for the solution using the LTC3588-1 in both voltage configurations, in conjunction with the voltage doubler with correct component values are shown in figures 5.6 and 5.7.

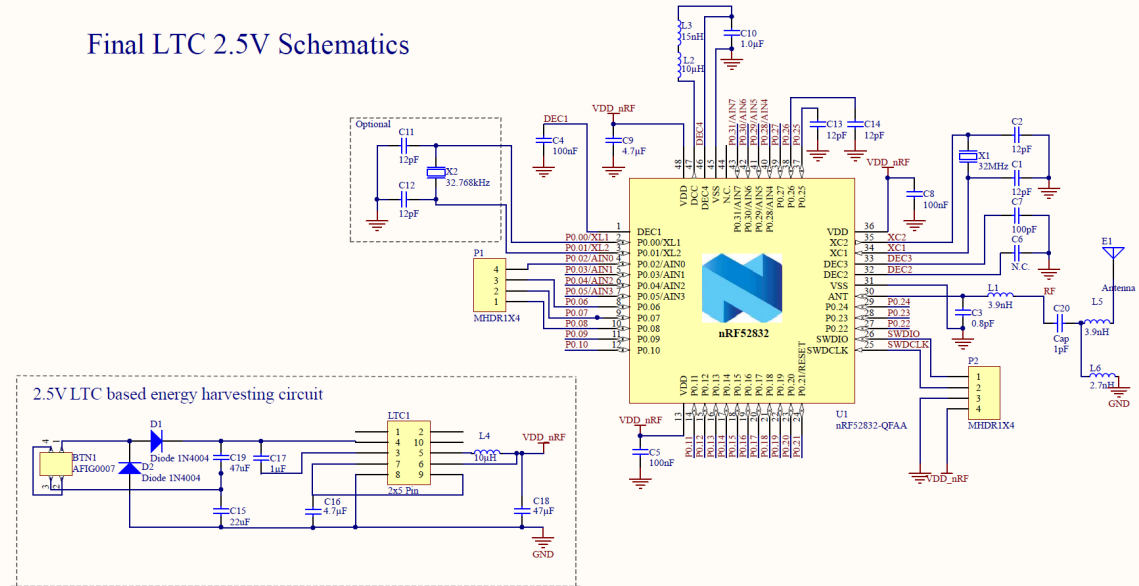


FIGURE 5.6: The finalized schematics for the final LTC solution 2.5V output.

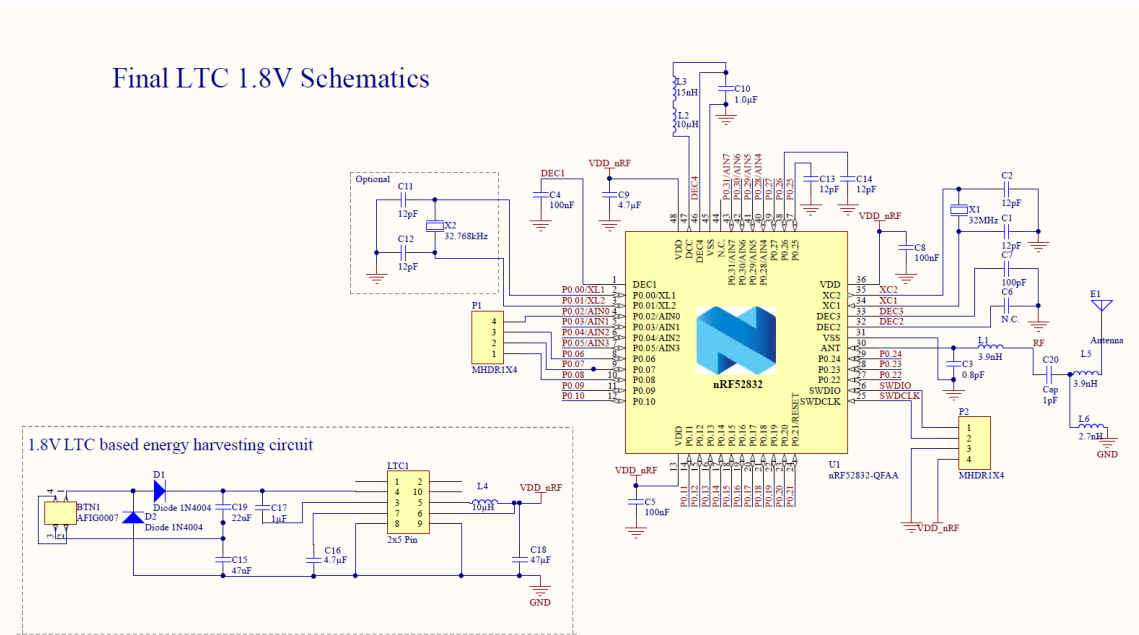


FIGURE 5.7: The finalized schematics for the final LTC solution 1.8V output.

### Final LTC Solution PCB Design (Original Layout)

The final PCB design, Altium Designer file in figure 5.8, and real life photo of the circuit after soldering in figure 5.9. These figures show the final LTC solution in its original layout. This one using the LTC3588-1 in its 1.8V output configuration.

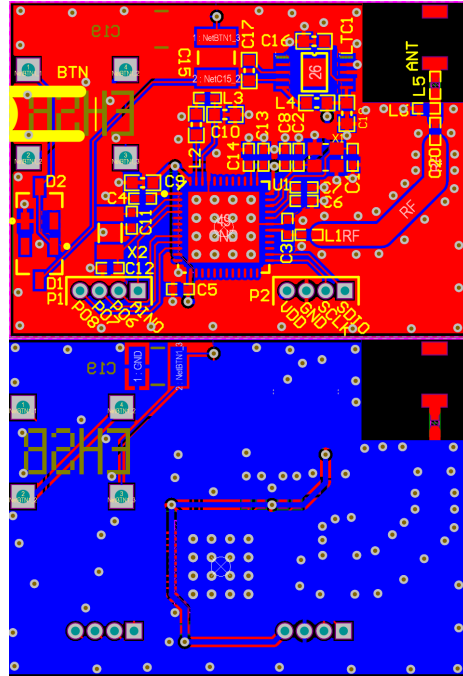


FIGURE 5.8: The original layout PCB design for the LTC solution, measured to be 30.05mm x 22.02mm. The red part being the top layer and the blue part being the bottom layer.



FIGURE 5.9: End product of the original layout for the LTC solution

### Final LTC Solution PCB Design (Showcase Layout)

The showcase PCB design, Altium Designer file in figure 5.10, and real life photo of the circuit after soldering in figure 5.11. These figures show the final LTC solution in its showcase layout. The via holes in the top-left and bottom-right corners are there to fasten the circuit board inside the stop button chassis. This one using the LTC3588-1 in its 2.5V output configuration.

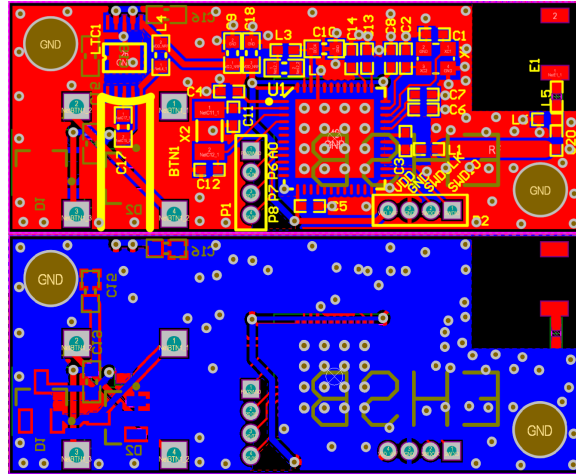


FIGURE 5.10: The showcase PCB design for the LTC solution, measured to be 34.14mm x 13.74mm. The red part being the top layer and the bottom part being the bottom layer

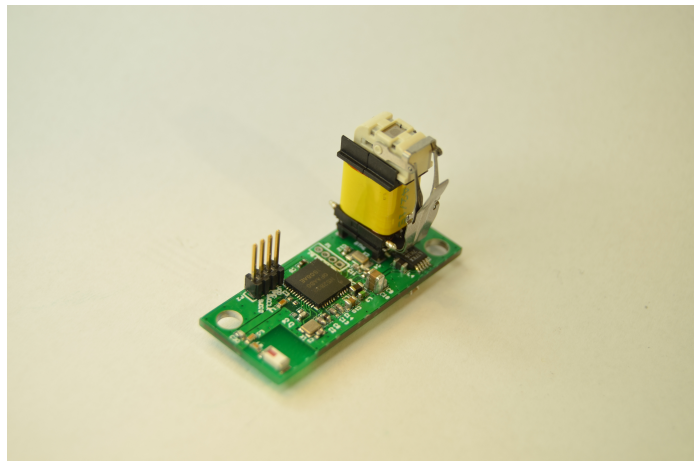


FIGURE 5.11: End product of the showcase PCB design for the LTC solution

### 5.1.3 3D Printing

This section presents the results of 3D prints made to showcase the project.

#### Central and Relayer Casings

A well known problem is that, during printing, the plastic may cool down too quick and pull up from the printing surface. This happened when printing the casings, leading to the lid not fitting properly, but as can be seen in figure 5.12, this was fixed with some tape. The central and relayer casings were used when field testing and held up considerably well.



FIGURE 5.12: Final central and relayer print

#### Stop Sign

Printing the stop sign was a straight forward job. The only element of uncertainty was how thin the writing had to be printed for the light to shine through. The first print did not quite turn out as intended, but after adjusting the model it worked nicely. See figure 5.13.

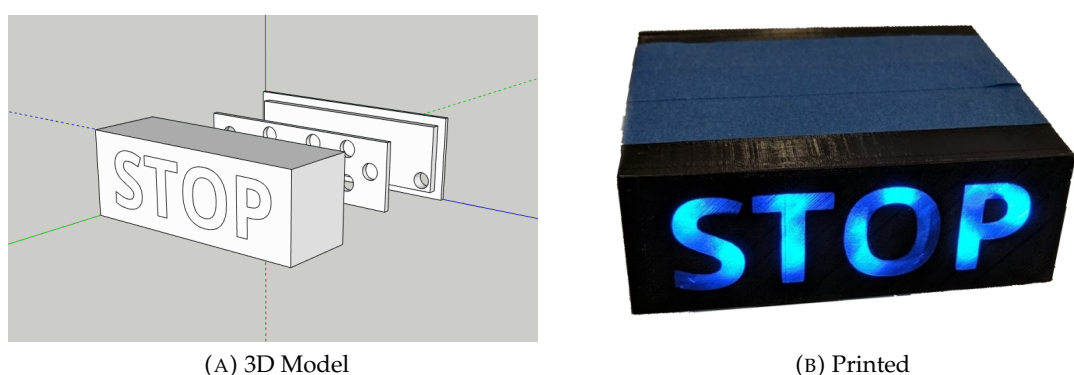


FIGURE 5.13: Stop sign modelled in SketchUp and printed product

**Stop Button Casing**

In the final casing there was made a platform to hold the PCB and support the generator when the button is pushed. See figure 5.14. The design is very similar to existing stop buttons, making it clear straight away what the product is intended for. See figure 5.15.



FIGURE 5.14: Inside the final stop button



FIGURE 5.15: Final printed stop button

## 5.2 BLE Event Statistics

This section contains BLE packet captures of the different solutions done with the BLE packet sniffer software using Wiresharks application interface. In addition, an oscilloscope was used to measure the duration of the regulated output signal from the regulator circuit over the nRF52. Note that the BLE packet sniffer captures one packet per event, so it is possible that it only captured the first packet in the last event, and that the nRF52 did not have enough energy to send the last two packets in the correlated event.

The tests and measurements display average results for the corresponding solution. The number of advertising events typically vary for each test, often between +(1-2) events depending on the push and release force applied to the electro-mechanical generator, and the SoftDevice advertising event randomization.

**Rough estimate of number of advertising packets based on the time the nRF52 is supplied between 1.7V to 3.6V, figure 5.16.**

Events	packets	Time
1	1-3	33ms
2	4-6	58ms
3	7-9	83ms
4	10-12	108ms
5	13-15	133ms
6	16-18	158ms

FIGURE 5.16: Advertising events and packets based on the duration of the input signal to the nRF52, based on 8ms start-up time and 25ms BLE event duration

### 5.2.1 Final Voltage Doubler Solution

No.	Time	Source	Destination	Protocol	Length	Info
1	0.000000000	c8:5d:ad:65:bb:1b	<broadcast>	LE LL	53	ADV_NONCONN_IND
2	0.021753000	c8:5d:ad:65:bb:1b	<broadcast>	LE LL	53	ADV_NONCONN_IND

FIGURE 5.17: BLE packet sniffer capturing two events (4-6 packets) advertised by the stop button

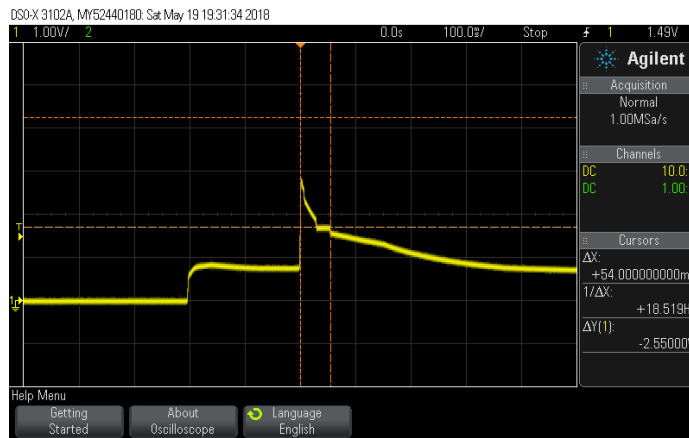


FIGURE 5.18: Oscilloscope measuring the duration of the output signal at 54ms

### 5.2.2 Final LTC Solution, 2.5V Output Voltage

No.	Time	Source	Destination	Protocol	Length	Info
1	0.000000000	f2:37:05:d8:78:e0	<broadcast>	LE LL	53	ADV_NONCONN_IND
2	0.025601000	f2:37:05:d8:78:e0	<broadcast>	LE LL	53	ADV_NONCONN_IND
3	0.051981000	f2:37:05:d8:78:e0	<broadcast>	LE LL	53	ADV_NONCONN_IND
4	0.080698000	f2:37:05:d8:78:e0	<broadcast>	LE LL	53	ADV_NONCONN_IND

FIGURE 5.19: BLE packet sniffer capturing four events (10-12 packets) advertised by the stop button

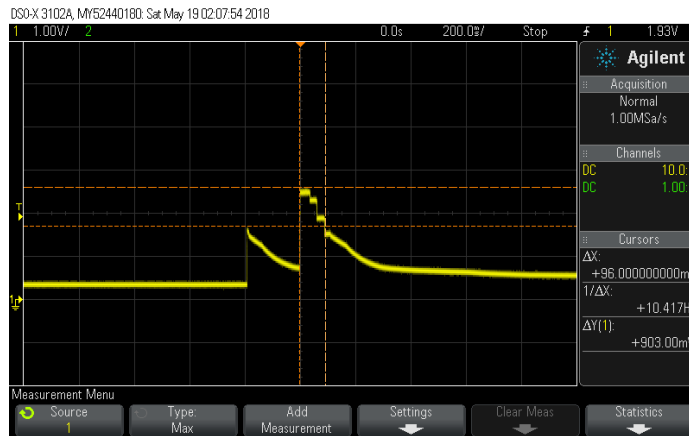


FIGURE 5.20: Oscilloscope measuring the duration of the output signal at 96ms

### 5.2.3 Final LTC Solution, 1.8V Output Voltage

No.	Time	Source	Destination	Protocol	Length	Info
1	0.000000000	fa:b8:b0:48:b9:19	<broadcast>	LE LL	53	ADV_NONCONN_IND
2	0.021026000	fa:b8:b0:48:b9:19	<broadcast>	LE LL	53	ADV_NONCONN_IND
3	0.042861000	fa:b8:b0:48:b9:19	<broadcast>	LE LL	53	ADV_NONCONN_IND
4	0.070265000	fa:b8:b0:48:b9:19	<broadcast>	LE LL	53	ADV_NONCONN_IND
5	0.091577000	fa:b8:b0:48:b9:19	<broadcast>	LE LL	53	ADV_NONCONN_IND

FIGURE 5.21: BLE packet sniffer capturing four events (13-15 packets) advertised by the stop button



FIGURE 5.22: Oscilloscope measuring the duration of the output signal at 105ms

## 5.3 Final System Field Tests

This section contains the final tests of the system using the different solutions. The system was tested in an articulated bus ranging approximately 19 meters. The central and relayer parameters utilized during this test and the stop button parameters can be found in section 4.1.4 and 4.1.4, respectively.

### 5.3.1 Final Voltage Doubler Solution

**Situation one** - The stop button was detected by the central 96 out of 100 times. 96% observation rate.



FIGURE 5.23: Central in front and stop button in back

**Situation two** - The stop button was detected either by the central or relayer 100 out of 100 times. 100% observation rate



FIGURE 5.24: Central in front, relayer in middle/back and stop button in back

### 5.3.2 Final LTC Solution, 1.8V Output Voltage

**Situation one** - The stop button was detected by the central 75 out of 100 times. 75% observation rate.



FIGURE 5.25: Central in front and stop button in back

**Situation two** - The stop button was detected either by the central or relayer 97 out of 100 times. 97% observation rate.



FIGURE 5.26: Central in front, relayer in middle/back and stop button in back

### 5.3.3 Final LTC Solution, 2.5V Output Voltage

**Situation one** - The stop button was detected by the central 99 out of 100 times. 99% observation rate.



FIGURE 5.27: Central in front and stop button in back

**Situation two** - The stop button was detected either by the central or relay 99 out of 100 times. 99% observation rate.



FIGURE 5.28: Central in front, relay in middle/back and stop button in back



## Chapter 6

# Conclusion and Discussion

Throughout this thesis, a series of questions have been presented. This chapter is dedicated to using the tests and results performed to reflect upon these questions, and how they were answered. This chapter will present a conclusion for the entirety of the project, and deem whether it was a success or not. The discussion will discuss what was done well and what could have been done better. What can be done to avoid future mishaps of the same nature, and how to fix any malfunctions or errors that still are present. Further work will present the most pressing concerns for the future of this project, and what aspects are subject of improvement and potential implementations.

### 6.1 Discussion

This section will discuss results, choices made before and during the project, and problems that occurred consecutively.

#### 6.1.1 Code

All prototypes performed surprisingly well in the final tests. It should be mentioned that all results were performed with the nRF52s LDO regulator enabled and not the DC/DC regulator. Measurements and calculations carried out during firmware development suggested that the DC/DC regulator would be noticeably more energy efficient than the LDO regulator. The reason for the sudden change of internal regulator, was because the firmware code would not flash correctly to the nRF52 in the final stop button designs. It is suspected that it has something to do with the external LC-filter that the DC/DC regulator utilizes when it regulates the output power from the regulator circuit. It is possible that this problem could have been avoided if the nRF52 reference design used as a base for the final designs had not been altered as much as they were. Based upon the energy measurements carried out during the firmware development the nRF52 should be about 40% percent less effective when utilizing the LDO regulator, which is substantial. Even without the DC/DC regulator, the results were more than satisfying enough.

The TX power setting in the stop button application was not altered during firmware development. By standard it is set to 0dBm. Even though power can be saved by setting a lower TX power, it was decided not to do so. Lets say that the stop button at 0dBm can advertise 50 meters. In a bus that is 20 meters it probably does not seem necessary to have the stop button advertise the last 30 meters. If the stop button were to advertise at a weaker signal strength, the weaker signal would be more easily affected by interference and electromagnetic noise. Something that can happen in worst case scenarios.

### 6.1.2 Transmission Range

As expected, the final LTC solutions advertised more BLE events at a single push of a button than the final voltage doubler solution. The thought was that the final system field test results would reflect the average difference in the number of BLE events advertised by the different solutions. This proved to be wrong. At some point, when two or more BLE events are advertised by the stop button, the scanning devices will observe the advertising event, no matter what, at least within the 20 meter range of the bus. Still, there is no downside to having the stop button advertise a few extra events above this limit, seeing as today, many people carry wireless devices that can affect the system in form of interference. The fact that in very crowded buses there are several potential devices that can cause interference. A fully crowded bus will also disturb the central to stop button line of sight. This taken into consideration, it seems like a good idea to choose a solution that advertise as many BLE events as possible. Of course, too many BLE events generated could again be a problem if the stop button advertises for several seconds on each button push.

### 6.1.3 Cost

Another discussion point is if the relayer should be used or not. Even though the relay provides greater redundancy to the system, it is not necessary to use it unless the central to stop button range exceeds 20 meters, possibly even further. Because of the relative time constraint of the project, the system was not tested in other application areas. It is possible that the system without the relay could be applicable to distances exceeding 20 meters, if the system is in an open area with line of sight and few to none interference sources. However, the relay is recommended due to the fact that worst case scenarios can occur, as stated in the section above.

The voltage doubler solution is the cheapest solution as it has a total estimate of 29.96\$ for the components, in comparison to the LTC solution which has an estimate of 33.90\$. For about 4\$ more you essentially get a solution that produces on average two BLE events more, and is safe against overload due to the LTC3588-1 regulating the voltage going in to the nRF52. It is a subject of discussion whether the LTC solution is worth the four extra dollars or not. Further system tests at worst case scenarios and stress tests of the solutions, would likely prove if it is or not.

### 6.1.4 Final System Field Tests

The system tests disclosed very good results across the different solutions. The LTC solution with a 1.8V output voltage, which was expected to be the best solution, underperformed. The reason why the observation rate of this specific solution was as low as 75% without the relay, was likely due to the original layout design being used instead of the showcase layout. As stated in section 4.2.2 the original layout PCB designs has not fully impedance matched antennas in contrary to the showcase layouts. Even though the original layout had a disappointing observation rate, it was interesting to see how much the original layout results deviated from the showcase layout results. In the same situation when the relay was connected to the system the observation rate rose to 97%. This is likely due to the extended range the relay provides, as the poor impedance matching in the original layouts is believed to cause a lower range than desired.

During the field tests, there were some faulty components or connections on the LTC solution outputting 1.8V, causing it to advertise 2-3 BLE events per button push, instead of

the expected average of five. With the voltage doubler solution sending the same amount of events, but having a 21% better observation rate, the theory that the PCB design with a poor impedance matching caused the lower observation rate, is strengthened. It should be mentioned that some of the events during all system tests likely was lost due to interference, electromagnetic noise, or the varying push and release force applied to the electro-mechanical button.

### 6.1.5 Circuit Design Choices

The voltage doubler in both solutions is designed with imbalanced capacitor values, making the circuit only produce one output signal instead of two. It essentially results in the nRF52 and LTC3588-1 only having to start up once per button push, and not twice, preserving energy, and increasing both the nRF52 and LTC3588-1s total lifetime. This was the main reason why the internal full-wave bridge rectifier in the LTC3588-1 was bypassed using a voltage doubler on the  $V_{IN}$  (pin 4) with imbalanced capacitors.

### 6.1.6 Work Environment

Throughout the project a lot of components malfunctioned or stopped working entirely, which spurred a lot of frustration. It is highly probable that the circuits and components during the project have been affected or damaged by ESD, due to a work environment that is not ESD secure. Another possible reason why the components, especially the LTC3588-1 malfunctioned was because it might have been exposed to higher voltages than its absolute maximum rating of 20V. There has been a lot of trial and error during this project, which sometimes has lead to very high voltage peaks if the circuitry was not connected properly or if capacitors are charged before introducing a load. It should also be mentioned that the LTC3588-1 is designed for vibration energy harvesting and not for energy pulses like the ones generated by the AFIG-0007. It is not unthinkable that some of the LTC3588-1s broke because of this fact. The absolute maximum rating of the LTC3588-1 is 20V, and with poorly optimized capacitors in the rectifier circuits it was exposed to, voltage peaks higher than 20V may have been generated.

If the work environment had been ESD secured and all necessary equipment, specifically a DC power analyzer, had been available throughout the project, the time it took to produce a functional circuit would likely be reduced by a few weeks, allowing for a more optimized final result as there would be more time to test what components were more efficient, and to do additional field tests.

### 6.1.7 Simulations of the LTC3588-1

In an energy pulse like the one output by the AFIG-0007, it is preferred to use as much as possible of the total energy output. In the AFIG-0007s case the output voltage varies from 0 to 20V, where the voltage between 3.77 and 20V is what the LTC3588-1 can use to output 1.8 and 2.5V, with the 3.3 and 3.6V needing a voltage input of 4.73V [46]. Based on this information alone it is safe to assume that the 3.3 and 3.6V output voltages will be less effective than the two only requiring 3.77V. The simulation in figure 4.57 shows that the LTC3588-1s lowest voltage output is to be preferred in this particular project, as it gives the necessary output voltage, and outputs for the longer amount of time.

Figure 4.1 shows actual tests done with the LTC3588-1s voltage output configurations, which further proves the 1.8V output to be the most efficient of the LTC3588-1s voltage configurations. As for the BLE event statistics shown in figure 5.21 shows the 1.8V output

advertising five BLE events on average, which no other configuration tests in that chapter were able to. All of these factors point to the 1.8V output configuration being the most efficient output voltage, even though the final test results in section 5.3 shows the 1.8V output configuration to have the lowest observation rate, although this is due to the earlier discussed faulty circuit board used.

### 6.1.8 Energy Measurements

Sadly, it was not enough time to measure the energy consumption of the final solutions using the DC power analyzer at Nordic Semiconductor. It would have been interesting to see exactly how many packets each of the solutions advertise, not just the approximate number of packets the BLE packet sniffer used in section 5.2 provides. Although the PPK measurements provided pretty accurate results, the nRF52s energy consumption was still measured on the nRF52DK, which will likely lower the measured circuits efficiency somewhat. The energy measurement of the nRF52 at 1.8V was estimated and not measured because of the restrictions of the PPK, but the estimated values were later confirmed by a DC power analyzer, which is a highly reliable tool. In the DC power analyzer test the solder bridges between the MCU and nRF52 was cut, enabling it to measure only over the nRF52.

## 6.2 Conclusion

The conclusion to this thesis is that the energy harvesting stop button is a viable alternative to today's bus stop buttons. This thesis proves that the EHSB has the range and observation rate required to function as a bus stop button to be utilized in the intended environment. This is by no means a finished product, but supplies the data and a proof of concept solution that the potential is there to make a device custom-made for this application.

A considerable amount of time has been dedicated to develop two stop button PCBs, both working as intended with no glaring issues. The differences between the two are mainly their redundancy factor and presumed longevity. There is also sufficient data to support the possibility to apply this concept in other applications, such as simple remotes and switches.

## 6.3 Further Work

This section will focus on what tasks would be prioritized first for further development of this idea. The tasks mentioned are what was found to be the most pressing tasks for future work, although there may be numerous other tasks to tackle. As stated before, the electro-mechanical switch can produce a total of 0.27mWs. This energy budget can be better utilized by further exploring and developing more energy efficient designs both in terms of firmware and hardware.

### 6.3.1 Synchronous Rectification

What might be the most pressing concern is that there was not done any research what so ever on synchronous rectification, as this seems to be a viable option for most energy harvesting circuits. The discovery of this method of rectification was made too late into the process to start designing a circuit around it, which is why this would be heavily focused if there were more time.

### 6.3.2 Optimization of Code

Another workload within further work would be to optimize the code more, even though it works and is already energy efficient enough to transmit a reasonable amount of BLE events. There is also an eagerness to, if possible, get a customized SoftDevice that bypasses the LFRC calibration process, advertising does not have to be as accurate as other processes. The calibration process drains  $\approx 600\mu\text{Ws}$  over 10 ms, which could be avoided. It is also possible to entirely bypass the SoftDevice, writing very bare bone code that utilizes the radio in a most effective way. The downside about bypassing the SoftDevice is that the product probably would no longer be within the BLE specification. The reason why the application code with the DCDC regulator enabled caused the nRF52 to behave strangely should also be uncovered. The DCDC regulator is less effective compared to the LDO regulator to not be used, at least in this specific application.

### 6.3.3 Mechanical Engineering

Although the current solution for button and central casing works fine, the 3D-prints used are pretty simple as no group members had any major experience with 3D modelling. The casings made in this project are only meant for use in the project presentation and are not made to be put in a bus. In potential future phases there would be a need for stop button and central casings that are engineered to be in a bus. Preferably another option than 3D printing should be used, as 3D printing is not the most cost effective way to produce the designs.

### 6.3.4 Central and Relayer PCBs

For this project, nRF52 DKs were used for the central and relayer, as there was no time making a circuit of that scale within the time constraints set in this project. In the future, a custom PCB design for the central and relayer would be preferred, both to optimize the circuit for the specific task it is set to do, and to give it its own design. This would also likely make the central and relayer noticeably smaller, making them easier to mount in the front and center of a bus.

#### Other Possible Implementations

- Central application interference
- GPS support for system integration of next stop location
- Other applications for the button
- Possibilities for multiple functions with a single button



# List of Figures

2.1	Basic MCU functional block diagram [7] . . . . .	3
2.2	nRF52 SoC functional block diagram [6] . . . . .	4
2.3	Bluetooth network topology . . . . .	4
2.4	BLE channel overview[32] . . . . .	5
2.5	BLE advertising packet structure[10] . . . . .	5
2.6	BLE advertising payload structure . . . . .	5
2.7	GATT data exchange process [18] . . . . .	7
2.8	GATT Profile structure [18] . . . . .	7
2.9	nRF52 software architecture . . . . .	8
2.10	Detailed nRF52 software architecture [41] . . . . .	8
2.11	The general system of energy harvesting . . . . .	9
2.12	Voltage before and after regulation [15] . . . . .	10
2.13	Comparison of types of energy storage devices. [44]	10
2.14	Inside the AFIG-0007s casing [50] . . . . .	11
2.15	Schematic representation of the piezoelectric effect in an X -quartz plate. The polarities indicated follow IEEE Standards on Piezoelectricity [19]. . . . .	12
2.16	Comparison between half- and full-wave rectification [20] . . . . .	13
2.17	Full-wave bridge rectifier [16] . . . . .	13
2.18	Schematics for both a half-wave and a full-wave voltage doubler [49] . . . . .	14
2.19	The difference between a normal step-down converter and a synchronous step-down converter.[1]. . . . .	15
2.20	A full-wave bridge rectifier supplying a buck-converter with power and an illustration of the output over a load. [3] . . . . .	15
2.21	Block diagram of the LTC3588-1 [46] . . . . .	16
2.22	Basic PCB layers [5] . . . . .	18
3.1	nRF52 internal regulator setup [34] . . . . .	21
3.2	ZF Electronics energy harvesting generator [12] . . . . .	22
3.3	Schematics that show the most efficient capacitor and inductor values for the LTC3588-1 and its voltage doubler . . . . .	24
3.4	Schematics that show the most efficient capacitor values for the voltage dou- bler circuit . . . . .	25
4.1	One BLE packet before and after code reduction displayed in the nRF Connect application . . . . .	28
4.2	ehsb_nordic_b application BLE advertising event. The three current peaks in the red area is the nRF52 advertising on channels 37, 38 and 39. . . . .	29
4.3	LED mapping relayer . . . . .	30
4.4	Button layout and LED mapping central . . . . .	31
4.5	Flowchart central and relayer application code . . . . .	32
4.6	PPK mounting . . . . .	33
4.7	nRF52DK voltage with PPK mounted on top . . . . .	34
4.8	PPK test setup [37] . . . . .	34

4.9	OPP generated results across different voltage levels, one BLE event . . . . .	35
4.10	PPK - LFXO - <b>startup + one BLE event</b> . . . . .	35
4.11	PPK - LFRC - <b>startup + one BLE event</b> . . . . .	35
4.12	PPK - LFXO - <b>one BLE event</b> . . . . .	35
4.13	PPK - LFRC - <b>one BLE event</b> . . . . .	35
4.14	Startup LFXO at 2.85V . . . . .	36
4.15	Startup LFRC at 2.85V . . . . .	36
4.16	DC Power Analyzer measuring current consumption of an LFRC calibration event. The LFRC calibration takes place between the cursors in both figures. . . . .	37
4.17	DC Power Analyzer measuring current consumption on the nRF52 at 1.8V . . . . .	39
4.18	PPK and DC power analyzer data comparison . . . . .	40
4.19	PPK measuring the additional current consumption . . . . .	40
4.20	DC power analyzer measuring the additional current consumption . . . . .	40
4.21	Stop button advertising 5 events, LFXO . . . . .	42
4.22	Current consumption of scanning central . . . . .	42
4.23	Scan parameters in relation to advertising and connection events . . . . .	43
4.24	Central in front and stop button in back . . . . .	43
4.25	Central in front, relay in back/middle and stop button i back . . . . .	43
4.26	Relay current consumption when scanning and communicating with the central. . . . .	44
4.27	Scan parameters in relation to advertising and connection events . . . . .	45
4.28	Central current consumption, new parameters . . . . .	45
4.29	Relay current consumption, new parameters . . . . .	45
4.30	Relay current consumption, new parameters, scan timeout at 120s . . . . .	45
4.31	nRF52 debug out setup [26] . . . . .	46
4.32	Piezoelectric elements were hard to get repetitive results on compared to the button, which gives the same output every time . . . . .	48
4.33	Single pulses first. Then the complete pulse, which is able to power the nRF52 for 40ms . . . . .	49
4.34	Holds a voltage able to power the nRF52 for 62ms . . . . .	49
4.35	The two voltage doubler solutions put up against each other. Both measured over a $2.2k\Omega$ resistor . . . . .	50
4.36	Schematics for the two rectifier circuits . . . . .	51
4.37	PCB design for the two rectifier circuits . . . . .	52
4.38	Schematics for the first LTC3588-1 circuit with its reference design and pins to configure the output voltage. . . . .	53
4.39	PCB for the first LTC3588-1 circuit with its reference design and pin headers to configure the output voltage and measure voltages between C1 and C3. . . . .	53
4.40	An LTC3588-1 break-out board from <a href="https://jlpcb.com/">https://jlpcb.com/</a> with all components mounted. . . . .	54
4.41	Schematics for the nRF52s reference design with additional pin headers for making measurements and programming the SoC. . . . .	55
4.42	PCB for the nRF52s reference design with additional pin headers for making measurements and programming the SoC. . . . .	55
4.43	Via stitching and shielding can be seen as small dark spots . . . . .	56
4.44	A so called finger before(left) and after removal(right) . . . . .	56
4.45	Saturn PCB Design Toolkit with the key values set . . . . .	58
4.46	LTC3588-1 block diagram, where instead of the current going in on pins PZ1 and PZ2, an already rectified signal goes directly into the $V_{IN}$ pin. . . . .	59

4.47 Schematics of the circuit in Altium, where the full-wave voltage doubler rectifies the energy from the button and sends it directly to pin 4 on the LTC3588-1. Pins 1 and 2 (PZ0 and PZ1) are not connected as the source connects directly to $V_{IN}$ . Note: component values here are not final. . . . .	60
4.48 AFIG-0007 circuit diagram (B) . . . . .	62
4.49 Push . . . . .	62
4.50 Release . . . . .	63
4.51 Total energy across different $R_1$ . . . . .	63
4.52 Measurements of the AFIG-0007 pulse over a total resistance of $33.77\Omega$ , $R_1 = 100\Omega$ . . . . .	63
4.53 The single button pulse used as the voltage source in simulations. $R_1$ set at $2.6k\Omega$ . . . . .	64
4.54 Current drawn by the LTC3588-1 at 10V DC input. The four configurations are all based on the same load, set to 100mA. $V_1 = 1.8V$ , $V_2 = 2.5V$ , $V_3 = 3.3V$ and $V_4 = 3.6V$ . . . . .	65
4.55 Efficiency diagram simulated in LTspice, of the LTC3588-1's output efficiency at its four $V_{OUT}$ settings . . . . .	65
4.56 The LTC3588-1's $V_{OUT}$ simulations over time for the four $V_{OUT}$ configurations with the same load of 100mA and an inductor value of $100\mu H$ . . . . .	66
4.57 Circuit schematics in LTspice of the four LTC3588-1 $V_{OUT}$ configurations. Simulations are based on these schematics with an input load of 100mA. . . . .	66
4.58 LTC3588-1 with different rectifying circuits, the diagram displays the energy harvested from both push and release, with the output configuration set at 1.8V and a constant load of 100mA. . . . .	67
4.59 Schematic for test setup of the LTC3588-1 . . . . .	68
4.60 Central and relayer casing modelled in SketchUp . . . . .	70
4.61 Stop sign modelled in SketchUp, front and middle part . . . . .	70
4.62 Stop sign modelled in SketchUp, back plate and complete model . . . . .	71
4.63 Button with moving parts . . . . .	71
4.64 Test using spring present on the generator . . . . .	72
4.65 Trying to implement a snap-back function . . . . .	72
4.66 First iteration of the stop button casing modelled in fusion 360 . . . . .	73
4.67 Second iteration of the stop button casing modeled in fusion 360 . . . . .	73
 5.1 The finalized schematics for the optimized voltage doubler solution . . . . .	75
5.2 The original layout PCB design for the voltage doubler solution, measured to be $30.43mm \times 16.49mm$ . The red part being the top layer and the blue part being the bottom layer . . . . .	76
5.3 End product of the original layout for the voltage doubler solution . . . . .	76
5.4 The showcase PCB design for the voltage doubler solution, measured to be $34.19mm \times 13.79mm$ . The red part being the top layer and the blue part being the bottom layer . . . . .	77
5.5 End product of the showcase layout for the voltage doubler solution . . . . .	77
5.6 The finalized schematics for the final LTC solution 2.5V output. . . . .	78
5.7 The finalized schematics for the final LTC solution 1.8V output. . . . .	78
5.8 The original layout PCB design for the LTC solution, measured to be $30.05mm \times 22.02mm$ . The red part being the top layer and the blue part being the bottom layer. . . . .	79
5.9 End product of the original layout for the LTC solution . . . . .	79

---

5.10 The showcase PCB design for the LTC solution, measured to be 34.14mm x 13.74mm. The red part being the top layer and the bottom part being the bottom layer . . . . .	80
5.11 End product of the showcase PCB design for the LTC solution . . . . .	80
5.12 Final central and relay print . . . . .	81
5.13 Stop sign modelled in SketchUp and printed product . . . . .	81
5.14 Inside the final stop button . . . . .	82
5.15 Final printed stop button . . . . .	82
5.16 Advertising events and packets based on the duration of the input signal to the nRF52, based on 8ms start-up time and 25ms BLE event duration . . . . .	83
5.17 BLE packet sniffer capturing two events (4-6 packets) advertised by the stop button . . . . .	84
5.18 Oscilloscope measuring the duration of the output signal at 54ms . . . . .	84
5.19 BLE packet sniffer capturing four events (10-12 packets) advertised by the stop button . . . . .	84
5.20 Oscilloscope measuring the duration of the output signal at 96ms . . . . .	84
5.21 BLE packet sniffer capturing four events (13-15 packets) advertised by the stop button . . . . .	85
5.22 Oscilloscope measuring the duration of the output signal at 105ms . . . . .	85
5.23 Central in front and stop button in back . . . . .	86
5.24 Central in front, relay in middle/back and stop button in back . . . . .	86
5.25 Central in front and stop button in back . . . . .	86
5.26 Central in front, relay in middle/back and stop button in back . . . . .	86
5.27 Central in front and stop button in back . . . . .	87
5.28 Central in front, relay in middle/back and stop button in back . . . . .	87

# Bibliography

- [1] Zhong Nie Ali Emadi Alireza Khaligh and Young Joo Lee. *Integrated Power Electronic Converters and Digital Control (Chapters 11 through 13)*. CRC Press, 2009.
- [2] *Buck-boost converters*. Available at <http://www.learnabout-electronics.org/PSU/psu33.php> 12.05.2018.
- [3] *Buck-converters*. Available at <http://www.learnabout-electronics.org/PSU/psu31.php> 12.05.2018.
- [4] Richard H. Caro. *Wireless Networks for Industrial Automation, Fourth Edition*. ISA, 2014.
- [5] *Circuit Board Drawing*. Available at <https://www.ourpcb.com/wp-content/uploads/2017/05/Circuit-Board-Drawing1.jpg> 16.04.2018.
- [6] *Cortex-M4F Processor*. Available at <http://www.agenox.com/blog/nordic-announces-new-line-of-cortex-m4-ble-socs/> 16.04.2018.
- [7] J. H. Davies. *MSP430 Microcontroller Basics*. Elsevier Ltd., 2008.
- [8] *Designing Mechanical Parts The Whoosh Machine*. Available at [https://www.shapeways.com/tutorials/designing\\_mechanical\\_parts\\_3d\\_printing\\_the\\_whoosh](https://www.shapeways.com/tutorials/designing_mechanical_parts_3d_printing_the_whoosh) 16.05.2018.
- [9] *Edge Coupled Microstrip Impedance*. Available at <https://www.eeweb.com/tools/edge-coupled-microstrip-impedance> 19.05.2018.
- [10] Digi-Key's North American Editors. *Comparing Low Power Wireless Technologies (Part 2)*. Available at <https://www.digikey.be/en/articles/techzone/2017/dec/comparing-low-power-wireless-technologies-part-2> 25.04.2018.
- [11] Nils Edvinsson. *Energy Harvesting Power Supply for Wireless Sensor Networks*. Available at <https://uu.diva-portal.org/smash/get/diva2:662618/FULLTEXT01.pdf> 18.04.2018.
- [12] ZF Electronics. *Energy Harvesting Generator*. Available at <http://switches-sensors.zf.com/us/product/energy-harvesting-generators> 16.04.2018.
- [13] Maurizio Di Paolo Emilio. *Microelectronic Circuit Design for Energy Harvesting Systems*. Springer, 2016.
- [14] Alper Erturk and Daniel J. Inman. *Piezoelectric Energy Harvesting*. Wiley, 2011.
- [15] *Faults in Power Supplies*. Available at [http://www.angelfire.com/planet/funwithtransistors/Book\\_TS\\_CHAP-5.html](http://www.angelfire.com/planet/funwithtransistors/Book_TS_CHAP-5.html) 16.04.2018.
- [16] *Full-wave Bridge Rectifier*. Available at <https://hackaday.com.files.wordpress.com/2014/12/bridge-rectifier-shunt-before.png> 16.04.2018.
- [17] GAP. Available at <https://learn.adafruit.com/introduction-to-bluetooth-low-energy/gap> 04.04.2018.
- [18] GATT. Available at <https://learn.adafruit.com/introduction-to-bluetooth-low-energy/gatt> 04.04.2018.
- [19] G. Gautschi. *Piezoelectric Sensors: Force, Strain, Pressure, Acceleration and Acoustic Emission Sensors, Materials and Amplifiers*. Springer, 2002.

- [20] *Half- and full-wave Rectification*. Available at <http://www.eblogbd.com/wp-content/uploads/2013/01/half-and-full-wave-rectification.jpg> 16.04.2018.
- [21] *Impedance-Calculator*. Available at <https://www.multi-circuit-boards.eu/en/pcb-design-aid/impedance-calculation.html> 19.05.2018.
- [22] Krzysztof Iniewski. *Optical, Acoustic, Magnetic, and Mechanical Sensor Technologies* (Pages 281-314). CRC Press, 2012.
- [23] DATAQ Instruments. *What's All This PPM Stuff?* Available at <https://www.dataq.com/blog/data-logger/whats-all-this-ppm-stuff/> 11.05.2018.
- [24] *Introduction to Linear Voltage Regulators*. Available at <https://www.digikey.com/en/maker/blogs/introduction-to-linear-voltage-regulators> 14.05.2018.
- [25] Haresh Khemani. *Inductive Transducers*. Available at <https://www.brighthubengineering.com/hvac/62717-about-inductive-transducers/> 08.05.2018.
- [26] Li. *Programming External/custom NRF52832 Board Using NRF52-DK*, *Forumpost*. Available at <https://devzone.nordicsemi.com/f/nordic-q-a/20536/programming-external-custom-nrf52832-board-using-nrf52-dk> 15.05.2018.
- [27] SEGGER Microcontroller Systems LLC. *Segger Embedded Studio IDE*. Download available at <https://www.segger.com/products/development-tools/embedded-studio/> 02.05.2018.
- [28] Inc. Measurement Specialities. *Piezo Film Sensors Technical Manual*. Available at <https://www.sparkfun.com/datasheets/Sensors/Flex/MSI-techman.pdf> 18.04.2018.
- [29] *NRF52832*. Available at <https://www.nordicsemi.com/eng/Products/Bluetooth-low-energy/nRF52832> 03.04.2018.
- [30] Panasonic. *DB3X209K0L Data Sheet*. Available at [https://industrial.panasonic.com/content/data/SC/ds/ds4/DB3X209K0L\\_E.pdf](https://industrial.panasonic.com/content/data/SC/ds/ds4/DB3X209K0L_E.pdf) 11.05.2018.
- [31] *PCB Basics*. Available at <https://learn.sparkfun.com/tutorials/pcb-basics-all.pdf> 05.04.2018.
- [32] Nordic Semiconductor. *Bluetooth Smart and the Nordic's Softdevices - Part 1 GAP Advertising*. Available at <https://devzone.nordicsemi.com/b/blog/posts/bluetooth-smart-and-the-nordics-softdevices-part-1> 25.04.2018.
- [33] Nordic Semiconductor. *Nordic UART Service Client*. Available at [https://infocenter.nordicsemi.com/index.jsp?topic=%2Fcom.nordic.infocenter.sdk5.v14.2.0%2Fble\\_sdk\\_app\\_nus\\_c.html&cp=4\\_0\\_0\\_4\\_2\\_0\\_5](https://infocenter.nordicsemi.com/index.jsp?topic=%2Fcom.nordic.infocenter.sdk5.v14.2.0%2Fble_sdk_app_nus_c.html&cp=4_0_0_4_2_0_5) 25.04.2018.
- [34] Nordic Semiconductor. *nRF52832 Internal Power Regulating*. Available at <http://infocenter.nordicsemi.com/index.jsp?topic=%2Fcom.nordic.infocenter.nrf52832.ps.v1.1%2Fpower.html> 03.05.2018.
- [35] Nordic Semiconductor. *nRF52832 Product Specification v1.4*. Available at [http://infocenter.nordicsemi.com/pdf/nRF52832\\_PS\\_v1.4.pdf](http://infocenter.nordicsemi.com/pdf/nRF52832_PS_v1.4.pdf) 09.04.2018.
- [36] Nordic Semiconductor. *Online Power Profiler*. Available at <https://devzone.nordicsemi.com/power/> 19.04.2018.
- [37] Nordic Semiconductor. *PPK User Guide v2.1*. Available at [http://infocenter.nordicsemi.com/pdf/PPK\\_User\\_Guide\\_v2.1.pdf](http://infocenter.nordicsemi.com/pdf/PPK_User_Guide_v2.1.pdf) 19.04.2018.
- [38] Nordic Semiconductor. *Reference Layout*. Available at [http://infocenter.nordicsemi.com/index.jsp?topic=%2Fcom.nordic.infocenter.nrf52%2Fdita%2Fnrf52%2Fpdflinks%2Fref\\_layout.html](http://infocenter.nordicsemi.com/index.jsp?topic=%2Fcom.nordic.infocenter.nrf52%2Fdita%2Fnrf52%2Fpdflinks%2Fref_layout.html) 19.05.2018.

- [39] Nordic Semiconductor. *SoftDevices*. Available at <http://infocenter.nordicsemi.com/index.jsp?topic=%2Fcom.nordic.infocenter.softdevices51%2Fdita%2Fnrf51%2Fsoftdevices.html> 09.04.2018.
- [40] Nordic Semiconductor. *SoftDevices*. Available at <https://www.youtube.com/watch?v=tZjlixQPO-Q&t=9s> 10.04.2018.
- [41] Nordic Semiconductor. *SoftDevices*. Available at [http://infocenter.nordicsemi.com/index.jsp?topic=%2Fcom.nordic.infocenter.s132.sds%2Fdita%2Fsoftdevices%2Fs130%2Fble\\_protocol\\_stack%2Fble\\_protocol\\_stack.html](http://infocenter.nordicsemi.com/index.jsp?topic=%2Fcom.nordic.infocenter.s132.sds%2Fdita%2Fsoftdevices%2Fs130%2Fble_protocol_stack%2Fble_protocol_stack.html) 09.04.2018.
- [42] Bluetooth® SIG. *Bluetooth® Core Specification*. Download available at <https://www.bluetooth.com/specifications/bluetooth-core-specification> 03.04.2018.
- [43] Bluetooth® SIG. *Bluetooth® Radio Versions*. Available at <https://www.bluetooth.com/bluetooth-technology/radio-versions> 03.04.2018.
- [44] David Squire and Forrest Huff. *Energy Harvesting for Low-Power Sensor Systems*. Available at <https://www.renesas.com/pt-br/media/solutions/home/energy-harvesting/Whitepaper-Energy-Harvesting.pdf> 18.04.2018.
- [45] Johanson Technology. *Antenna Selection Guide*. Available at <https://www.johansontechnology.com/chip-antenna-selection> 11.05.2018.
- [46] Linear Technology. *LTC3588-1 | Nanopower Energy Harvesting Power Supply*. Available at <http://www.analog.com/media/en/technical-documentation/data-sheets/35881fc.pdf> (12.04.2018).
- [47] *Voltage multiplier*. Available at <https://www.electronics-tutorials.ws/blog/voltage-multiplier-circuit.html> 17.04.2018.
- [48] *What is 3D printing*. Available at <https://3dprinting.com/what-is-3d-printing/> 16.05.2018.
- [49] *What is the Difference Between Half Wave Voltage Doubler and Full Wave Voltage Doubler?* Available at <https://electronics.stackexchange.com/questions/328477/what-is-the-difference-between-half-wave-voltage-doubler-and-full-wave-voltage-d> 17.04.2018.
- [50] *ZF Electronics Energy Harvesting Wireless Switches*. Available at <https://no.mouser.com/new/zf-electronics/cherry-energy-harvesting-switches/> 21.05.2018.



## Appendix A

# Bill of Materials

# Bill of Materials

## LTC solution

Component	Package	Quantity	Description	Supplier	Suppliers Part Number
LTC3588-1	10-MSOP	1	IC voltage regulator	Digi-Key	LTC3588EMSE-1#PBF
nRF52832	QFN48	1	Multi-protocol Bluetooth Low Energy and 2.4GHz proprietary system-on-chip	Nordic Semiconductor	NRF52832-QFAA-R
AFIG-0007	Custom in-house package	1	electro-magnetic transducer	Digi-Key	CH721-ND
2450AT18 A100(E)	Custom in-house package	1	2.4GHz chip antenna	Digi-Key	2450AT18A100E
DB3X209 K0LCT-ND	SOT-23N	2	Schottky diode	Digi-Key	DB3X209K0L
SAM10243- ND	MHDR1X4	2	Pin header 1x4	Digi-Key	TMS-104-01-L-S
Capacitor	CAPC 1005X04L	1	0.8pF Capacitor	Digi-Key	GRM1555C 2AR80BA01D
Capacitor	CAPC 1005X04L	1	1pF Capacitor	Digi-Key	GRM1555C 2A1R0CA01D
Capacitor	CAPC 1005X04L	6	12pF Capacitor	Digi-Key	GRM1555C 2A120JA01D
Capacitor	CAPC 1005X04L	1	100pF Capacitor	Digi-Key	CGA2B2C0G2 A101J050BA
Capacitor	CAPC 1005X04L	3	100nF Capacitor	Digi-Key	TMK105BJ104KV-F
Capacitor	CAPC 1608X06L	2	1 $\mu$ F Capacitor	Digi-Key	UMK107ABJ105MAHT
Capacitor	CAPC 1608X06L	2	4.7 $\mu$ F Capacitor	Digi-Key	CL10A475KL8NRNC
Capacitor	CAPC 1608X06L	1	22 $\mu$ F Capacitor	Digi-Key	CL10A226MO7JZNC
Capacitor	CAPC 1608X06L	2	47 $\mu$ F Capacitor	Digi-Key	CL10A476MQENRBE
Inductor	INDC 1005X04L	1	2.7nH Inductor	Digi-Key	LQG15HS2N7S02D
Inductor	INDC 1005X04L	2	3.9nH Inductor	Digi-Key	744765039A
Inductor	INDC 1005X04L	1	15nH Inductor	Digi-Key	LQG15WZ15NJ02D
Inductor	INDC 1608X06L	1	10 $\mu$ H Inductor	Digi-Key	GLFR1608T100M-LR
Inductor	INDC 1608X06L	1	100 $\mu$ H Inductor	Digi-Key	GLFR1608T101M-LR
Crystal oscillator	4-SMD, No Lead	1	32.0 MHz Crystal	Digi-Key	CX2016DB 32000D0WZRC1
Crystal oscillator	2-SMD, No Lead	1	32.768kHz Crystal	Digi-Key	ST2012SB32768E0HPWB

# Bill of Materials

## Voltage doubler solution

Component	Package	Quantity	Description	Supplier	Suppliers Part Number
nRF52832	QFN48	1	Multi-protocol Bluetooth Low Energy and 2.4GHz proprietary system-on-chip	Nordic Semiconductor	NRF52832-QFAA-R
AFIG-0007	Custom in-house package	1	electro-magnetic transducer	Digi-Key	CH721-ND
2450AT18 A100(E)	Custom in-house package	1	2.4GHz chip antenna	Digi-Key	2450AT18A100E
DB3X209 K0LCT-ND	SOT-23N	2	Schottky diode	Digi-Key	DB3X209K0L
SAM10243- ND	MHDR1X4	2	Pin header 1x4	Digi-Key	TMS-104-01-L-S
Capacitor	CAPC 1005X04L	1	0.8pF Capacitor	Digi-Key	GRM1555C 2AR80BA01D
Capacitor	CAPC 1005X04L	1	1pF Capacitor	Digi-Key	GRM1555C 2A1R0CA01D
Capacitor	CAPC 1005X04L	6	12pF Capacitor	Digi-Key	GRM1555C 2A120JA01D
Capacitor	CAPC 1005X04L	1	100pF Capacitor	Digi-Key	CGA2B2C0G2 A101J050BA
Capacitor	CAPC 1005X04L	3	100nF Capacitor	Digi-Key	TMK105BJ104KV-F
Capacitor	CAPC 1608X06L	1	1μF Capacitor	Digi-Key	UMK107ABJ105MAHT
Capacitor	CAPC 1608X06L	1	4.7μF Capacitor	Digi-Key	CL10A475KL8NRNC
Capacitor	CAPC 1608X06L	4	10μF Capacitor	Digi-Key	C1608X5R1A 106M080AC
Capacitor	CAPC 1608X06L	1	47μF Capacitor	Digi-Key	CL10A476MQENRBE
Capacitor	587-5448-1- ND	1	220μF Capacitor	Digi-Key	JMK325ABJ227MM-P
Inductor	INDC 1005X04L	1	2.7nH Inductor	Digi-Key	LQG15HS2N7S02D
Inductor	INDC 1005X04L	2	3.9nH Inductor	Digi-Key	744765039A
Inductor	INDC 1005X04L	1	15nH Inductor	Digi-Key	LQG15WZ15NJ02D
Inductor	INDC 1608X06L	1	10μH Inductor	Digi-Key	GLFR1608T100M-LR
Crystal oscillator	4-SMD, No Lead	1	32.0 MHz Crystal	Digi-Key	CX2016DB 32000D0WZRC1
Crystal oscillator	2-SMD, No Lead	1	32.768kHz Crystal	Digi-Key	ST2012SB32768E0HPWB



## **Appendix B**

# **Datasheets**

# Wireless Switches – Generator

## AFIG, AFIM Series

Energy Harvesting



### Description

The generator and generator with RF-Electronics PCB convert mechanical energy to electrical energy, enabling our Energy Harvesting wireless snap and rocker switches to provide data transfer via RF technology, eliminating the need for batteries. This also eliminates the need for complex wire assemblies and increases flexibility for use in previously inaccessible locations.

The generator is integral to the switches, and is also available as a stand-alone unit for use with your own mechanical switch. There are multiple frequencies available. A mono-stable and a bi-stable version are both available.

### Features

- Small size, with high energy efficiency
- 868 MHz and 915 MHz frequency bands allow global use within different applications
- Long mechanical life
- Protocols are sent up to 3 times

### Typical Applications

- Building Automation
- Industrial Automation
- Smart Home
- Lighting

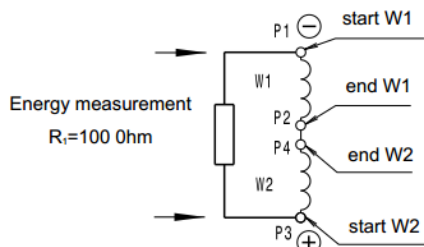
### Technical Specifications

Operating Temperature	-40 °C to 85 °C (-40 °F to 185 °F)
Mechanical Life	Up to 1,000,000 operations (Mono-stable) Up to 100,000 operations (bi-stable)
Frequency Bands, Generator with RF-Electronics (available with Mono-stable only)	868 MHz or 915 MHz
RF Distance with Cherry Energy Harvesting Switches (open area, Mono-stable only)	Up to 300 m (984')
RF Distance with Cherry Energy Harvesting Switches (buildings, Mono-stable only)	Up to 30 m (98')
Operating Force	13 N max (Mono-stable) 17 N max (Bi-stable)
Energy Generated	0.33 mWs actuating and releasing (Mono-stable) 0.33 mWs in each actuating direction (Bi-stable)

### Products

Part Number	Description
AFIG-0007	Generator, Mono-stable
AFIG-0006	Generator, Bi-stable
AFIM-1001	Generator (Mono-stable), RF-Electronics, ZF protocol wire, antenna, 868 MHz
AFIM-5002	Generator (Bi-stable), RF-Electronics, ZF protocol wire, antenna, 915 MHz

### Test Sequence



Observing the polarity a positive pulse is induced at press actuation and a negative pulse is induced at release actuation

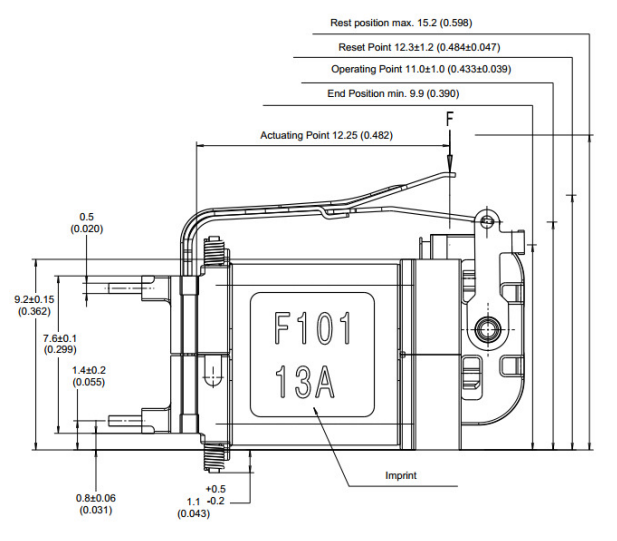
### PLEASE NOTE

CHERRY  
will become  
ZF in 2017.

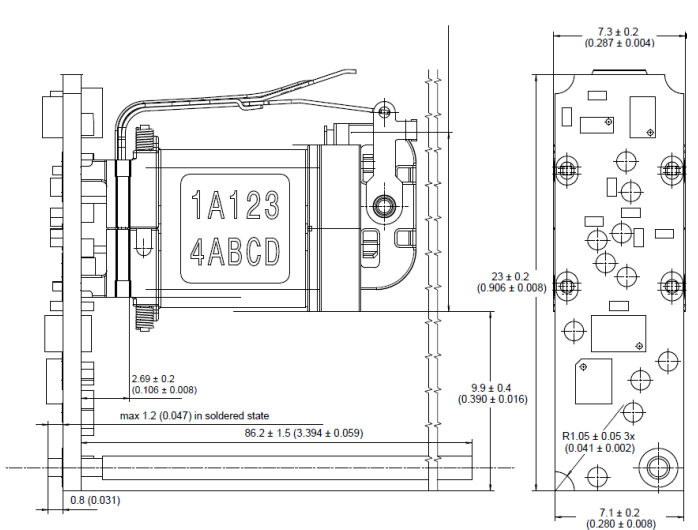


## Dimensions mm (inches)

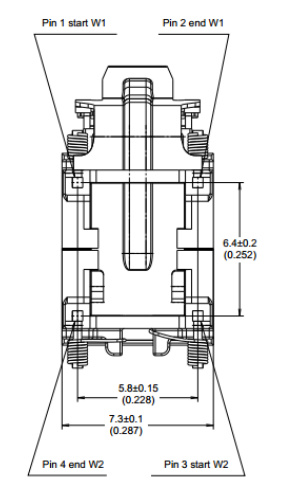
Mono-stable Generator



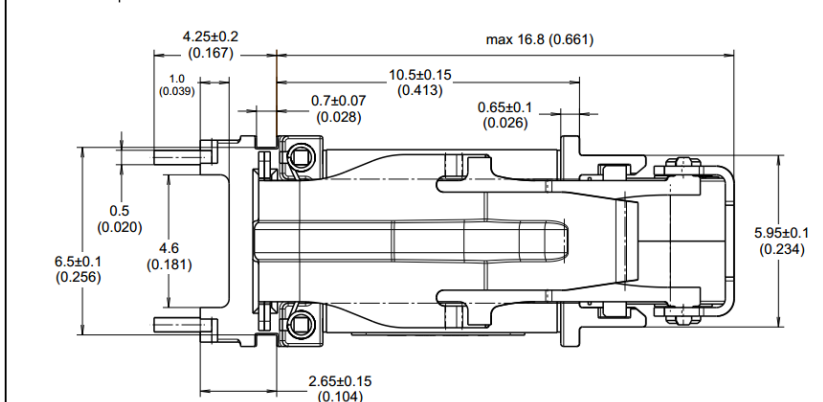
Mono-stable Generator with PCB and Wire Antenna



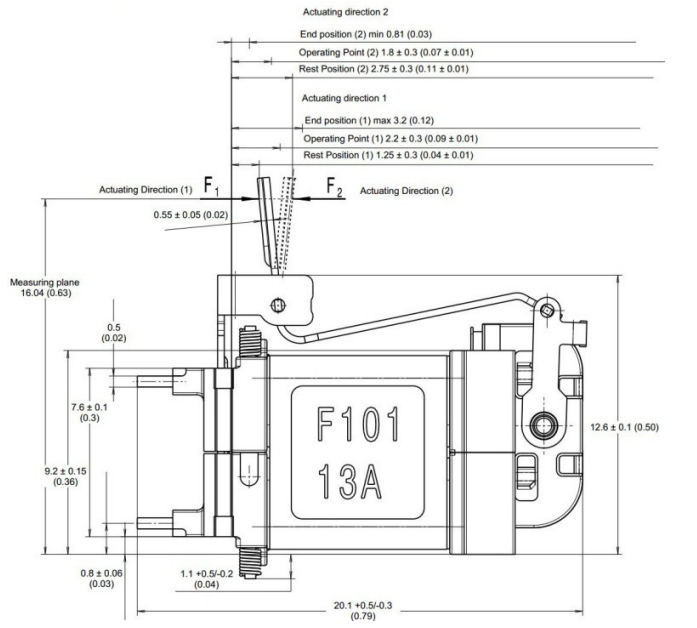
Generator Front View



Generator Top View



Bi-stable Generator





## Appendix C

# Schematics

### C.1 nRF52 Development Kit and Stop Button Central Schematics

# Nordic Semiconductor ASA

**nRF52832 Bluetooth Smart/ANT/2.4GHz RF Preview Development Board (PCA10036)**

- Sheet 1: nRF Radio
- Sheet 2: Interface MCU
- Sheet 3: Buttons and LEDs
- Sheet 4: Connectors
- Sheet 5: Power Supply
- Sheet 6: Stop Button Central Showcase



PCA10036 - Cover

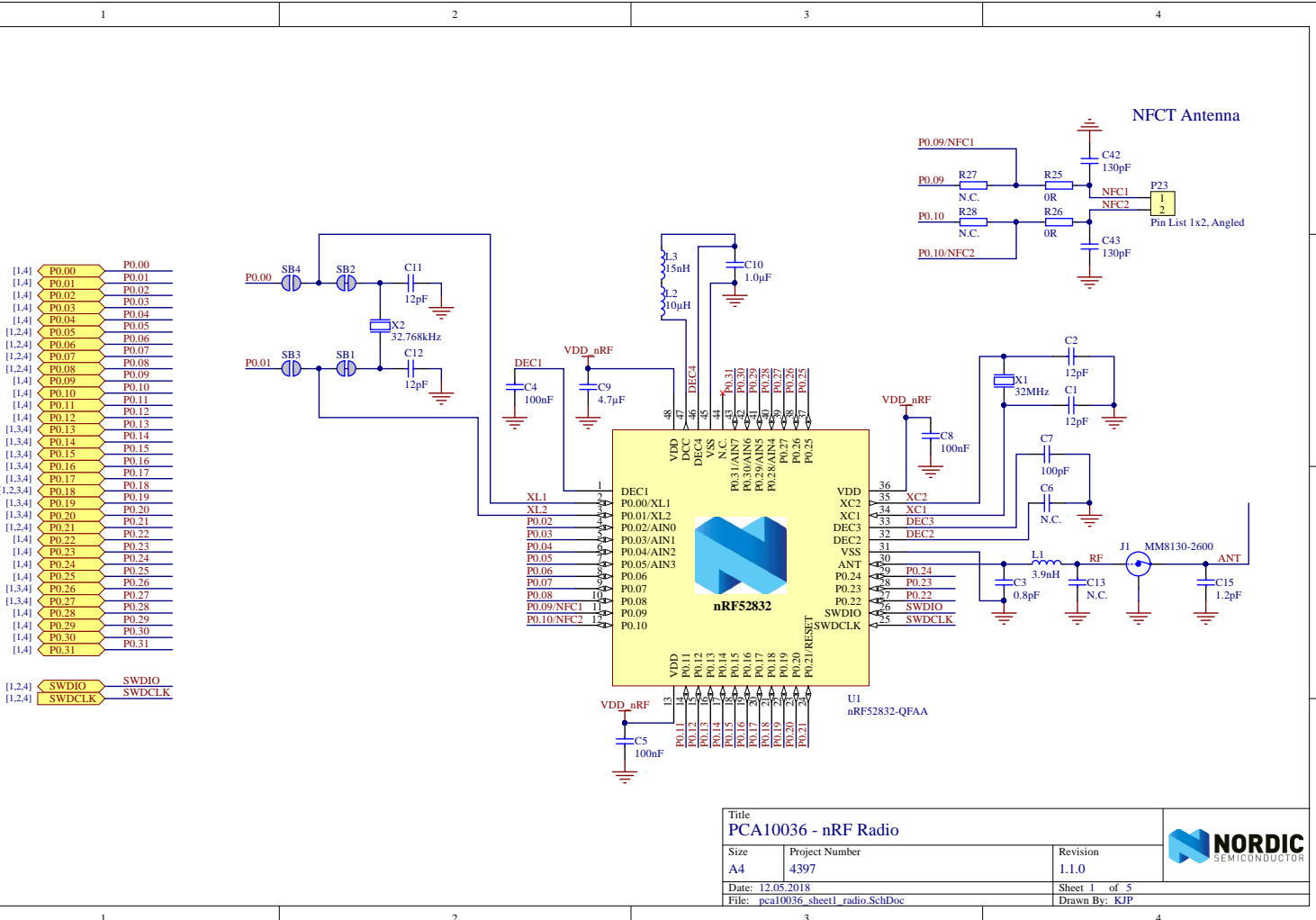
Size A3	Project Number 4397	Revision 1.1.0
------------	------------------------	-------------------

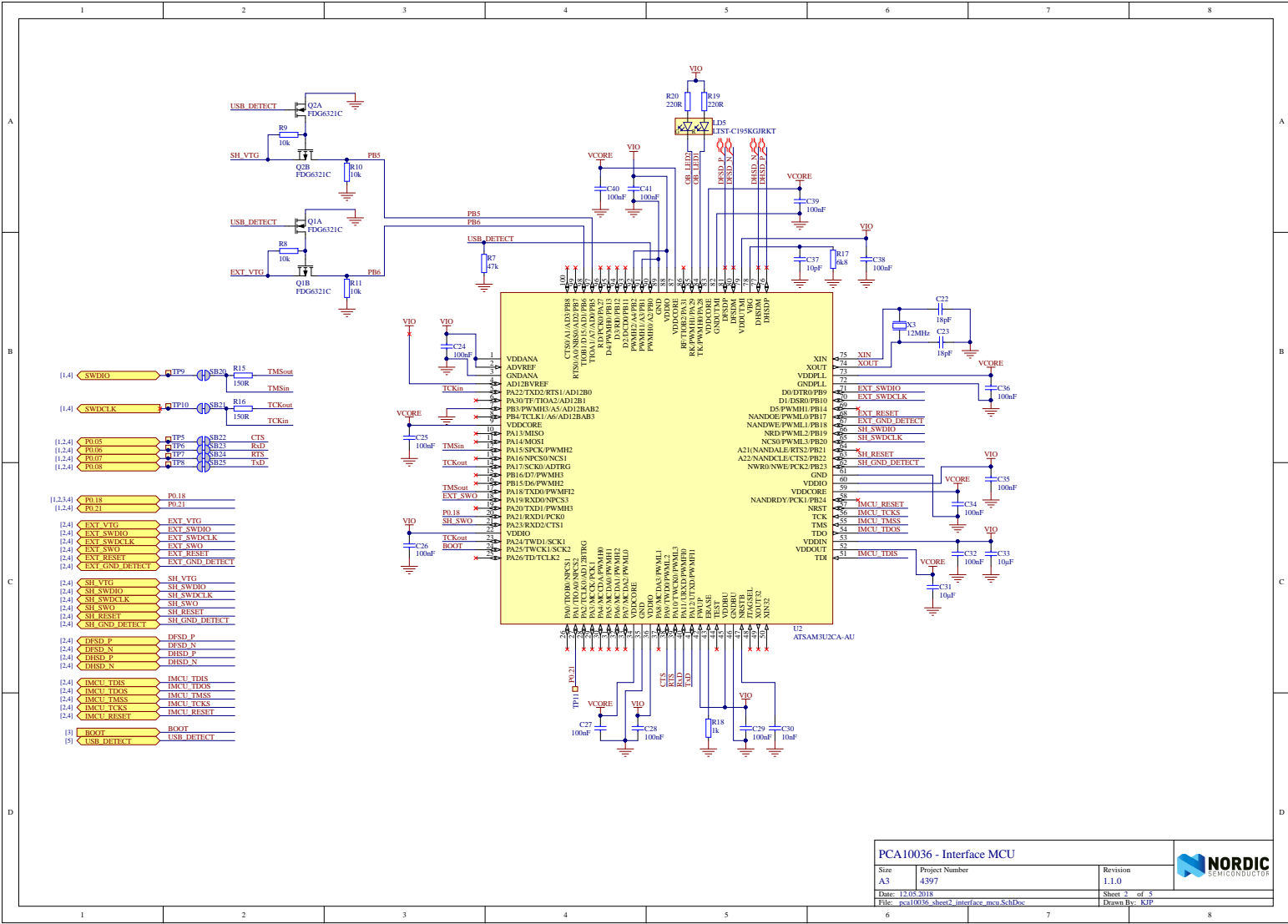
Date: 12.03.2018

File: pca10036\_sheet01\_cover.SchDoc

Sheet 0 of 5	Drawn By: KJP
--------------	---------------





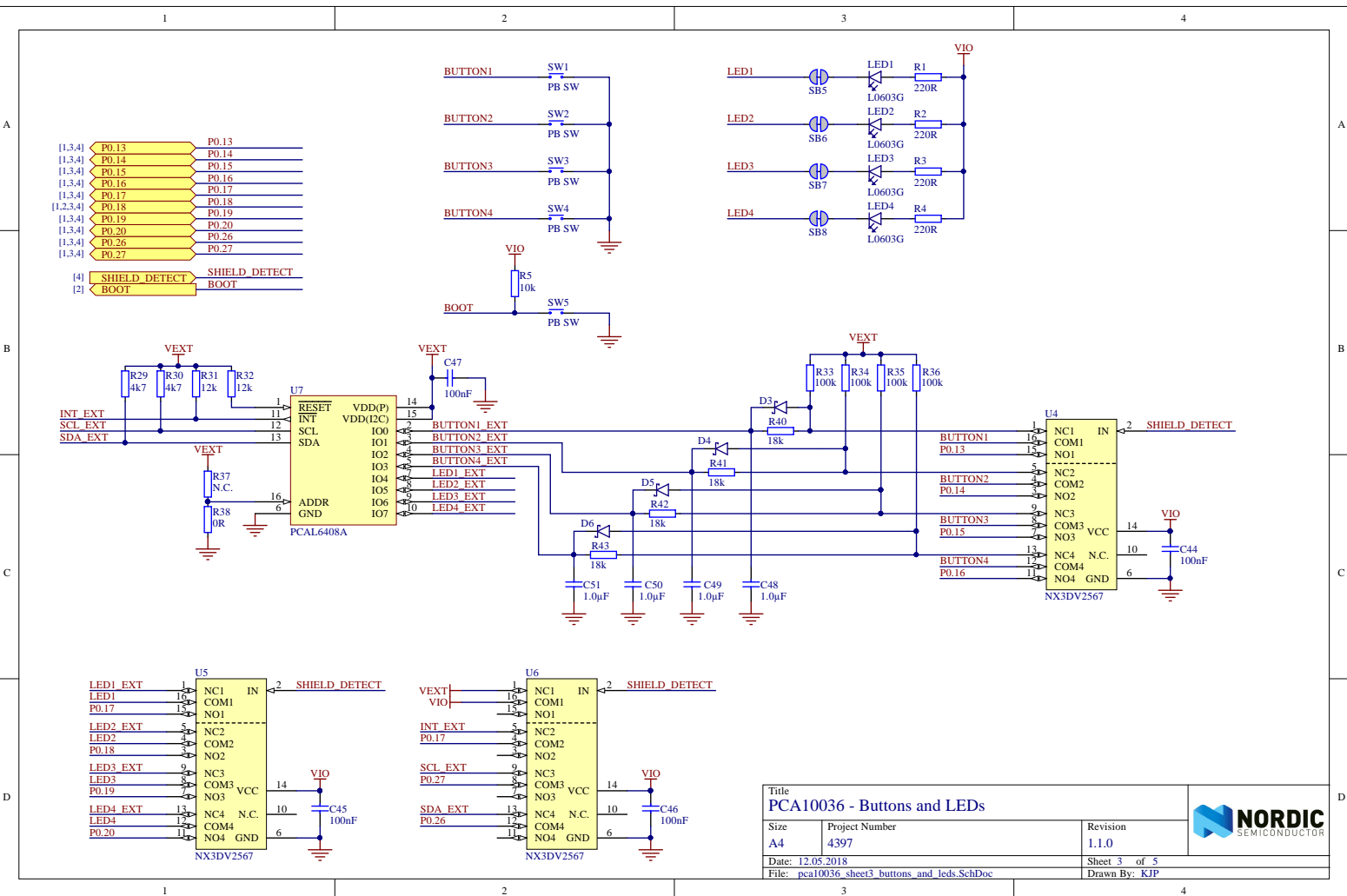


PCA10036 - Interface MCU

PCA9530S Interface MCC

Size <b>A3</b>	Project Number <b>4397</b>	Revision <b>1.1.0</b>
Date: <b>12.05.2018</b>		Sheet <b>2</b> of <b>5</b>
File Name: <b>PCA9530S-1_v2.1.1.5_061.D</b>		Printed: <b>05/18</b>

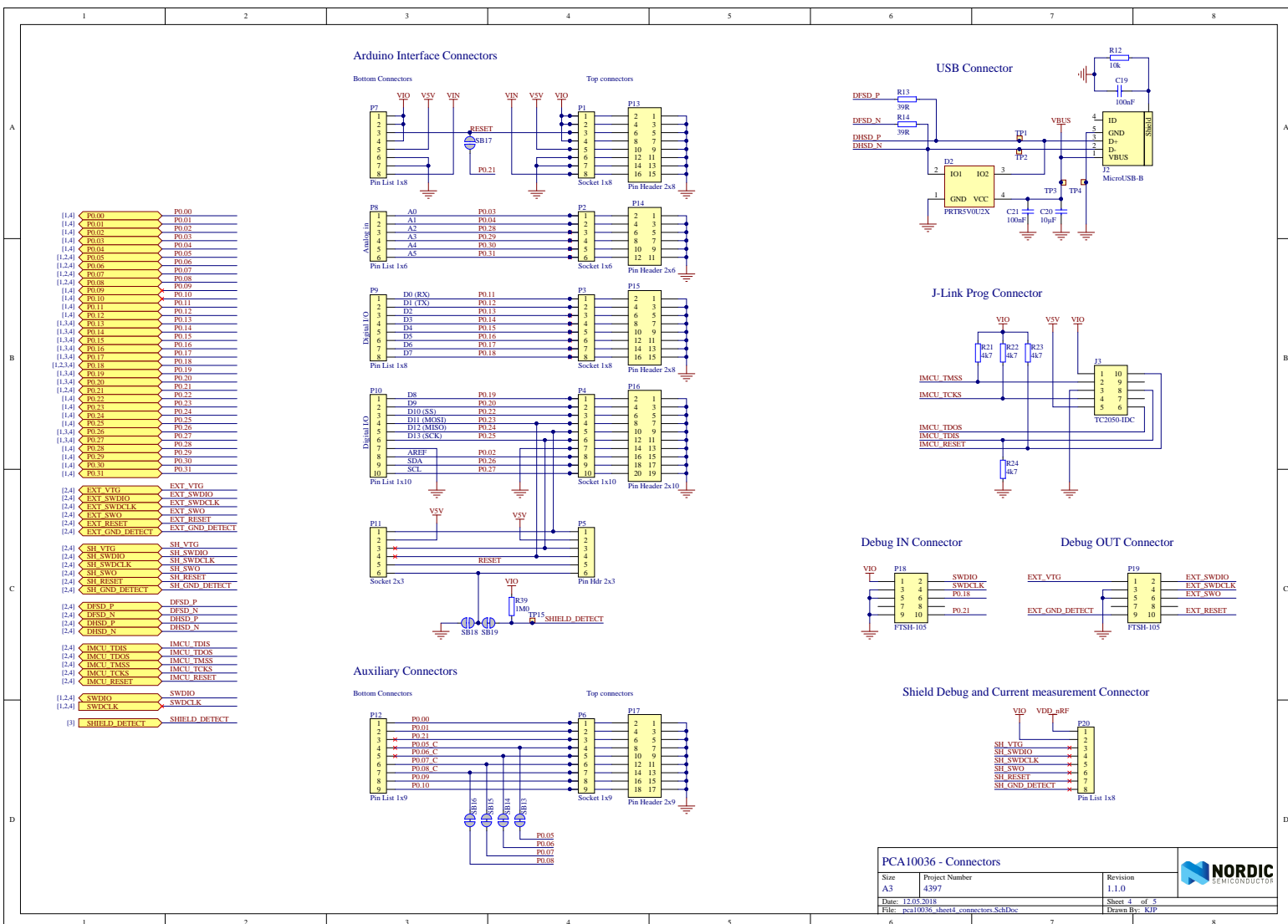


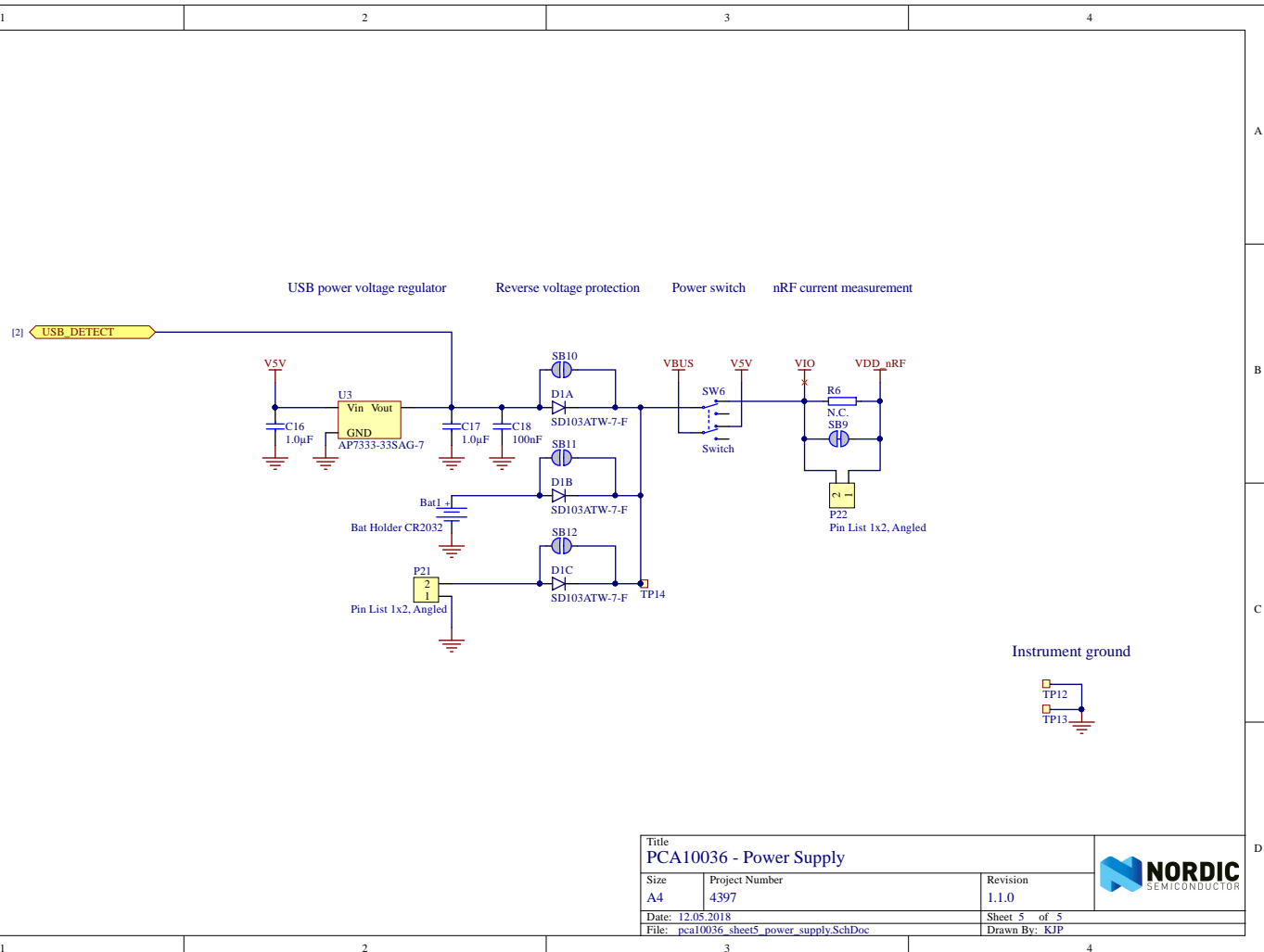


Title  
PCA10036 - Buttons and LEDs

Size	Project Number	Revision
A4	4397	1.1.0
Date: 12.05.2018	Sheet 3 of 5	
File: pca10036_sheet3_buttons_and_leds.SchDoc		Drawn By: KJP





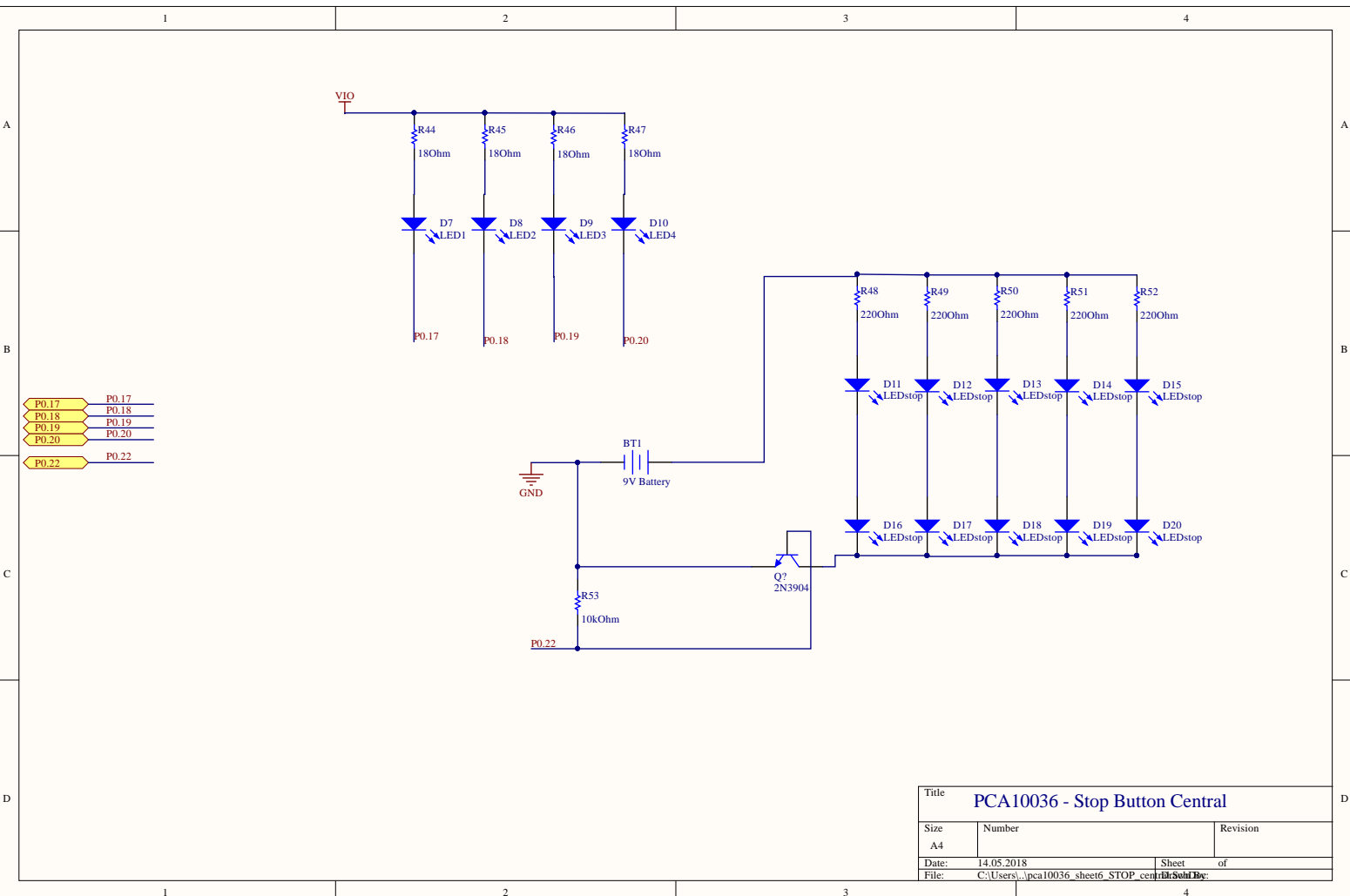


1

2

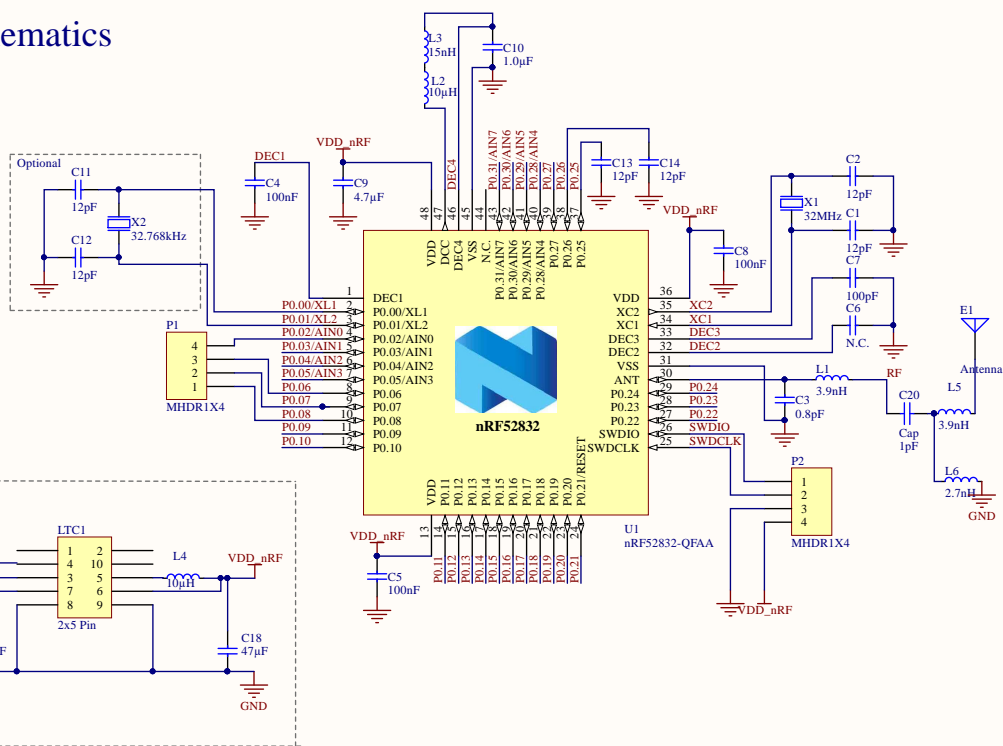
3

4

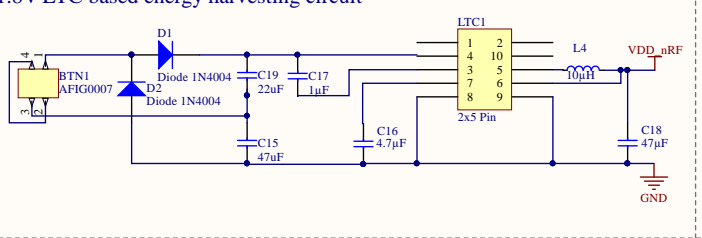


## **C.2 Energy Harvesting Stop Button Schematics**

## Final LTC 1.8V Schematics



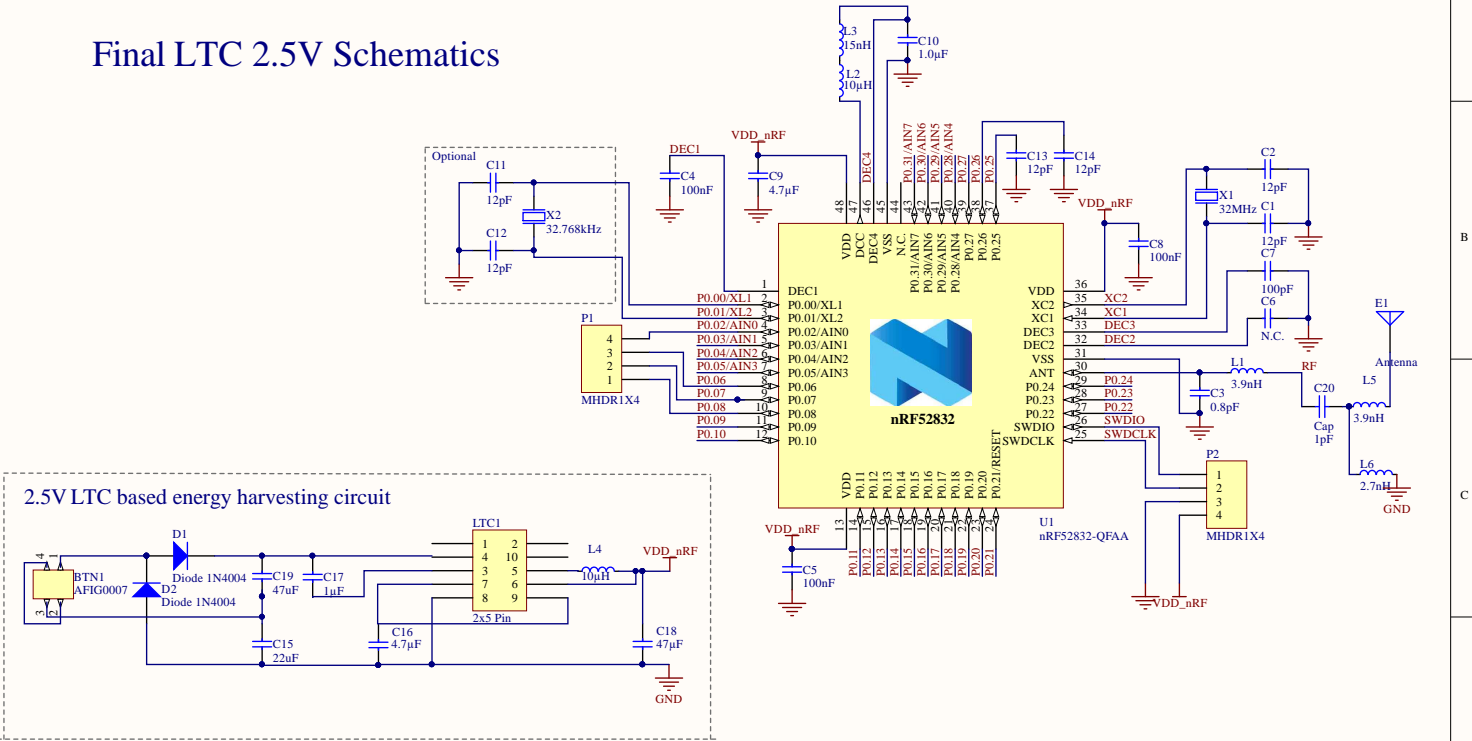
1.8V LTC based energy harvesting circuit



EHSB

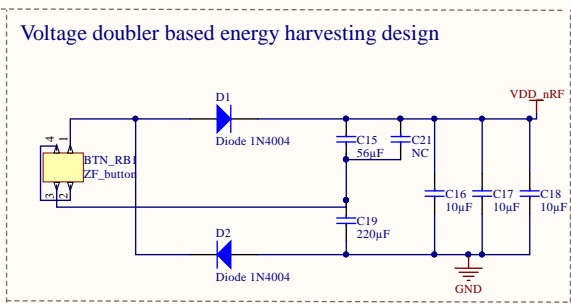
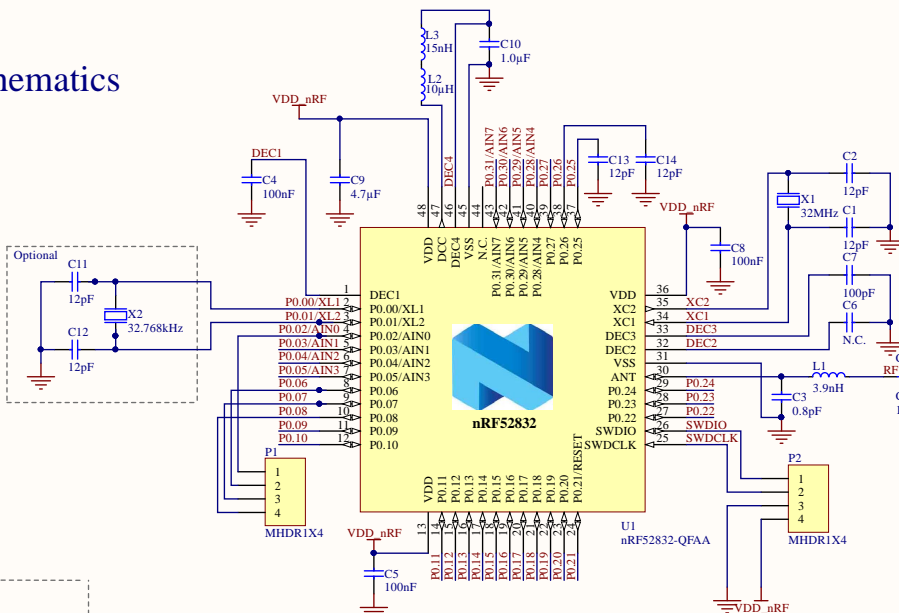
By Lundaas, Melheim, Olluri, Rømo and Røstad

# Final LTC 2.5V Schematics



EHSB  
By Lundaas, Melheim, Olluri, Rømo and Røstad

## Final Voltage Doubler Schematics



EHSB  
By Lundaas, Melheim, Olluri, Rømo and Røstad

## Appendix D

# CODE: Relayer

LISTING D.1: Initialisation of integer

```

1 /*Initialising 8-bit unassigned integer array with 16 positions , set every entry
   to 0*/
2 uint8_t adv_rep_uuid[16] = {0};
3 /*Initialising 16-bit integer that contains the length of adv_rep_uuid*/
4 uint16_t adv_rep_uuid_length = sizeof(adv_rep_uuid);

```

LISTING D.2: If statement that checks for eligibility

```

1 /*Event that gets generated by SoftDevice when an advertising report is ready */
2 case BLE_GAP_EVT_ADV_REPORT:
3 {
4     /*Access advertising report*/
5     ble_gap_evt_adv_report_t const * p_adv_report = &p_gap_evt->params.
6     adv_report;
7     /*Checks if the adv package carries a BR/RD not supported advertising flag*/
8     if(p_adv_report->data[2] == BLE_GAP_FLAG_BR_EDR_NOT_SUPPORTED \
9     /*Checks if the adv package carries a complete 128-bit UUID*/
10    && p_adv_report->data[4] == BLE_GAP_AD_TYPE_128BIT_SERVICE_UUID_COMPLETE)
11    {
12        /*Copy UUID to the adv_rep_uuid variable*/
13        memcpy(&adv_rep_uuid[0], &p_adv_report->data[5], 16);
14        /*Send content of variable to central via uart string*/
15        ble_nus_string_send(&m_nus, adv_rep_uuid , &adv_rep_uuid_length);
16    }
17 }break;

```

LISTING D.3: BLE event handler

```

1 /*The ble_evt_handler is a function that processes the events generated by the
   SoftDevice*/
2 static void ble_evt_handler(ble_evt_t const * p_ble_evt, void * p_context)
3 {
4
5     switch (p_ble_evt->header.evt_id)
6     {
7         /*Event generated when connection to central*/
8         case BLE_GAP_EVT_CONNECTED:
9
10            /*Event generated when disconnected from central*/
11            case BLE_GAP_EVT_DISCONNECTED:
12
13            /*Event generated when advertising report is ready*/
14            case BLE_GAP_EVT_ADV_REPORT:
15        }
16

```

LISTING D.4: Initialization of radio notification function

```
1 /*Initialize radio notification*/
2 static void radio_notification_init(void)
3 {
4     ret_code_t err_code;
5     uint32_t softdevice_evt_irq_priority;
6
7     err_code = sd_nvic_GetPriority(SD_EVT_IRQn, &softdevice_evt_irq_priority);
8     APP_ERROR_CHECK(err_code);
9
10    /*Make sure to use same IRQ priority as SD events to simplify state
11     information handling*/
12    err_code = sd_nvic_SetPriority(RADIO_NOTIFICATION_IRQn,
13        softdevice_evt_irq_priority);
14    APP_ERROR_CHECK(err_code);
15
16    err_code = sd_nvic_EnableIRQ(RADIO_NOTIFICATION_IRQn);
17    APP_ERROR_CHECK(err_code);
18
19    err_code = sd_radio_notification_cfg_set(
20        NRF_RADIO_NOTIFICATION_TYPE_INT_ON_INACTIVE,
21        NRF_RADIO_NOTIFICATION_DISTANCE_NONE);
22    APP_ERROR_CHECK(err_code);
23 }
24 void RADIO_NOTIFICATION_IRQHandler(void)
25 {
26     if (m_start_scanning)
27     {
28         m_start_scanning = false;
29         nrf_delay_us(2000);
30         scan_start();
31         NRF_LOG_INFO("Start scan after radio event");
32     }
33 }
```

## Appendix E

# CODE: Stop button

LISTING E.1: Information advertised by the ble\_app\_beacon

```

1  /* Manufacturer specific data and length defines */
2  #define APP_BEACON_INFO_LENGTH          0x17
3  #define APP_ADV_DATA_LENGTH             0x15
4  #define APP_DEVICE_TYPE                0x02
5  #define APP_MEASURED_RSSI              0xC3
6  #define APP_COMPANY_IDENTIFIER         0x0059
7  #define APP_MAJOR_VALUE               0x01, 0x02
8  #define APP_MINOR_VALUE               0x03, 0x04
9  #define APP_BEACON_UUID                0x01, 0x12, 0x23, 0x34, \
10                                         0x45, 0x56, 0x67, 0x78, \
11                                         0x89, 0x9a, 0xab, 0xbc, \
12                                         0xcd, 0xde, 0xef, 0xf0
13
14 /*Information advertised by the ble_app_beacon*/
15 static uint8_t m_beacon_info[APP_BEACON_INFO_LENGTH] =
16 {
17     APP_DEVICE_TYPE,
18     APP_ADV_DATA_LENGTH,
19     APP_BEACON_UUID,
20     APP_MAJOR_VALUE,
21     APP_MINOR_VALUE,
22     APP_MEASURED_RSSI
23 };
24
25 /*Function that initialises the data to be advertised*/
26 static void advertising_init(void)
27 {
28     ble_advdata_t advdata;
29     uint8_t        flags = BLE_GAP_FLAG_BR_EDR_NOT_SUPPORTED;
30
31     ble_advdata_manuf_data_t manuf_specific_data;
32
33     manuf_specific_data.company_identifier = APP_COMPANY_IDENTIFIER;
34     manuf_specific_data.data.p_data = (uint8_t *) m_beacon_info;
35     manuf_specific_data.data.size    = APP_BEACON_INFO_LENGTH;
36
37     /*Build and set advertising data*/
38     memset(&advdata, 0, sizeof(advdata));
39
40     advdata.name_type      = BLE_ADVDATA_NO_NAME;
41     advdata.flags          = flags;
42     advdata.p_manuf_specific_data = &manuf_specific_data;
43 }
```

LISTING E.2: Information advertised by the ehsb\_nordic\_b application

```

1 /*Defines values used in advertising data*/
2 #define APP_BLE_CONN_CFG_TAG          1
3 #define EHSB_SERVICE_UUID_TYPE        0x02
4 #define BLE_UUID_EHSB_SERVICE         0x0001
5 #define EHSB_BASE_UUID                0x9F, 0xCA, 0xDC, 0x24, \
6                                         0x0E, 0xE5, 0xA9, 0xE0, \
7                                         0x93, 0xF3, 0xA3, 0xB5, \
8                                         0x00, 0x00, 0x40, 0x6E
9
10 /*Struct that takes in ehsb service uuid and ehsb service type*/
11 static ble_uuid_t m_adv_uuids[] =
12 {
13     {BLE_UUID_EHSB_SERVICE, EHSB_SERVICE_UUID_TYPE}
14 };
15
16 /*Function that initializes the data to be advertised*/
17 static void advertising_init(void)
18 {
19     ble_advdata_t           advdata;
20     uint8_t                 flags = BLE_GAP_ADV_FLAG_BR_EDR_NOT_SUPPORTED;
21
22     /*Build and set advertising data*/
23     memset(&advdata, 0, sizeof(advdata));
24
25     advdata.flags            = flags;
26     advdata.uuids_complete.uuid_cnt = sizeof(m_adv_uuids)/sizeof(m_adv_uuids[0])
27 ;
28     advdata.uuids_complete.p_uuids = m_adv_uuids;
29
30     /*Add UUID to softdevice*/
31     ble_uuid128_t ehsb_base_uuid = EHSB_BASE_UUID;
32     err_code = sd_ble_uuid_vs_add(&ehsb_base_uuid, &m_adv_uuids[0].type);
33 }
```

## Appendix F

# CODE: Central

LISTING F.1: Whitelist initiation

```

1 /* Two-dimensional array to hold the UUIDs that should be "whitelisted" */
2 uint8_t whitelist[30][16] = {0};

```

LISTING F.2: Whitelist storage function

```

1 /*NRF_FSTORAGE instance*/
2 NRF_FSTORAGE_DEF(nrf_fstorage_t whitelist_storage) =
3 {
4     /* Set a handler for fstorage events. */
5     .evt_handler = fstorage_evt_handler,
6     .start_addr = 0x3e000,
7     .end_addr   = 0x3ffff,
8 };
9
10 int main(void)
11 {
12     ret_code_t rc;
13
14     /*Initiate the fstorage instance*/
15     rc = nrf_fstorage_init(&whitelist_storage, &nrf_fstorage_sd, NULL);
16     APP_ERROR_CHECK(rc);
17 }

```

LISTING F.3: Whitelist read function

```

1 /*Function for reading UUIDs from flash and putting them in whitelist on start-
2  up*/
3 static void read_flash(void)
4 {
5     ret_code_t err_code;
6     /*Read flash at the address where uuid_number is stored*/
7     err_code = nrf_fstorage_read(&whitelist_storage, 0x3e000, &uuid_number, 4);
8     APP_ERROR_CHECK(err_code);
9
10    /*If nothing has previously been written to flash, uuid_number will equal
11     255*/
12    if(uuid_number == 255)
13    {
14        uuid_number = 0;
15    }
16    else
17    {
18        /*Read out as many UUIDs as indicated by uuid_number*/
19        for(uint8_t i = 0; i < uuid_number; i++)
20        {
21            nrf_fstorage_read(&whitelist_storage, flash_addr, &whitelist[i], 16)
22        }
23    }
24 }

```

```

20         flash_addr += 0x10;
21     }
22 }
23 }
```

LISTING F.4: Administrating the whitelist

```

1 /* Function for handling button actions*/
2 void button_handler(uint8_t pin_no, uint8_t button_action)
3 {
4     ret_code_t err_code;
5
6     /*Button 2 is for adding a new UUID to the system.
7      A push of the button sets add_uuid = true
8      and release sets add_uuid = false, meaning that the button
9      needs to be held down in order to add a new UUID*/
10    if(pin_no == BUTTON_2 && button_action == APP_BUTTON_PUSH)
11    {
12        if(uuid_number > 30)
13        {
14            NRF_LOG_INFO("\\"Whitelist\\" full");
15            nrf_gpio_pin_clear(LED_2);
16            nrf_gpio_pin_clear(LED_4);
17            existing_uuid = true;
18        }
19        else
20        {
21            /*Timer to toggle LED_4 every 500ms*/
22            app_timer_start(m_add_uuid_timer_id, APP_TIMER TICKS(500),
23 add_uuid_timeout_handler);
24            add_uuid = true;
25        }
26    if(pin_no == BUTTON_2 && button_action == APP_BUTTON_RELEASE)
27    {
28        /*Stop the toggling of LED_4*/
29        app_timer_stop(m_add_uuid_timer_id);
30        nrf_gpio_pin_set(LED_4);
31        /*If a UUID has been added flash needs to be updated*/
32        if(new_uuid_added)
33        {
34            uuid_number += 1;
35            new_uuid_added = false;
36
37            /*Erase old uuid_number from flash and write the new one*/
38            err_code = nrf_fstorage_erase(&whitelist_storage, 0x3e000, 1, NULL);
39            APP_ERROR_CHECK(err_code);
40
41            NRF_LOG_INFO("Writing \"%x\" to flash.", uuid_number);
42            err_code = nrf_fstorage_write(&whitelist_storage, 0x3e000, &
43 uuid_number, 4, NULL);
44            APP_ERROR_CHECK(err_code);
45        }
46
47        else if(existing_uuid)
48        {
49            nrf_gpio_pin_set(LED_2);
50            existing_uuid = false;
51        }
52
53        add_uuid = false;
54    }
55    /*Holding button 3 erases "whitelist" after 4 seconds of toggling all LEDs*/
56 }
```

```

55     if(pin_no == BUTTON_3 && button_action == APP_BUTTON_PUSH)
56     {
57         erasing_whitelist = true;
58         scan_stop();
59         nrf_gpio_pin_set(LED_2);
60         nrf_gpio_pin_set(LED_3);
61         nrf_gpio_pin_set(LED_4);
62         /*Timer to toggle all the LEDs and show that flash is about to be erased
63         */
64         app_timer_start(m_erase_whitelist_timer_id , APP_TIMER TICKS(250) ,
65         erase_uuids_timeout_handler);
66     }
67     if(pin_no == BUTTON_3 && button_action == APP_BUTTON_RELEASE)
68     {
69         /*If the button is released to early – abort deletion*/
70         if(!whitelist_erased)
71         {
72             app_timer_stop(m_erase_whitelist_timer_id);
73             if(connected)
74             {
75                 nrf_gpio_pin_clear(LED_3);
76             }
77             nrf_gpio_pin_set(LED_2);
78             nrf_gpio_pin_set(LED_4);
79             if(!connected)
80             {
81                 nrf_gpio_pin_set(LED_3);
82             }
83             scan_start();
84             erasing_whitelist = false;
85             delete_counter = 0;
86         }
87     }

```

LISTING F.5: Is UUID in whitelist?

```

1  /*Check for eligible UUID*/
2  if(p_adv_report->data[2] == BLE_GAP_ADV_FLAG_BR_EDR_NOT_SUPPORTED \
3      && p_adv_report->data[4] == BLE_GAP_AD_TYPE_128BIT_SERVICE_UUID_COMPLETE)
4  {
5      for(int8_t i = 0; i < button_number; i++)
6      {
7          /*Compare received UUID to the entries in whitelist*/
8          if(memcmp(adv_uuid, whitelist[i], sizeof(adv_uuid)) == 0)
9          {
10              nrf_gpio_pin_set(STOP_SIGN);
11              nrf_gpio_pin_clear(LED_2);
12              reset = true;
13          }
14      }
15 }

```

LISTING F.6: Adding advertised UUID to "whitelist"

```

1  /*Advertising report*/
2  case BLE_GAP_EVT_ADV_REPORT:
3  {
4      ble_gap_evt_adv_report_t const * p_adv_report = &p_gap_evt->params.adv_report
5      ;
6      uint8_t adv_uuid[16] = {0};
7      memcpy(&adv_uuid, &p_adv_report->data[5], 16);
8
9      else if (add_uuid)
10     {
11         /*Check RSSI, flag and UUID type to ensure that advertising device is
12          close and of right kind.*/
13         if (p_ble_evt->evt.gap_evt.params.adv_report.rssi > -35 \
14             && p_adv_report->data[2] == BLE_GAP_ADV_FLAG_BR_EDR_NOT_SUPPORTED \
15             && p_adv_report->data[4] ==
16             BLE_GAP_AD_TYPE_128BIT_SERVICE_UUID_COMPLETE)
17         {
18             /*Check if UUID is already present in whitelist*/
19             for (uint8_t i = 0; i < uuid_number; i++)
20             {
21                 if (memcmp(adv_uuid, whitelist[i], sizeof(adv_uuid)) == 0)
22                 {
23                     app_timer_stop(m_add_uuid_timer_id);
24                     nrf_gpio_pin_set(LED_4);
25                     nrf_gpio_pin_clear(LED_2);
26                     existing_uuid = true;
27                 }
28             }
29             if (!new_uuid_added && !existing_uuid)
30             {
31                 /*Copy the UUID from advertisement report to the next slot in
32                  whitelist*/
33                 memcpy(&whitelist[uuid_number], &p_adv_report->data[5], 16);
34
35                 app_timer_stop(m_add_uuid_timer_id);
36                 nrf_gpio_pin_clear(LED_4);
37                 new_uuid_added = true;
38
39                 /*Write the added UUID to flash*/
40                 NRF_LOG_INFO("Writing \"%x\" to flash.", whitelist[uuid_number]);
41                 err_code = nrf_fstorage_write(&whitelist_storage, flash_addr,
42                     whitelist[uuid_number], sizeof(whitelist[uuid_number]), NULL);
43                 APP_ERROR_CHECK(err_code);
44                 NRF_LOG_INFO("Done.");
45
46                 flash_addr += 0x10;
47             }
48         }
49     }
50 } break;

```

## Appendix G

# Energy Harvesting Stop Button Poster



NTNU

# Energy Harvesting Stop Button

Jonathan L. Lundaas, Tor André Melheim, Besart Olluri, Simon Rømo, Simen S. Røstad

Faculty of Information Technology and Electrical Engineering - Department of Electronic Systems

Norwegian University of Science and Technology

NORDIC SEMICONDUCTOR



## Assignment

A single public transport bus in Trondheim has more than 24 stop buttons that are intricately wired. The idea with this project is to replace these with wireless stop buttons that can be put anywhere in the bus, reducing the cost of installation and maintenance. The energy harvesting aspect will remove the need to change batteries in current wireless alternatives. Using Nordic Semiconductors nRF52 system on a chip and its Bluetooth Low Energy functionality to send a wireless signal to a central in the bus, which signals the bus to stop. Even though this is presented as a stop button, the possible applications are countless.

## 1 Energy Harvesting

Using an electromechanical generator as the source of energy to run the stop button, the AFIG-0007 from ZF Electronics, depicted in figure 1, was chosen.



**Figure 1:** The AFIG-0007 Electromechanical generator

Generating an energy pulse on both press and release, approximately 0.27mWs was generated by each button push, which in theory should be enough power to run the nRF52 long enough to send a Bluetooth Low Energy signal.

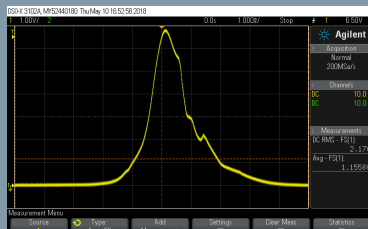


**Figure 2:** One energy pulse created by a press of the button

As the power from the button is an AC, it has to be rectified and regulated into a DC output that is within the operating voltage of the nRF52 (1.7 to 3.6 Volts).

## 2 nRF52832

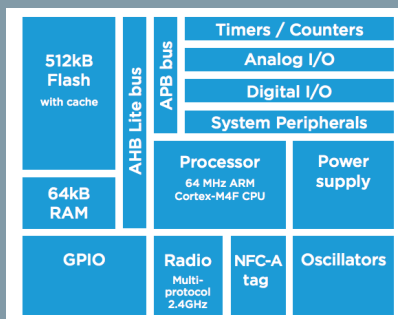


**Figure 3:** nRF52 System on a Chip

The nRF52 System on a Chip is a powerful, highly flexible ultra-low power multiprotocol system on a chip ideally suited for Bluetooth Low Energy and 2.4GHz ultra low-power wireless applications. The nRF52 is built around a 32-bit ARM Cortex-M4F CPU with 512kB flash storage + 64kB RAM. The embedded 2.4GHz transceiver supports Bluetooth Low Energy which is utilized in this project.

## 3 Network Setup

The flowchart in figure 4 illustrates the different processes occurring in the central and relayer devices. Showing how they scan for Bluetooth Low Energy signals from the stop button and how they communicate.

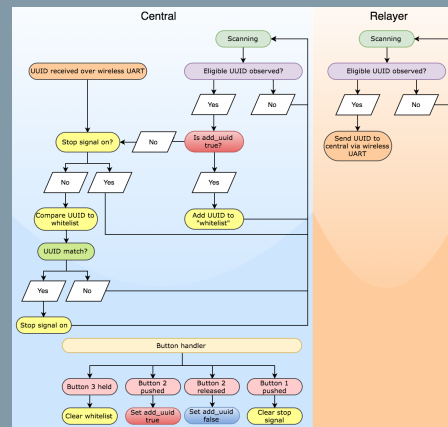


**Figure 4:** System flowchart

The stop button is a non-connectable broadcasting device that advertises a 128-bit custom UUID. The custom UUID is either observed directly by the central or via the relayer, setting a stop signal.

## 4 Circuit Board Design

PCB design is a vital part of today's electronics devices. A PCB is a multi-layered board that mechanically supports and electrically connects a circuit.

The main concern when designing the circuit board was that the size had to fit inside a generic bus stop button casing. The circuit board design was based on the nRF52's reference design, and combined with the energy harvesting circuitry made for this project. The final design had a total of 35 components on a  $4.71\text{cm}^2$  circuit board.

Having all the components soldered onto a single circuit board provides the mechanical backbone needed to handle the stress such an application is exposed to.

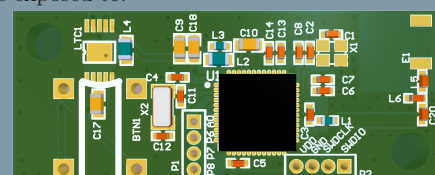


**Figure 5:** A 3D fabricated PCB design of the final circuit board.

## 5 3D Design

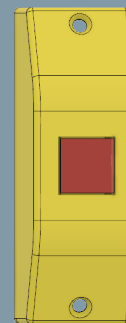


**Figure 6:** Stop button

For the purpose of this project, the button design is restricted to a prototype that looks and functions in a similar fashion as today's bus stop button design. The final 3D design of the button casing is shown in figure 6.

The 3D printed casing supports the build of the circuit board design, and makes it suitable for hard handling, increasing the stop buttons lifespan.

## 6 Final Product

Looking at the buses that are present today (2018) in Trondheim, the length of a bus vary from 9 to 19 meters. To make sure that all stop buttons can reach the central with their respective Bluetooth Low Energy signal, the stop button was made to be able to transmit a signal 20 meters to the central.

To add an option for articulated, and other buses exceeding 20 meters, a relay able to forward the stop buttons Bluetooth Low Energy signals to the central, was made to be mounted near the middle of a bus.

## 7 Further Work

- Improve and optimize the energy harvesting circuit.
- Test active rectification technology to reduce energy loss and prevent reverse current.
- Firmware optimization
- Reduce cost per unit.

## 8 GitHub

For more information on this project, check out the GitHub link below.

[https://github.com/simenrostad/Bachelor-Nordic\\_Semi](https://github.com/simenrostad/Bachelor-Nordic_Semi)

